Genetically Programmable Pathogen Sense and Destroy

by

Saurabh Gupta

B.Tech, Electrical Engineering (2004)
Indian Institute of Technology, Roorkee, India

SUBMITTED TO THE DEPARTMENT OF BIOLOGICAL ENGINEERING
IN PARTIAL FULFILLMENT OF THE REQUIREMENTS FOR THE DEGREE OF

DOCTORATE OF PHILOSOPHY

AT

THE MASSACHUSETTS INSTITUTE OF TECHNOLOGY

JUNE 2012

Signature of Author.....

Saurabh Gupta
Department of Biological Engineering
March 21, 2012

Certified by.....

Ron Weiss
Associate Professor of Biological Engineering
Thesis Supervisor

Accepted by.....

Doug Lauffenburger
Ford Professor of Bioengineering
Chair, Biological Engineering Graduate Committee

Genetically Programmable Pathogen Sense and Destroy

by

Saurabh Gupta

ABSTRACT

Twenty five percent of all the deaths worldwide are caused by infectious diseases. They are also the biggest cause of mortality among children under five years of age. Among them diarrheal diseases alone cause as many deaths as AIDS or TB and malaria combined. Also up to 80% of traveler's diarrhea is bacterial in nature. *Vibrio cholerae* (cholera), *Salmonella spp* (typhoid fever), *Shigella spp* (shigellosis) and a variety of enteropathogenic *Escherichia coli* strains are among the principle bacterial agents that cause this type of diarrhea.

Improvements in hygiene and access to adequate nutrition are good strategies but immunization against specific diseases still offers the best solution to fight these infections. Unfortunately the wide diversity of bacterial and viral agents that cause diarrhea complicates accurate diagnosis and makes the development of vaccines difficult. Antibiotics used in timely manner and in appropriate doses can be effective but the diagnosis is usually made too late for the therapy to be effective. Moreover frequent use of over-the-counter drugs without any medical supervision has led to multidrug resistance in most of the bacterial strains.

To counter this problem I demonstrate a proof of principle of a novel cell therapy against *Pseudomonas Aeruginosa* (major cause of urinary tract disease and hospital infections). Using principles of Synthetic Biology I genetically modified a probiotic strain of *E. coli* to specifically detect PAO1 and respond by secreting a novel, pathogen-specific engineered toxin. Additionally, I translated the bacterial system into mammalian cells and established a foundation for an adaptive system where the sentinel cells secrete an alternate toxin if the pathogen becomes resistant to the first one. Finally, based on this system I proposed designs against highly pathogenic strains of *Shigella*, *Salmonella* and *Vibrio cholerae*.

This cell therapy remains inert until a threat is detected, and then serves as an early detection and rapid response agent. Furthermore this platform can be tuned to release minimum but sufficient amounts of very narrow spectrum antimicrobial proteins to control the early stages of infection before the disease becomes systemic. Therefore this system's rapid, automated and highly specific response can be helpful in reducing the occurrence of dose dependent resistance. This approach offers a single integrated solution to eradicating multiple threats with a strategy that is a rapid, selective, and highly sensitive.

Thesis Supervisor: Ron Weiss
Title: Associate Professor of Biological Engineering

CONTENTS

LIST OF FIGURES

ACKNOWLEDGEMENTS

"He is a wise man who does not grieve for the things which he has not, but rejoices for those which he has."
~ Epictetus

Before coming to graduate school I read an interesting story in one of the leading national daily newspapers in India. It was about a very cool research where a group in the US had modified bacteria so that it makes ring like patterns by fluorescing different colors. I clearly remember wishing that someday I would love to do this. I didn't know that one day I will graduate from the same research group and finish my PhD under the same advisor. I'm incredibly thankful to Prof. Ron Weiss for his support and guidance throughout my stay and for giving me the opportunity to work in an exciting new scientific discipline. My stay in his lab has been very interesting to say the least. He taught me to constantly push the limits of engineering solutions for biological problems and always encouraged a highly critical super-charged scientific dialogue. In addition I'm honored to have Prof. Doug Lauffenburger, Prof. Marcia Goldberg and Prof. Jacquin Niles as my thesis committee members. I'm much obliged for their invaluable feedback and constructive criticisms on my thesis. I don't have words to describe the support I received from my thesis chair, Prof. Douglas Lauffenburger. This work wouldn't have been possible without the help and suggestions from Prof. Thomas Silhavy of Princeton University. As little as half hour meetings with him gave me enough ideas and direction to my work. His graduate course in microbiology was one of the most intense learning experiences for me. He taught me how to 'think like a bacteria' which is extremely useful as a biological engineer.

I met some amazing people throughout my graduate school and made life-long friends. First of them is Noah Davidson who has been my labmate, roommate and a fellow passenger. I'm a fan of his undying optimism and deeply cherish our wonderful times in and outside the lab. Dr. Patrick Guye always bowled me over by his pure logic and exceptional scientific advice. Thanks to Dr. Liliana Wrobleska who was always warm and compassionate shoulder to lean on. Despite being incredibly busy she helped me with all my mammalian cell culture experiments. I'm deeply indebted to Dr. Sairam Subramanium and Dr. David Karig who mentored me at the beginning of my PhD and uplifted my spirits with encouraging words. I deeply cherish intellectual discussions with Dr. Eran Bram. His extraordinary analytical insight proved an asset to me. I'm thankful to Dr. Johnathan Babb for reading my thesis from beginning to end and for his unique perspective on everything from politics to research. I am grateful to Allen Lin for helping me with MATLAB simulations. Furthermore I believe Weisslab is incomplete without our lab manager Steve Firsing who works tirelessly to keep our lab clean and organized and deserves special thanks for his efforts.

I'm indebted to my parents for teaching me the importance of perseverance and hard work in life. I met my wife during my graduate studies and even though she didn't help me start this huge endeavor she was certainly instrumental in finishing it. I will be forever thankful to her for all the sacrifices she made to ensure that I could spend most of my time in the lab. She always showed a silver lining in everything and is the 'bestest BuBu in the whole world'. I dedicate my thesis to her as a small token of appreciation.

In the end, I am profoundly thankful to two funding agencies, Office of Naval Research and Bill and Melinda Gates foundation for their generous monetary support without which this work wouldn't have been possible.

to my family...

CHAPTER 1 –INTRODUCTION

Synthetic Biology is a scientific discipline where researchers use engineering principles to analyze biological data and then use this knowledge to engineer sophisticated systems for various applications. The focus of the field is slowly diverging from characterizing basic building blocks to engineering more complex systems with multiple modules interacting with each other [1, 2]. Researchers in the field are using engineering approaches and biological methods to propose novel solutions to tackle numerous medical and environmental problems faced by the world today. For example conventional medicines faces key limitations [3] including a constant need to find novel compounds, determine precise drug-dosing regimens and avoid causing drug-resistance [4-6]. Synthetic Biology holds promise for breakthrough solutions to circumvent some of these challenges [7]. Rational design and engineering of complex and high-precision programmable organisms that couple sensing and delivery mechanisms have the potential to offer better solutions against more complex diseases such as diabetes and cancer [7]. For instance researchers are using the regenerative power of stem cells to develop a new therapy for Diabetes Mellitus [8]. For this purpose stem cells are being engineered such that out of a seed population a portion will differentiate into insulin producing beta cells while another portion of the cells continuously monitor the net amount of available beta cells (unpublished work). Similarly, a recent publication [7] illustrates the use of a synthetic genetic circuit to identify a cancer cell (HeLa). The engineered cells with this circuit simultaneously sense the levels of half a dozen biomarkers to establish whether the cell in question is cancerous or not. If the result is positive, it triggers cell death. This approach offers a novel way of diagnosing a disease based on the detection of relevant markers and executing a certain course of action.

With this foundation I propose a novel solution to the growing problem of antibiotic resistance. In this dissertation, I implemented an *in vitro* proof of principle novel pathogen 'Sense and destroy' cell therapy using the principles, techniques and tools of Synthetic Biology. I demonstrated that the engineered cells are capable of precisely detecting an infectious pathogen and executing a highly tailored response that specifically kills the pathogen.

I. Thesis Statement

Worldwide, nearly 15 million people per year die from infectious diseases, which are the second biggest cause of mortality after cardiovascular diseases [9]. Pathogens responsible for these diseases have become increasingly resistant to "first-line" drugs and second or third line drugs are much more expensive and toxic [10-12]. Inappropriate prescription and widespread overuse of antibiotics with inadequate compliance by patients are some of the causes for this growing resistance [11, 13]. Another major issue with using antibiotics is that they also kill commensal bacteria along with the pathogens and thereby make the human body more vulnerable to future infections [14, 15]. With even fewer new antibiotics in the pipeline [16] there is a growing interest and need for alternate strategies to fight these infectious agents.

To address such critical issues, I envision an auxiliary, automated and benign live synthetic cell therapy platform capable of rapidly responding to a large variety of pathogens in multiple contexts. This approach will offer a single integrated solution to eradicate multiple threats with a rapid, selective, and highly sensitive strategy. As shown in **Figure 1** this system will sense its environmental conditions, process input signals to determine whether a pathogen is present and execute an "intelligent" response by utilizing multiple, customized treatments. Engineering cells in this manner for the detection and targeted destruction of pathogens provides several important advantages over existing antimicrobial strategies :

- The engineered cells can act as sentinel/killer cells that function without human intervention. Therefore they can be deployed in difficult to access environments including, for example, the gastrointestinal tract or water supply systems. They will be embedded and remain inert until a threat is detected, and then serve as an early detection and rapid response system.
- Engineered sentinel cells may serve as a high-throughput screening platform for the discovery of the next generation of antibiotics [17-20].
- These cells can be used as smart bandages in the case of severely burnt patients where the circulatory system is destroyed and hence the antibiotics cannot protect against incoming infections.

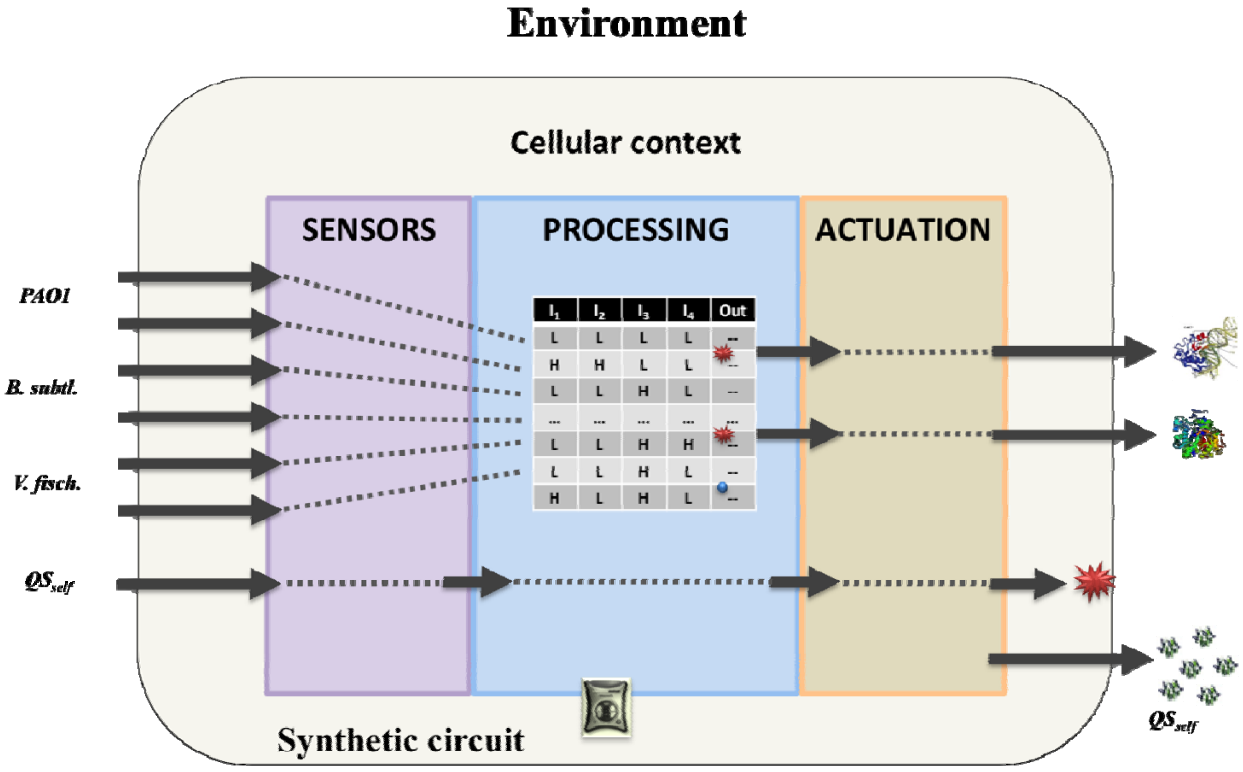

Figure 1: Architecture of the 'Sense and Destroy' system.
The system consists of genetically programmed cells which can act as a sensor, a processor and an actuator. It will first sense quorum sensing signals produced by pathogenic and non-pathogenic bacteria. Then the engineered cells will process that information to determine whether a pathogen is present in the neighborhood and what is its identity. Finally, if the pathogen is present, the engineered cells will release a toxin to specifically kill the pathogen present in the neighborhood.

Depending on the specific context these cells can be bacterial or mammalian. For example the human body hosts 10 times more bacterial cells than its own [21].and commensal bacteria can prove to be excellent vectors for carrying synthetic gene circuits that are engineered to fight infections of the human gastrointestinal tract. The gut flora is the largest reservoir of human microbiome and these microbiota constituents are already well tolerated by the innate immune system. Conversely engineered mammalian cells are more suitable for fighting affliction of sterile environments such as blood infections or skin infections in burn victims.

With this motivation this thesis focusses on proving the following hypothesis :

> An *in vitro* cell therapy can be engineered by genetically programming *E. coli* cells that explicitly detect a common human pathogen, *Pseudomonas Aeruginosa* and respond by secreting a novel, pathogen-specific engineered toxin.

More specifically in this work I engineered a lab strain of *E. coli,* MG1655 that detects the presence of a wildtype strain of *Pseudomonas Aeruginosa* (PAO1) and secretes bacteriocins that kill this pathogen with high specificity. Similar 'Sense and Destroy' designs against two additional pathogens, *Shigella* and *Vibrio cholera,* are also illustrated. I also genetically programmed mammalian cells, HEK293 FT, to detect PAO1 and express bacterial toxins in response. Furthermore, I created and evaluated designs and obtained preliminary results for an innovative adaptive two-phase 'Sense and Destroy' system that monitors the progression of a given treatment and executes secondary lines of attack upon failure of the first attempt to eradicate the pathogen.

II. Significance of PAO1

Pseudomonas aeruginosa (PAO1) is a common gram-negative bacterium, which is found in soil, water, skin flora, and most man-made environments and causes disease in animals, including humans [22]. Its ability to thrive in normal as well as hypoxic conditions has allowed it to successfully colonize many natural (i.e. lakes, soil, streams etc.) and artificial environments (i.e. drinking water supply systems) alike. It uses a wide range of organic material for food and can even grow in distilled water [23]. This bacterium is also found on medical equipment, including catheters, causing cross infections in hospitals and clinics. Its versatility enables the organism to infect damaged tissues and immune-compromised people. If PAO1 infects critical body organs,

such as the lungs, the urinary tract, and kidneys then the results are often fatal. PAO1 also colonizes the lungs of most individuals with Cystic Fibrosis.

P. aeruginosa is a widely researched organism due to its substantial medical importance, and its genome was sequenced very recently [24]. There is also scientific evidence of interspecies signaling in *Pseudomonas aeruginosa* [25-30]. It has been known for quite some time that PAO1 uses 3OC12HSL as a specific Quorum Sensing signaling molecule [31]. This molecule has been widely implicated in the pathogenicity of PAO1 and provides a good mechanism to detect the pathogen. These attributes make PAO1 an appropriate pathogen to target in order to demonstrate a proof of principle of 'Sense and Destroy' system.

III. Thesis outline and Summary of Contributions

The overall structure of my thesis is given in **Figure 2** and shows a flowchart of steps taken in the direction of achieving a proof of principle of the 'Sense and Destroy' system. PAO1 is the pathogen of choice for demonstrating the proof of concept. Experimental results proving complete bacterial 'Sense and Destroy' system against PAO1 are discussed in Chapter 2. In Chapter 3 I illustrate preliminary designs and experimental progress made towards achieving a mammalian 'Sense and Destroy' system against PAO1. Chapter 4 presents the schematics and experimental results of an adaptive 'Sense and Destroy' system. Finally the designs of the genetically programmable pathogen 'Sense and Destroy' against *Shigella flexneri* and *Vibrio cholerae* are discussed in Chapter 5.

a) Bacterial Sense and Destroy for PAO1

Figure 3 shows the schematic of bacterial the 'Sense and Destroy' system. As shown in the figure, bacterial sentinels are engineered for selective and sensitive pathogen detection using components of canonical quorum sensing (QS) pathways present in bacteria with elements from the Las system of PAO1. The sentinels are able to differentiate between gram-negative and gram-positive pathogen as well as non-pathogenic bacteria because they are programmed to express a toxin only in the presence of signals produced by gram-negative bacteria which in this case is PAO1.

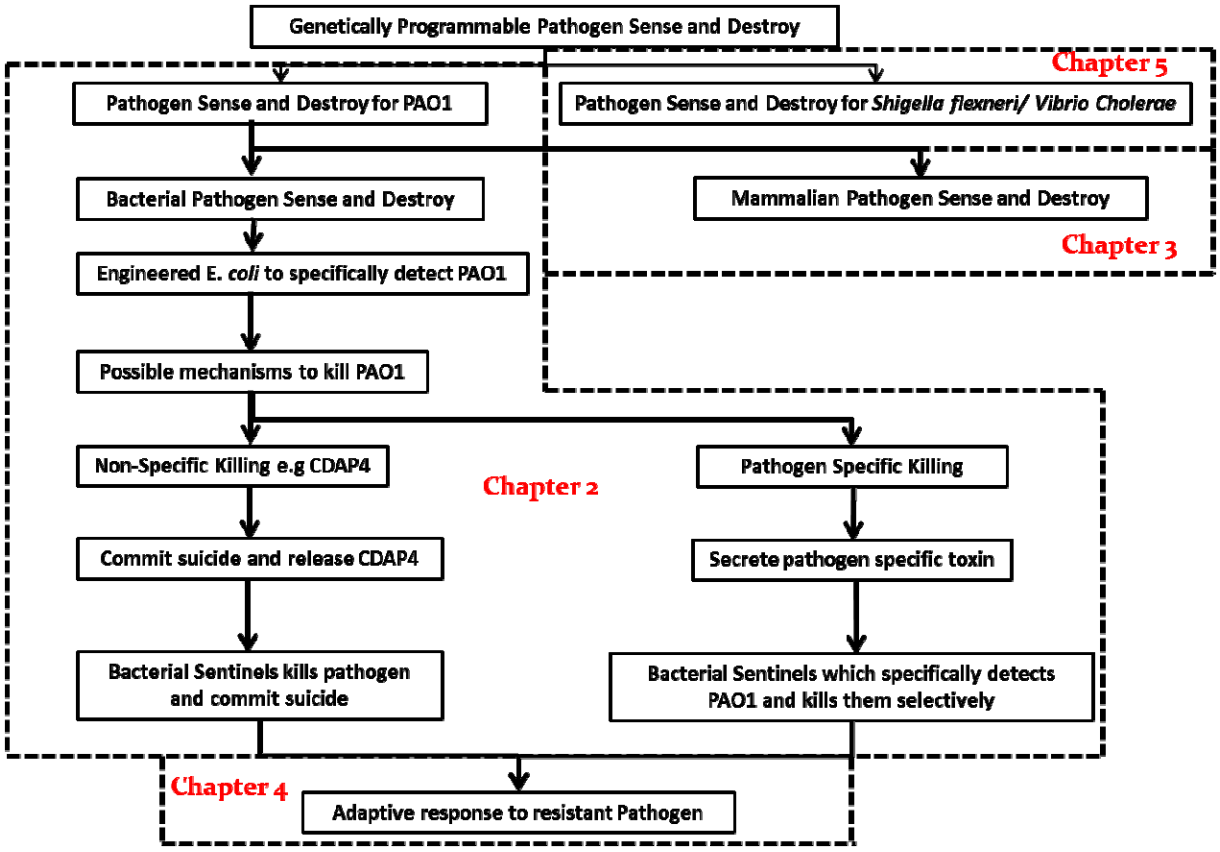

Figure 2: Organization of this thesis

Genetically programmable pathogen 'Sense and Destroy' system is divided into bacterial or mammalian 'Sense and destroy' based on the host of the system. Chapter 2 deals with experimental validation of the bacterial 'Sense and destroy' against PAO1. This chapter outlines three important modules of the system. First is the 'Detection' module which allows sentinels to detect PAO1 specifically. Second is the 'killing' module which employs strategies to specifically destroy PAO1 and the third is the 'Secretion' module which uses different strategies to release the toxin into the extracellular medium. Mammalian 'Sense and Destroy' against PAO1 is discussed in Chapter 3. In Chapter 4 I introduce possible mechanisms by which the sentinels can adapt to the resistant pathogen. The system against *Shigella flexneri/ Vibrio cholerae* is described in Chapter 5.

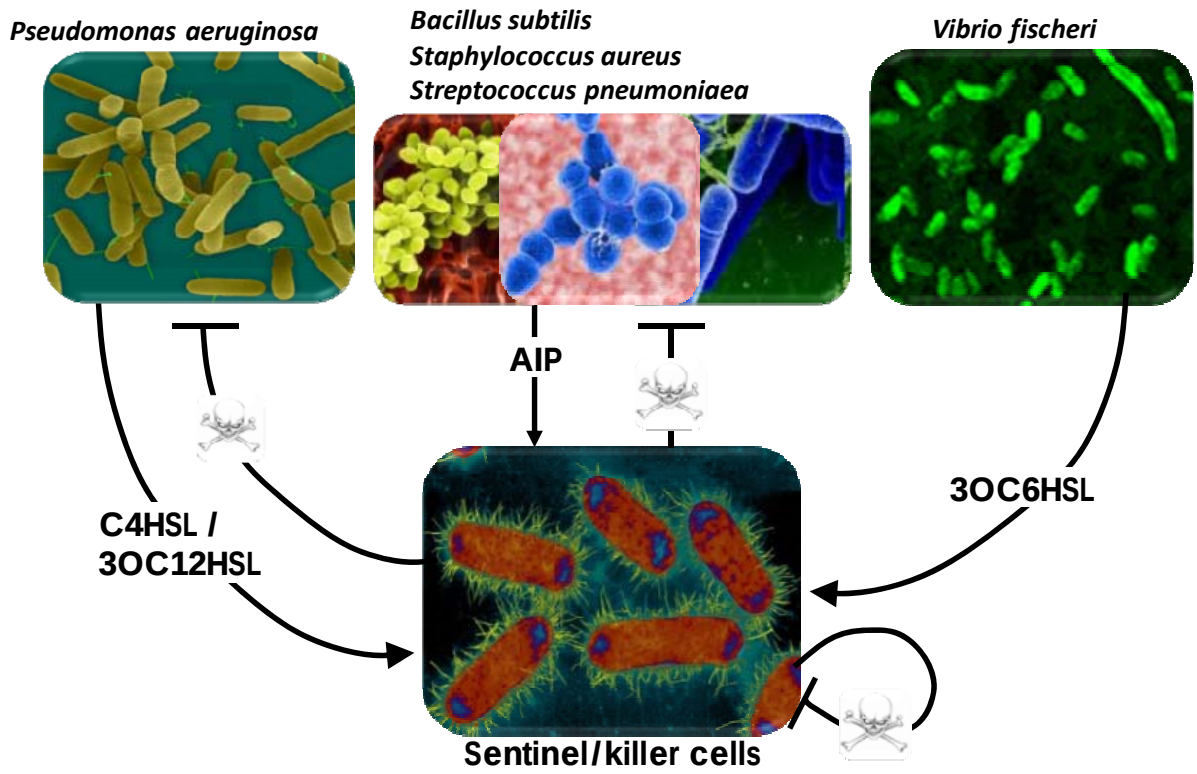

Figure 3: Schematic representation of the 'Sense and Destroy' system.
Sentinel/killer cells can be bacterial or mammalian cells depending on the system's context of deployment. As described in Figure 1 the sentinels will differentiate between pathogenic and non-pathogenic bacteria based on the signals produced by them. For example gram-negative pathogenic bacteria *Pseudomonas aeruginosa* produce two quorum sensing molecules namely C4HSL and 3OC12HSL whereas gram-positive pathogen, *Staphylococus aureus*, produces a different quorum sensing peptide namely autoinducing peptide (AIP). Similarly a non-pathogenic bacterium like *Vibrio fisheri* produces a different quorum sensing molecule called 3OC6HSL. Sentinels will be capable of specifically detecting different signals and respond by producing toxic proteins to specifically kill the invading pathogen. Sentinels will not respond to signals produced by non-pathogenic bacterium which in this case is 3OC6HSL.

For this purpose a novel toxin, CoPy, which is specifically toxic to PAO1, was created and characterized. The high specificity of CoPy is confirmed by incubating the protein with several different strains of bacteria and subsequently monitoring their growth. A new mechanism to secrete CoPy into the extracellular milieu of gram-negative bacteria is discussed and simultaneously employed to transport CoPy in response to PAO1. Efficiency of the secretion of CoPy was ascertained using western blots. Fully engineered *E. coli* sentinels were further co-cultured with PAO1 to establish the required killing ratio of sentinels versus PAO1. This ratio was further corroborated by optical microscopy.

b) Mammalian Sense and Destroy for PAO1

In Chapter 3 I leverage the design of bacterial 'Sense and Destroy' to move to a more challenging context. The overall design for mammalian 'Sense and Destroy' system will remain the same as the bacterial system as shown in **Figure 3** except that the sentinels will be engineered mammalian cells. I described the experimental progress made towards realizing a complete mammalian 'Sense and destroy' system. Mammalian cells were programmed to fluoresce in response to 3OC6HSL and 3OC12HSL. PAO1 specific toxin, CoPy was codon optimized and successfully expressed in the mammalian cells. Two secretion tags, *SecPen* and *SS*, were fused to CoPy and immunostained for expression. The killing and secretion efficiency remain to be tested. In the future, the individual components can be integrated into a functional mammalian 'Sense and Destroy' system and compared to its bacterial counterpart.

c) Bacterial and Mammalian Adaptive Response System

Antibiotic resistance is a growing concern and any antimicrobial strategy is incomplete without the provision for the sentinels to adapt to resistant pathogen. Hence in Chapter 4 I will introduce circuit designs for a bacterial and mammalian adaptive 'Sense and Destroy' system. This adaptive response strategy is executed in two phases. In the first phase, sentinels respond to an invading pathogen by launching a narrow spectrum attack. This phase is similar to the standalone 'Sense and Destroy' system discussed above. In the adaptive response strategy, the sentinels further monitor the efficacy of the first phase attack by continuously detecting the signals produced by the pathogen. If the signal is higher than a pre-determined threshold even after a certain amount of time then it is an indication of a resistant pathogen or failure of the first phase attack. In response, the sentinels will trigger the second phase in which the engineered sentinels produce a broad spectrum toxin and lyse themselves to deliver large quantities of the the broad

spectrum toxin into the medium. Both of these toxins together will guarantee the complete elimination of the pathogen.

I tested a broad spectrum toxin, CDAP-4 and characterized its dosage response against PAO1. Initial delay circuits were constructed and characterized for adaptive mammalian 'Sense and Destroy' system. Finally the adaptive response of mammalian sentinels was modeled and simulated to understand the dynamics of such a technique. In the future, it will be crucial to understand and choose optimal parameters, which are necessary for stable and predictable system performance.

d) Sense and destroy against *Shigella* and *Vibrio cholerae*

In Chapter 5 I present new designs of bacterial 'Sense and Destroy' system against two highly pathogenic strains of bacteria namely *Shigella* and *Vibrio cholerae*. Every year infections due to *Shigella* and *Vibrio cholera* kill millions of people in the developing countries. Implementation of 'Sense and destroy' against these pathogens can potentially offer alternate prevention therapy and significantly reduce the mortality in the future.

IV. Background and Related Work

In this section I will discuss relevant background information used to design and engineer different modules of bacterial and mammalian 'Sense and Destroy' system.

a) Antibiotic Resistance mechanisms

Antibiotic overuse and misuse due to incorrect diagnosis is one of the major causes of growing antibiotic resistance [32]. Overuse in animal farming also creates drug resistant bacteria which then eventually get transmitted to humans. Bacteria may be innately resistant or acquire resistance to antimicrobial agents [33-35]. Acquired resistance can be either genetic or phenotypic. Genetic resistance arises from: (i) mutations in genes (chromosomal mutation), (ii) gene transfer from one microorganism to another by plasmids (conjugation or transformation), transposons (conjugation), integrons and bacteriophages (transduction). Phenotypic resistance arises due to changes in the bacterial physiological state, such as the stationary or log growth phase or the dormant state. Antibiotics kill bacteria by inhibiting important cell or metabolic processes. Based on these processes antibiotics are divided into five major classes:

i) **Cell Wall Inhibitors-** Antibacterial drugs such as beta-lactams (e.g. Penicillin) and glycopeptides (e.g. Vancomycin) inhibit bacterial cell wall synthesis by interfering with the enzymes required for synthesis of the peptidoglycan layer. Vancomycin binds to the terminal D-alanine residues of the nascent peptidoglycan chain and prevents cross-linking.

ii) **Inhibitors of nucleic acid synthesis-** Drugs such as Fluoroquinolones inhibit DNA synthesis causing double-strand DNA breaks during DNA replication whereas sulfonamides and trimethoprim (TMP) block the pathway for folic acid synthesis, which ultimately inhibits DNA synthesis.

iii) **Protein synthesis inhibitors-** Some drugs take advantage of the fact that bacterial ribosomes differ from their eukaryotic counterparts in structure and selectively inhibit bacterial growth by inhibiting protein synthesis. Macrolides, aminoglycosides, and tetracyclines bind to the 30S subunit of the ribosome, whereas chloramphenicol binds to the 50S subunit.

iv) **Anti-metabolites**- These are drugs which inhibit other naturally occurring metabolites that participate in normal metabolism. For example antifolates interfere with the use of folic acid.

v) **Damage the cell membrane-** Antibacterial drugs such as Polymyxin B causes bacterial cell contents to leak by increasing cell permeability. Cyclic lipopeptide Daptomycin causes membrane depolarization and eventual death.

Bacteria can acquire genetic resistance against antibacterial agents in each class by accumulating chromosomal mutations or by transferring resistance genes [36, 37]. Spontaneous mutations may cause resistance by (1) altering drug permeability or uptake (e.g. change in Neisseria gonorrhoea porin protein causes resistance to Penicillin and Tetracycline), (2) upregulating pumps that increase the drug efflux from the cell (e.g. efflux of fluoroquinolones in *S aureus* or Tetracycline binds to mutated repressor and activates transcription and translation of an efflux pump), (3) enzymatic inactivation (e.g. beta-lactamases can cleave beta-lactam antibiotics and cause resistance or erythromycin ribosomal methylase in *staphylococci*), (4) alteration of the drug target (e.g. a -15C to T promoter mutation causes over-expression of the drug target InhA, and lead to a low-level isoniazid (INH) resistance in *M. tuberculosis* or Vancomycin resistance is caused by the change of D-Ala-D-Ala to D-Ala-D-lactate), (5) loss of enzymes required for the activation of pro-drugs (e.g. nitroreducatse is needed to transform Metronidazole into reactive species that damage the DNA and kill the cell. Mutations in this enzyme cause resistance to Metronidazole).

Genetic resistance is also caused by the transfer of resistance genes through mobile genetic elements [34, 37, 38]. For example Streptomycin resistant genes such as strA and strB are carried on a plasmid. This mechanism is called horizontal evolution and may occur between strains of the same species or between different bacterial species through conjugation, transduction, and transformation. During conjugation the resistance genes are transferred from one bacterium to another through an elongated pilus whereas during transduction the resistance genes on plasmids are transferred through bacteriophages. Some bacteria release their DNA into the growth environment during cell lysis. This DNA can be taken up by live cells by transformation and can be incorporated into their genome. For example qnr gene encodes pentapeptide which is a DNA mimic. Bacterial cells that express this pentapetide are quinolone resistant because this DNA mimic binds to DNA gyrase preventing the quinolone binding it. Bacteria can also acquire antibiotic resistance by changing their physiological state. Susceptible bacteria become unsusceptible because they stop growing. This type of phenotypic resistance poses significant problems in biofilm infections and TB chemotherapy. For example planktonic *P. aeruginosa* is susceptible to 1 ug/ml imipenem but require at least 1024 ug/ml when in the biofilm form [37, 39, 40].

No one antibacterial strategy is sufficient to prevent the increase in antibacterial resistance. Besides the development of new antibacterial compounds other disease and drug management strategies are critical. For example better disease surveillance, education of health care professionals and improved hygiene are also important. Recently, combinations of more than one bioactive compound have shown improved efficacy especially against microorganisms that are known to develop resistance relatively quickly, such as *Pseudomonas aeruginosa* [38]. This is due to the fact that the chance of mutants resistant to two antimicrobials is a product of mutation frequencies, provided that resistance mechanisms are independent. Measures to promote prudent use of antibiotics and compliance with inflectional control measures can be equally effective in reducing resistance, preserving the efficacy of anti-pseudomonal agents until the development of new options against multidrug-resistant *P. aeruginosa* strains.

b) Signal Detection

Bacterial cells sense population density through the phenomenon of Quorum Sensing (QS) which also provides bacteria a means to regulate many other processes, including: virulence factor secretion and biofilm formation [41, 42]. QS consists of synthesis, secretion and detection of

strain specific chemical signaling molecules referred to as autoinducers [43]. Autoinducer concentration increases with the population density and at a certain threshold concentration triggers population-wide alteration of gene expression. There are three general QS mechanisms: gram-negative, gram-positive, and a hybrid between the two first discovered in *Vibrio harveyi* [43-45]. In the classical gram-negative Quorum Sensing system, an I-protein synthase produces acylated homoserine lactone (AHL) autoinducers, which diffuse freely between the cytoplasm and the environment, then directly interact with R-protein transcriptional regulators to control the expression of target genes [43-45].

P. aeruginosa harbors two QS systems. The first one is the Las system which uses 3OC12HSL as a signal and the second one is the Rhl system which uses C4HSL as a signal [26, 30]. QS elements LasI/R and RhlI/R from the pathogen can be cloned in *E. coli* to produce GFP in response to natural 3OC12HSL produced by *P. aeruginosa*. Similar to bacterial sensors, mammalian 3OC6HSL sensors were designed and fabricated before as part of initial efforts to build a synthetic mammalian cell to cell communication system [8, 46]. These designs were constructed with a LuxR based signal transducer expressed constitutively through $Hef1_{alpha}$ (Human Elongation Factor 1a) promoter. The 3OC6HSL signal transducer LuxRm is a chimeric LuxR-activator protein created by fusion of mammalian activation domains to native bacterial LuxR. It was found that the most effective design resulted from fusing a p65 activation domain from the mammalian ReLa protein to the N-terminus of a mammalian codon-optimized LuxRm which is a hypersensitive LuxR mutant. These two domains are separated by a helical linker to preserve their individual functionality. An NLS was appended to the C terminus for proper nuclear targeting. Since bacterial promoters don't work in mammalian cells, synthetic lux promoters were constructed by fusing different number of lux operators to a minimal CMV promoter. Out of several different variants, a promoter with seven lux boxes worked the best and is thus called pLuxO7. A variety of lux signal transducers were also designed and tested [47-49]. In the presence of 3OC6HSL, LuxRm binds and activates transcription from the mammalian lux promoter pLuxO7. Microscope images and FACS data demonstrated that the optimized design resulted in highly functional mammalian 3OC6HSL receivers upon induction with 0.1mM 3OC6HSL

c) Engineering Artificial Signaling Pathways

Synthetic gene networks, analogous to electronic circuits such as an oscillator [50-53] or a toggle switch [54] can precisely control gene activity in living cells. The biochemical computation performed by these biological circuits thus serves to extend or modify the behavior of the cells. Concentrations of specific DNA binding proteins and inducer molecules represent logic signals. Logic gates perform computation using inducers that interact with transcriptional regulatory proteins and promoters that control expression of the proteins [55, 56]. Naturally occurring components have widely varying kinetic characteristics and arbitrarily composing them into circuits is unlikely to work. Thus it is imperative to match the logic gates such that their coupling produces correct behavior. One way to address this issue is to modify the encoding genetic elements based on the mathematical modeling using directed evolution until the desired behavior is achieved [57-60]. Similar techniques can be used to design and optimize signal detection and pathogen destruction pathways that work correctly and reliably.

A circuit illustrated in [61] uses engineered cell-cell communication to obtain ring-like fluorescence structures (based on LuxR/I QS elements from *V. fischeri*). Pattern formation was achieved through interactions between two engineered strains: sender and band-detect receiver cells. Based on computational models, various genetic elements were mutated in order to achieve multiple rings that have different response thresholds, i.e. they produce rings with different widths and at different distances from the center. Liquid and solid phase behaviors of circuit mutants were quantified. These cells express GFP only when exposed to pre-specified concentration ranges of AHL. Similarly the sentinels can be engineered to pinpoint the location of AHL emitting pathogen.

d) Signal Amplification

Sometimes the transcriptional responses to a synthetic circuit are weak or undetectable by conventional means. This problem can be resolved by integrating a signal amplifier into the circuit. The literature [62, 63] and previous experimental experience [59, 61] suggests that cI is a very efficient transcriptional repressor. Even small increases in cI levels, normally undetectable in fluorescence observations, produce large changes in $\lambda_{P(R)}$ activity, and therefore yield easily observable changes in final signal output. It is important to note that the performance of signal amplification depends heavily on matching the kinetics of QS promoter activation and repression of $\lambda_{P(R)}$ by cI. To gain a better understanding of this issue, a mathematical model of the signal

amplification gene network was developed [64]. It shows that the system response can be modulated by changing the binding efficiency of cI/O_{R1}. This amplifier circuit can be useful to increase the sensitivity of the sentinels to the invading pathogen.

The circuit design of a transcriptional cascade that amplifies weak 3OC6HSL signals in mammalian cells is described in [8]. Similar to cI, rtTA (Reverse Tetracycline Trans-activator) is a strong activator of transcription and requires only the presence of a few molecules of itself and DOX (Doxycycline) to maximally activate the TRE (Tet Response Element) promoter. Hence through this design even trace amount of 3OC6HSL leads to changes in rtTA which in turn translates into amplified EGFP response. It is shown that the mammalian sensors with the amplifier circuit were able to respond to an order of magnitude smaller concentration of 3OC6HSL than the sensors without the amplifier circuit.

e) Secretion of Proteins

Effective secretion of functional proteins is a complex but crucial module for the success of 'Sense and Destroy' system because the killing dynamics of PAO1 will depend on the amount of functionally active toxin secreted into the medium by the sentinels. An ideal secretion system must fulfill at least two criteria. First, it should be able to secrete proteins into the extracellular space in one step as the non-secreted residual toxin in the periplasm can compromise the permeability barrier of the outer membrane [65]. Second, the secretion system should secrete fully or at least partially folded proteins or else the secreted protein would be rendered inactive. Gram negative bacteria have seven known distinct secretion pathways, classified as Type I–VII, that enable transfer of proteins across the inner and outer membranes [65-72]. The complex Type IV system is only superficially characterized in *E. coli* and has not been employed for secretion or display of recombinant proteins thus far [65]. Type VI [73, 74] and Type VII (only identified in *Mycobacterium* spp.; [75]) secretion systems have only been recently identified and the details about the secretion mechanism are still emerging. Type II and V are two-step secretion mechanisms. Type-I, Sec, ABC and type III secretion systems secrete unfolded proteins [76]. Type III and IV secretion systems are mostly used by pathogenic bacteria to transport proteins from the bacterial cytoplasm to eukaryotic cytoplasm. Bacterial flagellar system is similar to type III system except that it is used by the bacteria as a one-step mechanism to secrete partially folded flagellar components into the extracellular environment and to assemble flagella. Hence a flagellar system

was used to transport toxins and is discussed in Chapter 2. Salient features of all type I-VI secretion systems prevalent in *E. coli* are discussed below.

(i) Type I Secretion System (T1SS)

This type of secretion mechanism is used by *E. coli* to secrete alphahemolysin (HlyA) into the extracellular medium. Secretion occurs in a Sec-independent manner and is a continuous process across both the inner and outer membranes. This system consist of three proteins: an outer membrane protein which forms pores, a membrane fusion protein, and an inner membrane ATP-binding cassette (ABC) protein. These proteins are represented in *E. coli* by TolC, HlyD and HlyB, respectively. Secretion signal specific to this system is located within the C-terminal end of the secreted protein. When this signal interacts with the dedicated ABC transporter, interaction of the membrane fusion protein (HlyD) and outer membrane protein (TolC) is triggered that allows secretion of HlyA into the external milieu. An important characteristic of this mechanism is that it is a one step process and proteins secreted by this mechanism are not processed during secretion and do not form distinct periplasmic intermediates.

(ii) Type II Secretion System (T2SS)

This is a complex two step secretion process where the protein is first translocated into the periplasmic space by either Sec or Tat system and subsequently exported across the outer membrane by a dedicated secretion apparatus consisting of complexes of 12 to 16 proteins spanning the periplasm and connecting the inner and outer membrane. The protein in the periplasm will be either unfolded or fully folded depending on whether Sec or Tat is used for the first stage of the transport. Once in the periplasm, the signal sequence is cleaved off by a periplasmic peptidase [77].

(iii) Type III Secretion System (T3SS)

Similar to the type I secretion system, this system translocates its effector molecules across both the inner and outer membranes in a Sec-independent manner in one step. It has been shown that the region encoding the first 20 amino acids (either the untranslated mRNA or the first 20 amino acids of the polypeptide) is essential for secretion and the process is highly regulated. After the protein is targeted to the cytoplasmic side of this secretion system it is secreted through a needle-like structure into the extracellular medium without forming periplasmic intermediates. The needle-like structure is composed of approximately 20 different proteins.

An important characteristic of T3SS is that it is used by pathogenic bacteria to target effector proteins directly into the eukaryotic cells. In some cases the phenomenon is triggered when the bacterium comes in contact with a eukaryotic cell. Nonetheless, not all T3SS are contact dependent. Some effector molecules are released into the extracellular medium. The factors on which this decision is based is an active area of research. Some factors include contact with the surface of the target cells, shift in temperature to 37C, change in extracellular pH or iron concentration and depletion of calcium ions. Initially it was thought that the secretion signal is present in the amino terminal sequence in the protein but this hypothesis was proved wrong when it was shown that relatively radical changes in the amino acid sequence did not affect secretion. This led to the belief that the secretion signal is conformational rather than sequence based [78]. Initially it was argued that the signal was embodied within the 5' region of the mRNA coding for the substrate and that secretion was coupled to translation [79]. More recent research has indicated the presence of a chaperon binding domain located within the first 100 amino acids of the effector protein [80]. This domain is present downstream from a short and uncleaved amino terminal export signal. Whether or not T3SSs contain a conserved signal sequence has long been debated and research has predominantly focused on Yop effectors of *Yersinia spp*. In many cases, close homologs of effector proteins of one species are not secreted in others. This has even led some to argue that the T3SS acts randomly, secreting proteins based on their abundance and proximity to the secretion apparatus.

(iv) Type IV Secretion System (T4SS)

Similar to TTSS this secretion system is one-step [81, 82]. This system is broadly divided into three functional types. The first type is used to transfer DNA from one cell to the other in a cell-cell contact-dependent manner. This event is called conjugation and is utilized by the bacteria for horizontal gene transfer. It represents a major mechanism used by pathogenic bacteria to spread antibiotic resistance genes. A well-studied model is the DNA transfer system in *Agrobacterium tumefaciens*. Another type IV secretion system mediates DNA uptake (transformation) and release from the extracellular space. The two so far characterized systems are the *Helicobacter pylori* ComB system, which take up DNA from the extracellular milieu, and the *Neisseria gonorrhoeae* gonococcal genetic island (GGI) which secretes DNA to the extracellular milieu. A third type of T4SS is used to transport a wide variety of virulence proteins into the host cell. Only limited information is available regarding protein secretion by the T4SS.

Direct contact is essential for T4SS mediated transfer but little is known about these interactions. In all subfamilies of T4SS the substrates for secretion are recruited by coupling proteins. These proteins selectively interact with the translocation signals of the appropriate substrate molecules. For example a simple cluster of positively charged residues at the C-terminus has shown to act as a functional translocation signal in the case of *A. tumefaciens* VirB/VirD4 and the *L. pneumophila* Dot/Icm T4SS. But other known *Bartonella* effector proteins (BepA–BepG) that are translocated through VirB/VirD4 have more complex bipartite signals. The CagA effector of *H. pylori* carries a 20 amino acid C-terminal signal adjacent to a larger interaction domain for its secretion chaperone CagF.

(v) Type V Secretion System (T5SS)

This is a two-step secretion system similar to T2SS [81]. There are three known subfamilies of this system: (i) the autotransporter (AT) system, (ii) the two-partner secretion pathway and (iii) the type Vc system. Not only are the proteins secreted through this pathway structurally similar, but they also have shown similarity in their biogenesis. They use an amino terminal secretion signal for inner-membrane export of the secreted protein through Sec pathway. This signal sequence is cleaved in the periplasm. Further, the carboxy-terminal region inserts itself into the outer membrane to form a beta-barrel pore. This pore then uses a linker domain to translocate the passenger protein to the bacterial surface or the extracellular space where it may or may not undergo further processing.

(vi) Type VI Secretion System (T6SS)

This recently discovered system is mostly found in pathogenic bacteria [73, 74, 83-85]. Similar to TTSS this export mechanism is linked to virulence during host infection. Recent studies have showed that T6SS of *Pseudomonas, Burkholderia* and *Vibrio* species is used to export virulent toxic proteins in both the bacterial and eukaryotic target cells in a cell–cell contact-dependent process. It is unclear whether transport is a one-step or a two-step process. Most of the identified T6SS substrates lack an established hydrophobic (Sec) or arginine-rich (Tat) N-terminal signal sequence. Very little is known about the mechanisms involved in the transport of toxic proteins through this system [86]. The latest model proposes that the first step in the secretion process is the formation of a base-plate complex that initiates Hcp (haemolysin co-regulated protein) tube polymerization which forms rings. gp25 (a major component of the T4 phage tail baseplate), VgrG (valine–glycine repeats) and other T6SS proteins constitute the base-plate complex which spans the inner membrane, peptidoglycan and outer membrane. Subsequently VipA/ VipB heterodimers

polymerize to form a sheath around the Hcp tube. It has been proposed that an unknown extracellular signal triggers a conformational change in the base-plate complex. This change results in sheath contraction which in turn leads to translocation of the VgrG/Hcp tube complex into the adjacent target cell membrane. Additional effector proteins can also translocate using the Hcp tube as a conduit. After this ClpV ATPase detaches and disassembles the contracted sheath. Disassembled VipA/B dimers are recycled to form a new extended T6SS apparatus. Hcp and VgrG proteins are released into the extracellular space as secreted proteins in the absence of target cell penetration.

In mammalian cells the Endoplasmic Reticulum/Golgi mediated secretion pathway can be used to secrete proteins by attaching an N-terminal sequence of about 30 amino acids that targets the protein to the ER [48, 87]. This technique can be used to secrete cytoplasmic proteins and is applicable to secrete even heterologous proteins from diverse organisms. Researchers showed that α-amylase, an enzyme native to the *Bacillus stearothermophilus* that degrades starch, can be secreted from mammalian cells by fusing a signal peptide 90 (METDTLLLWVLLLWVPGSTGD) derived from the murine Ig k-chain V-J2-C region [48, 88]. Some of the commonly used secretion signals described in [8] are (i) *ILCO1,* which is an alteration of the interleukin-2 (IL-2) N-terminal signal peptide (ii) *SS,* which is the secretion signal originally derived from a piscine vitellogenin (Vtg) gene of *Oreochromis aureus* [88-90] (iii) *Sec,* which is a recently identified secretion signal that is a part of the C-terminal of the Engrailed-2 homeodomain protein present in Drosophila melanogaster. SEAP (Secreted Alkaline Phosphate) is naturally secreted from mammalian cells. Endogenous secretion signal from SEAP was removed and a library of plasmids incorporating the three secretion signals mentioned above was built to test their relative efficiencies. These plasmids were transfected in HEK 293FT cells and assayed using the 'Great Escape chemiluminescence kit' (Clontech). This characterization data can be used to select the best possible secretion tag for the mammalian 'Sense and Destroy' system and can further act as a foundation to build a bigger library of secretion tags.

f) Synthetic Cascades for Delayed Expression of Genes

It was discussed in Section III (c) that as part of the adaptive response circuit the sentinels monitor the signal produced by the pathogen for a '*certain amount of time'* before they decide whether or not to launch the second phase attack. This delay, during which the sentinels analyze the efficacy of the first phase attack, can be generated by integrating synthetic cascades into the

circuit. One, two, and three stage cascades and the delay introduced by them have been characterized [58, 59]. Steady state analysis of these cascades demonstrated that the response to input dosages becomes more digital as the cascade depth increases and correlated well with stochastic models. The experimental and modeling results suggested that these cascades can be used as independent modules and it is feasible to construct large, robust circuits out of these components. Temporal analysis of transcriptional cascades revealed that two and three stage cascades exhibit delayed responses relative to a one stage cascade. In the one stage cascade when aTc is added, it induces EYFP transcription from pLtet-O1, resulting in a rapid increase in fluorescence that stabilizes after 120 min. For the two-stage cascade, aTc induction results in the decay of EYFP that reaches the final low level after 400 min. The fluorescence of a three-stage cascade begins to increase 140 min after aTc induction, reaches half maximal expression after 300 minutes, and stabilizes after 600 min. An important factor that affects the dynamics of these circuits is the protein decay rate, which for all proteins used in this study (TetR, LacI, CI, and EYFP) is roughly equal to the cell division rate because these proteins are highly stable. Another important feature of these transcriptional cascades is ultrasensitivity. In the context of pathogen 'Sense and Destroy' system, such a cascade can detect very low levels of an input and respond in a highly amplified fashion. The cascade genetic circuit can be directly integrated into the bacterial 'Sense and Destroy' system or can be modified with mammalian genes to become part of the adaptive mammalian 'Sense and Destroy' system.

CHAPTER 2 -GENETICALLY PROGRAMMABLE BACTERIAL SENSE AND DESTROY

I. Introduction

The experimental progress made towards a bacterial 'Sense and Destroy' system against PAO1 is described in this chapter. **Figure 4** gives a detailed architecture of the bacterial 'Sense and Destroy' system against PAO1. The system is divided into three separate modules. The first module is the 'Detection' module that enables the bacterial sentinels to differentiate between pathogenic and non-pathogenic microbes by detecting specific QS signaling molecules produced by these bacteria. If required, the sentinels can use signal amplification capability to magnify any hard to detect signals. The second module is the 'Kill' module that let the sentinels produce an engineered pathogen specific toxin. The third module is the 'Secrete' module that allows the sentinels to secrete/release the toxin either by using a secretion tag or by self-lysis. The first three sections in this chapter discuss the three separate modules of the system: PAO1 Detection, PAO1 Kill and Secretion of PAO1 specific toxins. The fourth section reviews the experiments and characterization data obtained after co-culturing the sentinels and PAO1.

II. Bacterial Sensors of PAO1

It has been shown that *P. aeruginosa* has a 50% lethal dose of $3*10^7$ CFU in adult mouse [22, 31, 91, 92] acute pneumonia model. High Cell Density (HCD) is necessary for *P. aeruginosa* to form biofilms and cause clinical manifestations in Cystic Fibrosis (CF) patients. These patients have $>10^9$ bacteria/ml of sputum in their lungs. Further, it was also demonstrated that the absence of a complete las and or rhl quorum-sensing system significantly attenuated the ability of *P. aeruginosa* to colonize the host, induce inflammation, disseminate, and cause mortality in an adult mouse acute-pneumonia model. Mean concentrations of 3OC12HSL, which is the quorum sensing signal produced by PAO1, found in the biofilm samples is of the order of 2-3 uM [93]. This concentration of 3OC12HSL is shown to initiate inflammatory response [94].

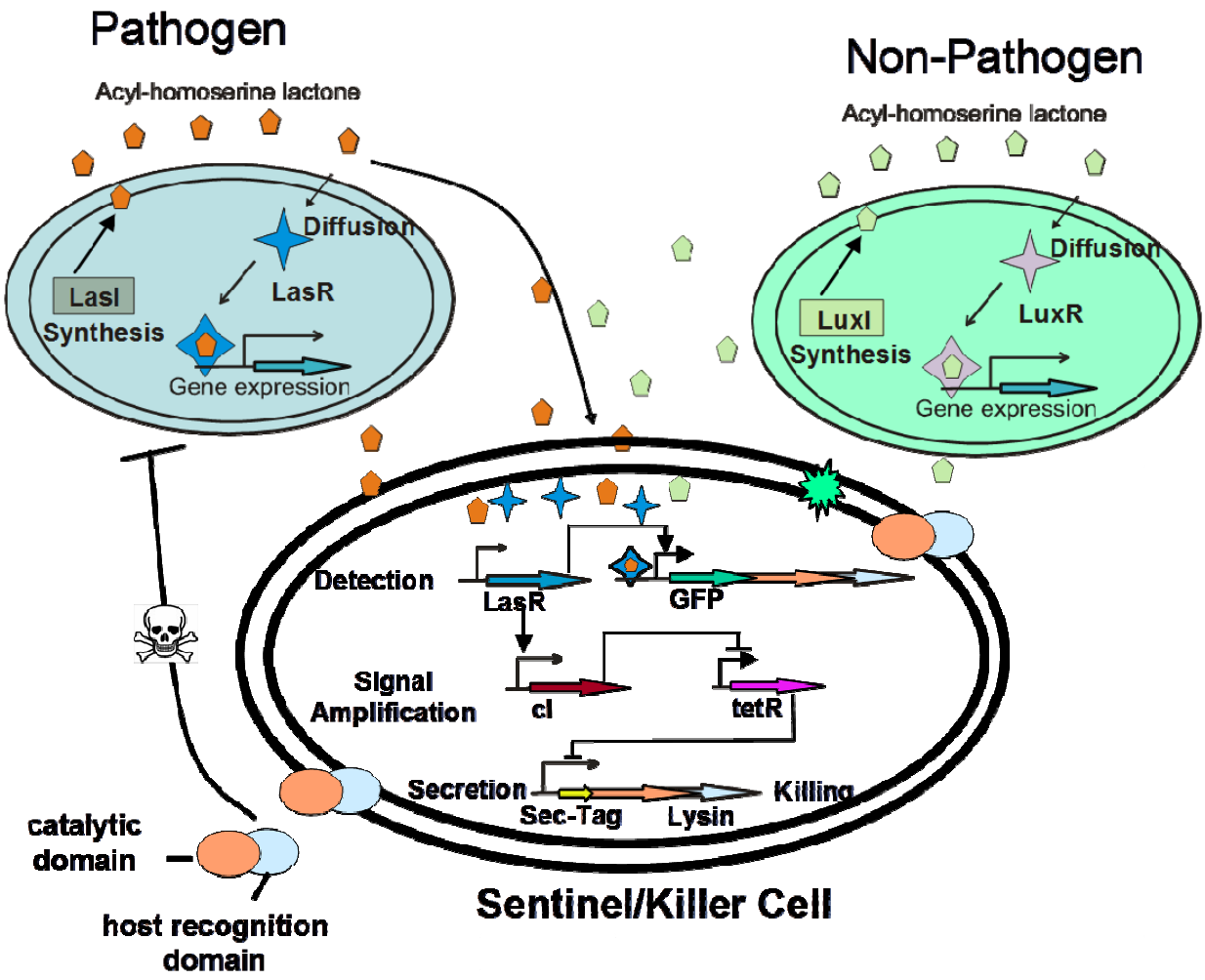

Figure 4: Architecture of the bacterial 'Sense and Destroy' system.
This system is divided into three modules. The first module is the 'Detection' module wherein a diffusible AHL autoinducer (produced by gram-negative cells with an I/R system for e.g. *V. fischeri or P. aeruginosa*) is detected with a LasR-protein activated pathway in the sentinels. Detection of a specific AHL results in the production of a color-coded output. The signal amplification module is an optional module, which can be used to amplify weak signals from the pathogen. Another module is the 'kill' module. Once the presence of pathogen is verified, this module will synthesize pathogen specific toxin. The last module is the 'Secretion' module which uses a secretion tag to transport the toxin into the environment and kill the pathogen specifically.

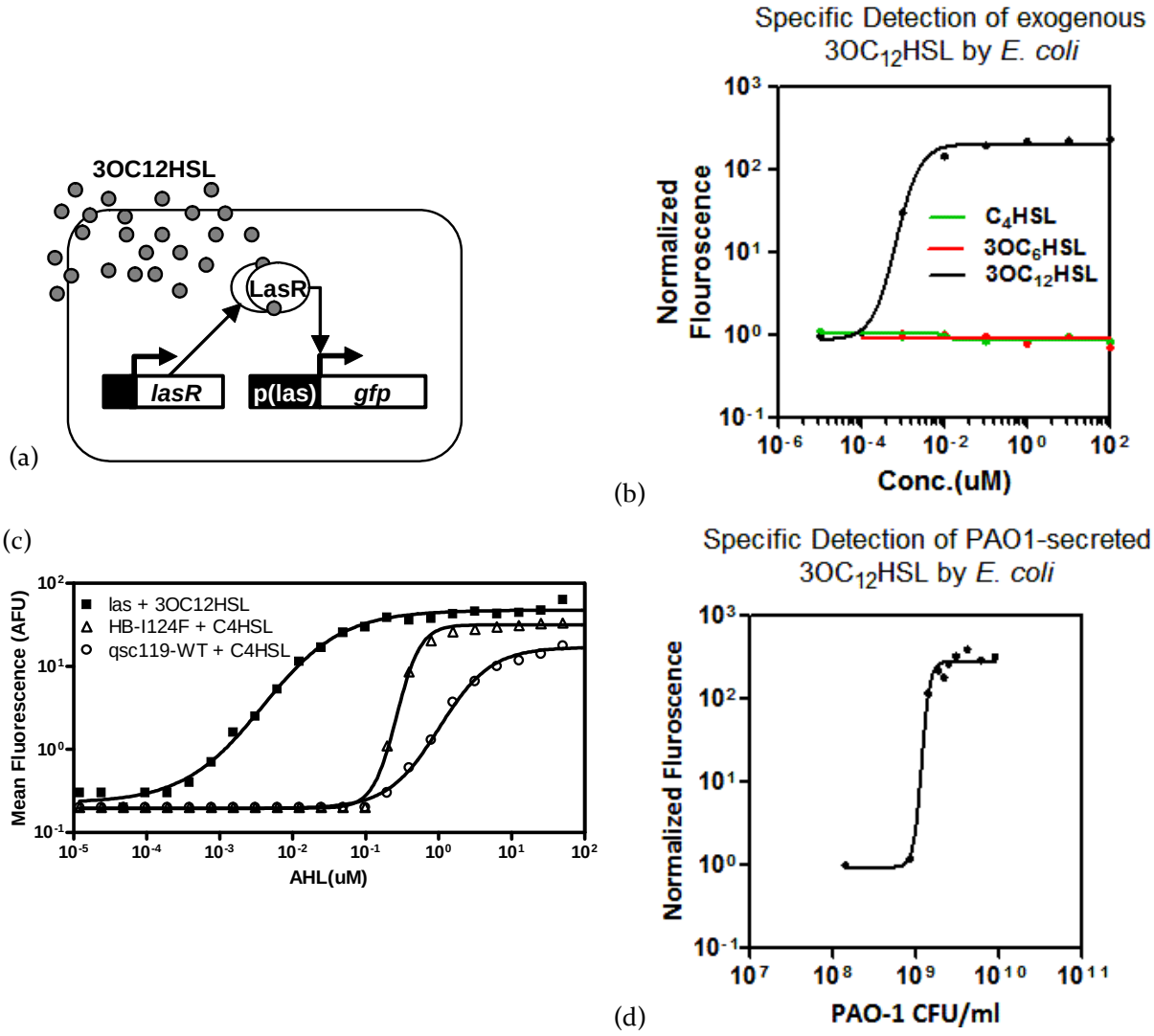

Figure 5: *P. aeruginosa* signal detection.
(a) Genetic circuit for Las sentinel. (b) 3OC12HSL response curves for Las sentinel. Las promoter is activated only by 3OC12HSL but not by 3OC6HSL and C4HSL. (c) Dosage response curves for Las sentinel and two Rhl sentinel variants (one with wildtype qsc119 and RhlR and the other with HB-I124F). This figure is adapted from [64]. (d) Fluorescence of sentinels grown in PAO1 supernatant.

In levels higher than 5 uM, 3OC12HSL stimulates production of mRNAs for multiple inflammatory chemokines, neutrophils and cytokines *in vivo.* It is the exuberant induction of the chemokine IL-8 and the subsequent infiltration of neutrophils that cause tissue destruction during chronic *P. Aeruginosa* infections in CF patients [91, 92, 94].

Based on these findings, synthetic gene networks were constructed in *E. coli* that produce GFP in response to 3OC12HSL and shown in **Figure 5 (a)**. Sentinels were grown to an O.D. of 0.5 and then induced and incubated with different concentrations of exogenous 3OC12HSL for 3 hours. The resulting fluorescence was measured using flow cytometry and the dosage response curve is shown in **Figure 5 (b).** *P. aeruginosa* harbors another QS system, the Rhl system which uses C4HSL as a signal, but may be inferior to the las system for the purpose of sensing PAO1 [26, 30]. To select between these two potential detection options, several genetic circuits were constructed. These constructs were used to compare the Las response to 3OC12HSL versus the responses to C4HSL of two different optimized variants of the Rhl pathway (**Figure 5 (c)**). As shown, the Las response is more sensitive than that of the Rhl response. Furthermore, the Las system is more suitable for earlier detection because it is implicated in initial *P. aeruginosa* QS activity. Therefore, subsequent efforts focused on the implementation of Las system (3OC12HSL sensitive) for a bacterial sensor.

In order to understand whether the sentinels respond specifically to PAO1, these sentinels were induced and incubated with two other inducers: 3OC6HSL, which is produced by *Vibrio fisheri*, and C4HSL, which is produced by PAO1 albeit at a later stage of forming biofilms. As evident from **Figure 5 (b),** sentinels do not respond to 3OC6HSl and C4HSL and respond specifically to 3OC12HSL. It is evident that the engineered sentinels can detect and exhibit full response to the clinically relevant concentration of 1 uM 3OC12HSL. The sentinels were further tested for their response to AHL directly produced by PAO-1. *P. aeruginosa* was grown to different O.D. and supernatant was subsequently collected and filter sterilized. The supernatant contains the signals produced by the pathogen for quorum sensing but the cells are filter sterilized. After this, 0.5 O.D. of the sentinels were incubated in the supernatant for two hours and their fluorescence was measured. The graph in **Figure 5 (d)** explains the relationship between pathogen density and 3OC12HSL levels.

Figure 5 demonstrates that the sentinels already operate within clinically relevant densities of PAO-1. In the future, the response sensitivity of the las system can be further improved by integrating a signal amplifier. Amplifier cascade for 3OC12HSL will be similar to the

one previously implemented for C4HSL [60]. The circuit of C4HSL signal amplifier is discussed in Chapter 1. As shown in **Figure 4** this circuit will amplify the response by fusing cI downstream of the las promoter and having $\lambda_{P(R)}$ regulates tetR expression. TetR will further control the expression of pathogen specific toxin. In the absence of PAO1 there will be no cI and hence tetR will shut down the toxin production. In the presence of very little 3OC12HSL, few molecules of cI are produced, enough to completely repress $\lambda_{P(R)}$ and relieve TetR repression of the toxin. Hence the toxin is expressed even in the presence of minute quantities of 3OC12HSL. The pathogen detection circuit can be fine tuned by measuring the performance of several different $\lambda_{P(R)}$ mutants by titrating with exogenous 3OC12HSL until highly sensitive detection capabilities are achieved. The limits of *P. aeruginosa* detection can be characterized by co-culturing the pathogen with sentinels harboring the best signal amplifier. This analysis can be carried out using a microplate reader with dual wells that have a permeable 0.22μm membrane between them [60, 64]. Wildtype *P. aeruginosa* will be grown in one well, while signal amplifying *E. coli* sentinels will be grown in the adjoining well. 3OC12HSL will diffuse freely through the connecting permeable membrane. This microplate reader setup will help to determine the minimal *P. aeruginosa* culture density required for the detection by signal amplifying *E. coli* sentinels.

III. Engineered Pathogen Specific Toxins

In the previous section I engineered the 'Detection' module which allows sentinels to successfully detect the pathogen. In this section I discuss the 'Killing' module. For this functionality, engineered bacteriocins were used to specifically kill the pathogen, PAO1. Bacteriocins are toxic proteins produced by several strains of bacteria and are active on related species but not on the producing cells [95-98]. Bacteriocins are highly specific and potent toxins produced during stressful culture conditions and result in rapid elimination of neighboring cells that are not immune to their effect. Under stressful conditions characterized by nutrient depletion, overcrowding, stationary phase of growth or high temperatures a small portion of the cells produce bacteriocins [99]. Bacteriocins are evolved to bind various cell surface receptors that are outer membrane (OM) proteins important for the entry of specific nutrients such as nucleosides, siderophores, and vitamins. This characteristic prevents the target cells to escape from the bacteriocins. For example, BtuB is the receptor in *E. coli* for both Vitamin B12 and a bacteriocin called 'Colicin E'. Colicins are the bacteriocins produced by certain strains of *E. coli* that are lethal to related strains of *E. coli* but not to the producing strain.

(a)

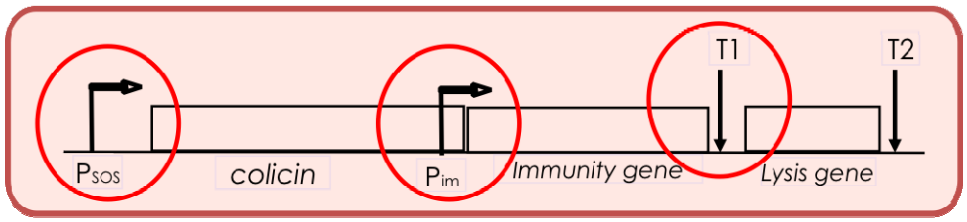

(b)

(c)

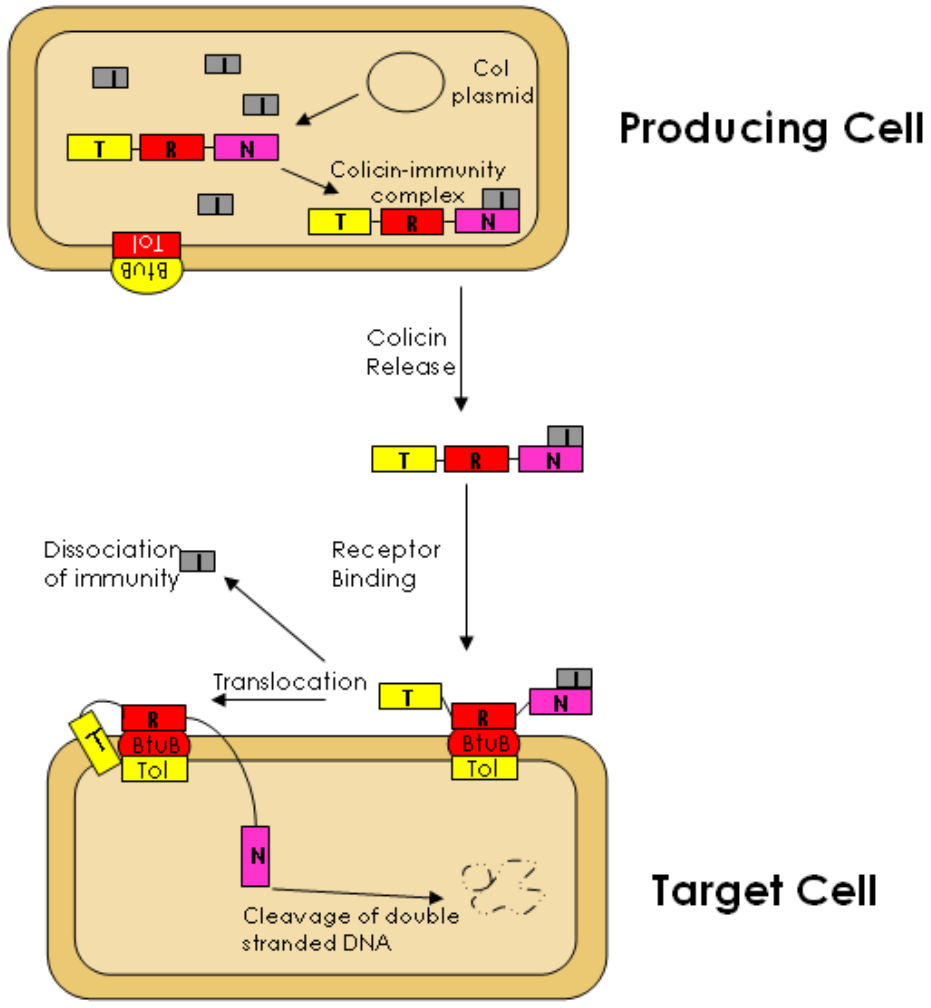

Figure 6: Colicin operon, structure and mechanism of action.
(a) Organization of the colicin operons. SOS promoter (Psos), the immunity promoter (Pimm), and the transcription terminators (T1 and T2) are indicated by arrows. (b) Various domains of a typical colicin (c) Schematic representation of the mechanism of killing by colicin. Nuclease Domain is translocated into the cytoplasm by an unknown mechanism [99].

Analogous to colicins, the new families of bacteriocins carry the name of the producing species followed by the suffix –cin. Thus, pyocins come from *Pseudomonas pyogenes*, cloacins come from *Enterobacter cloacae* and marcescins come from *Serratia marcescens* etc [99]. **Figure 6 (a)** shows the natural operon regulating colcins. In all colicin operons, the first gene is the gene encoding the activity protein, called *cxa*, which stands for colicin X activity. The gene encoding the immunity protein is designated either *cxi*, for colicin X immunity, or *imX*, and is located downstream from the activity gene for colicin. Immunity protein is under the regulation of two promoters: the LexA promoter (the bacterial SOS response promoter) of the colicin operon and its own constitutive promoter (P_{imm}) that allows a constitutive production of the immunity protein in order to ensure that there is never free colicin, which would kill the producing cell. This separate promoter is located within the structural gene encoding *cxa*. Transcription from Psos results in formation of two mRNA transcripts due to the presence of two transcription terminators, T1 and T2. The major RNA corresponds to the colcin gene and the immunity gene. Colicin and immunity gene are coordinately transcribed and translated, and both gene products associate immediately after the synthesis to form a dimeric complex devoid of any enzymatic activity. An additional promoter present upstream (Pimm) of immunity gene allows higher production of immunity protein than that of the colicin in order to block colicin from killing the producing cells. The minor RNA is the largest one, as it corresponds to a transcript of the entire operon that includes colicin, immunity protein and the lysis protein. The lysis protein is encoded by the last gene of the colcin operon and named *cxl* for colicin X lysis protein. Expression of the lysis protein allows the release of colicin by lysing the producing cell. The lysis gene is transcribed at lower levels than the colicin gene. This allows cells to express huge amounts of colicin before they lyse themselves to release it into the medium. Cell lysis only happens due to the lysis protein. Cells expressing colicin without the lysis protein do no die. The fraction of the cell population expressing colicin varies depending upon the severity of the stress. Colicins are not synthesized under normal conditions since the colicin operon is under SOS response promoter. Whether colicin is produced in small amounts by all the cells of a culture or in large amounts by a fraction of cells during either the spontaneous or the induced production of colicin has long been a subject of controversy. One study suggests that 0.1% of cells produce colicin E2 under normal conditions compared to 50% after UV irradiation. Another study demonstrated that only 3% of the cells produce colicin K under nutrient limitation [100].

The bacteriocins produced by *Pseudomonas* species are called pyocins [101, 102]. Pyocins are further classified into different types, namely R, F, and S pyocins. S-type pyocins are more related to the colicins based on domain organization [103-106]. Pyocin S3 is produced by *P. aeruginosa* P12 that is isolated from a Cystic Fibrosis patient [103]. S3 uses Ton transporters and ferripyoverdine FpvA as a receptor [99]. These bacteriocins are highly similar to each other in structure. As shown in **Figure 6 (b)** bacteriocin activity proteins have three distinct domains arranged from N to C terminus known as the receptor, translocase and nuclease (with immunity protein-binding) domains respectively. The translocation-domain and the receptor-binding domain are species specific. The nuclease-domain can be DNase or RNase and it kills the cell by cleaving its DNA or RNA.

Figure 6 (c) explains the mechanism of colicin killing [99, 107, 108]. The recognition-domain recognizes specific receptors on the surface of target species. The translocase-domain then forms a complex with Tol or Ton transporters. This complex dissociates immunity protein from the nuclease-domain and translocates the nuclease-domain into the cell. This nuclease-domain then kills the cell by cleaving its DNA or RNA or by inhibiting lipid synthesis. The producing cell is protected from its own colicin because the colicins are translationally coupled to an immunity protein and are produced together. Immunity protein forms a tight complex with the nuclease-domain. This complex disassociates only when the translocation-domain binds to the corresponding transporter on the cell surface. This mechanism provides advantage to the producing cell over the sensitive cells, which lack the immunity protein.

It has been reported that the distinct domains of bacteriocins are interchangeable. In order to engineer a protein that selectively kills PAO1, recognition and translocation domains of colcin E3 were replaced by that of the Pyocin S3 [105, 109] as shown in **Figure 7 (a).** The resulting chimeric protein, CoPy, only recognizes the cell surface receptors of *P. aeruginosa* and translocates the nuclease domain (originally from E3) into the pathogen, leaving the *E. coli* cells intact. Since *P. aeruginosa* does not express immunity protein against the nuclease domain of colicin E3 it becomes susceptible to CoPy. **Figure 7 (b)** describes the mechanism of action of CoPy. Once CoPy is released into the extracellular medium, its receptor domain binds the corresponding receptor, which is FpyA, on the surface of *P. aeruginosa*, and the translocase domain forms a complex with Ton transporters. This allows immunity protein to break free and nuclease domain enters the cell. *Pseudomonas* does not have immunity against this nuclease domain as it came from *E. coli* and hence PAO1 dies.

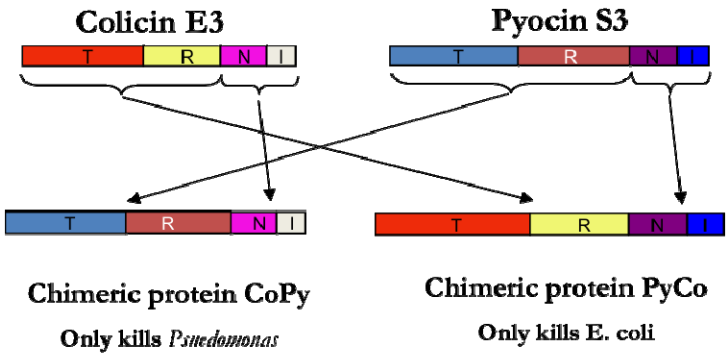

(a)

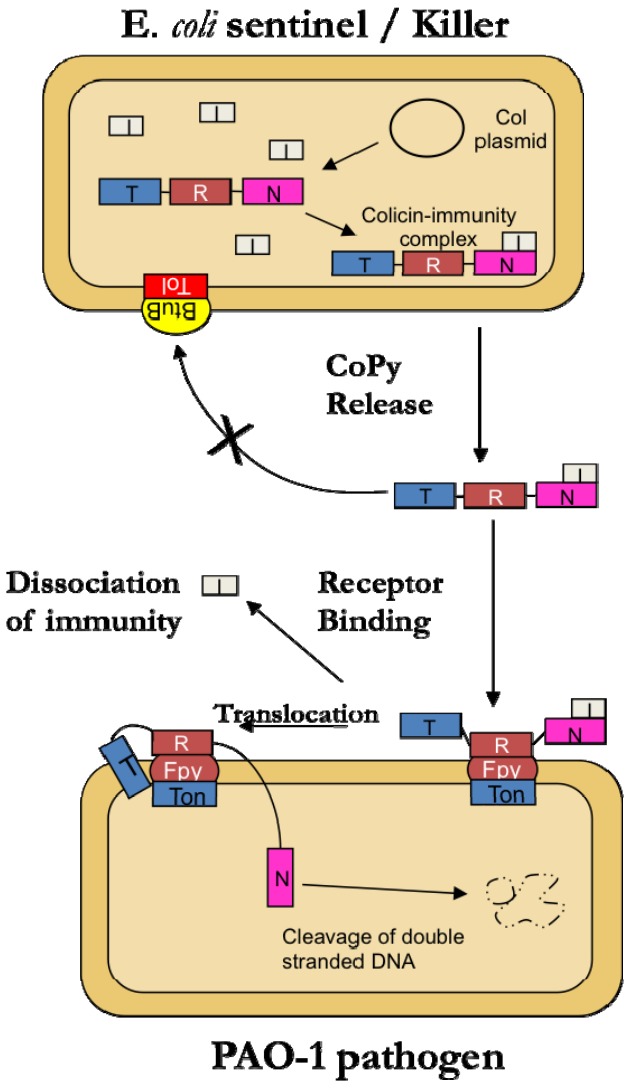

(b)

Figure 7: Colicin engineering
(a) Engineering of chimeric proteins (b) Schematic representation of the killing by chimeric protein which specifically kills PAO1 and does not kill *E. coli*.

Cells expressing CoPy survive by two mechanisms. First, only the producing cells have the immunity protein against the nuclease domain. Second, the recognition domain can only recognize receptors of the sensitive cell, PAO1, and hence does not bind to the producing cell surface receptors. This was verified experimentally as shown in **Figure 8 (a).** CoPy was cloned under the control of pltetO1 which is maximally induced by 100ng/ml of anhydrotetracycline (aTc). Growth of cells expressing CoPy is comparable to cells not expressing CoPy demonstrating that expressing CoPy with the corresponding immunity protein in a cell is not detrimental to growth. In order to test whether exogenous CoPy kills PAO1, 0.1 O.D. of PAO1 was incubated in the cell lysate of the CoPy producing cells. The result of this experiment is shown in **Figure 8 (b),** indicating that the cell lysate which contains CoPy inhibits the growth of PAO1. Further experiments were done to corroborate this result. CoPy was purified using a HisTag fused to its N-terminal (His-Tag purification protocol is given in Chapter 6, Section 1.a and commassie blotting protocol is given in Chapter 6, Section 1.f [104, 109]) and the resulting commassie blot is shown in **Figure 8 (c).** Cells capable of expressing CoPy were grown to 0.7 O.D. and then induced and incubated with 100ng/ml of aTc to induce expression at 37C for 4 hours. CoPy was then purified from the resulting cell pellet using Nickel bead columns. Concentration of the purified CoPy was 163 ng/ul where 1 ug=11.793 pmol (picomoles) and 1 ul=1.92 pmol.

In order to characterize the dosage response of CoPy, 0.1 O.D. of PAO1 was grown in a 96 well plate with different amounts of purified CoPy. **Figure 9 (a)** shows three representative dosage response curves. Half Maximal Inhibitory Concentration (IC50) of purified CoPy was calculated by plotting [65] under different concentrations. This curve is shown in **Figure 9 (b)** and can be used to calculate the 50% inhibitory concentration of CoPy which is approximately 100 nM of purified CoPy. All the growth curves of PAO1 under different concentrations of CoPy were curve fitted with a sigmoidal dosage response equation with variable slope and for each curve two parameters were estimated, EC50 and HillSlope. In this case, EC50 represents the time to reach 50% of the difference between $O.D._{max}$ and $O.D._{min}$. HillSlope is inversely proportional to the growth rate of individual curves and is shown in **Figure 9 (c).** HillSlope is smaller for steeper curves.

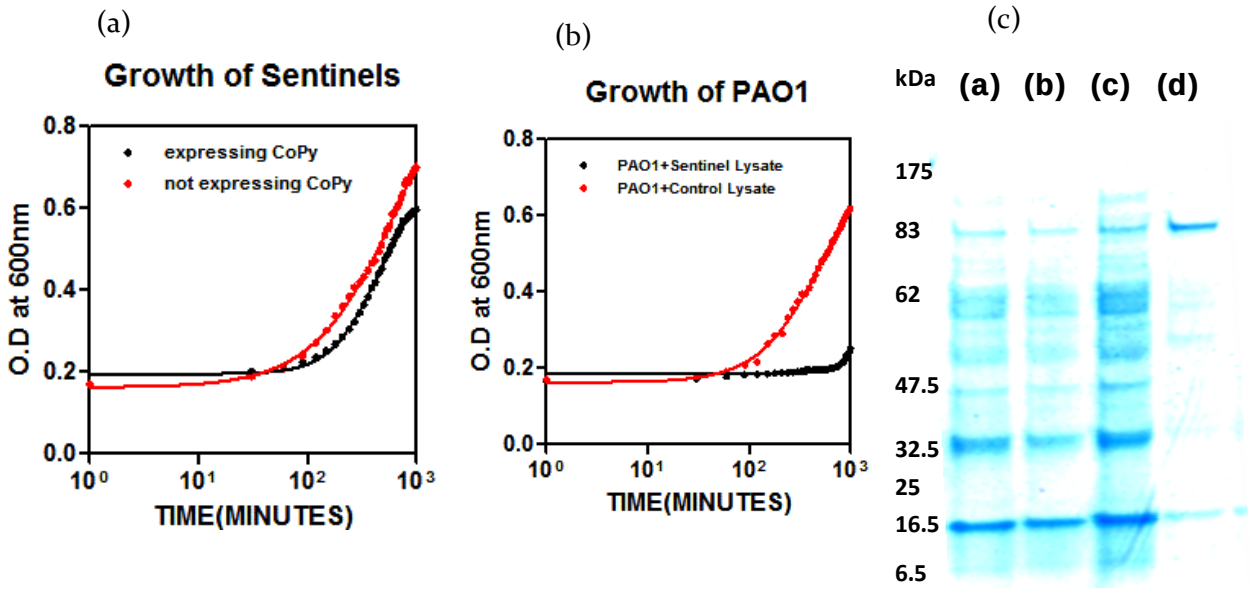

Figure 8: Purification and characterization of CoPy.
(a) Growth of the sentinels expressing CoPy was compared to control cells not expressing CoPy in a 96well plate reader. Sentinels are not significantly affected by CoPy when produced and retained in the cytoplasm. (b) Efficient killing by exogenous CoPy of PAO1 was demonstrated by observing growth of PAO1 when incubated with the same amount of cell lysate from sentinels (expressing CoPy) and control cells (not expressing CoPy). (c) Commassie blot of purified CoPy. Different lanes are as follows (lane a) 20 ul of recombinant protein wash 1 (lane b) 20 ul recombinant protein wash 2 (lane c) 20 ul of recombinant protein from the sentinel cell lysate (lane d) 20 ul purified CoPy using Nickel beads. Length-670 aa, Molecular Weight- 84.797 KDa.

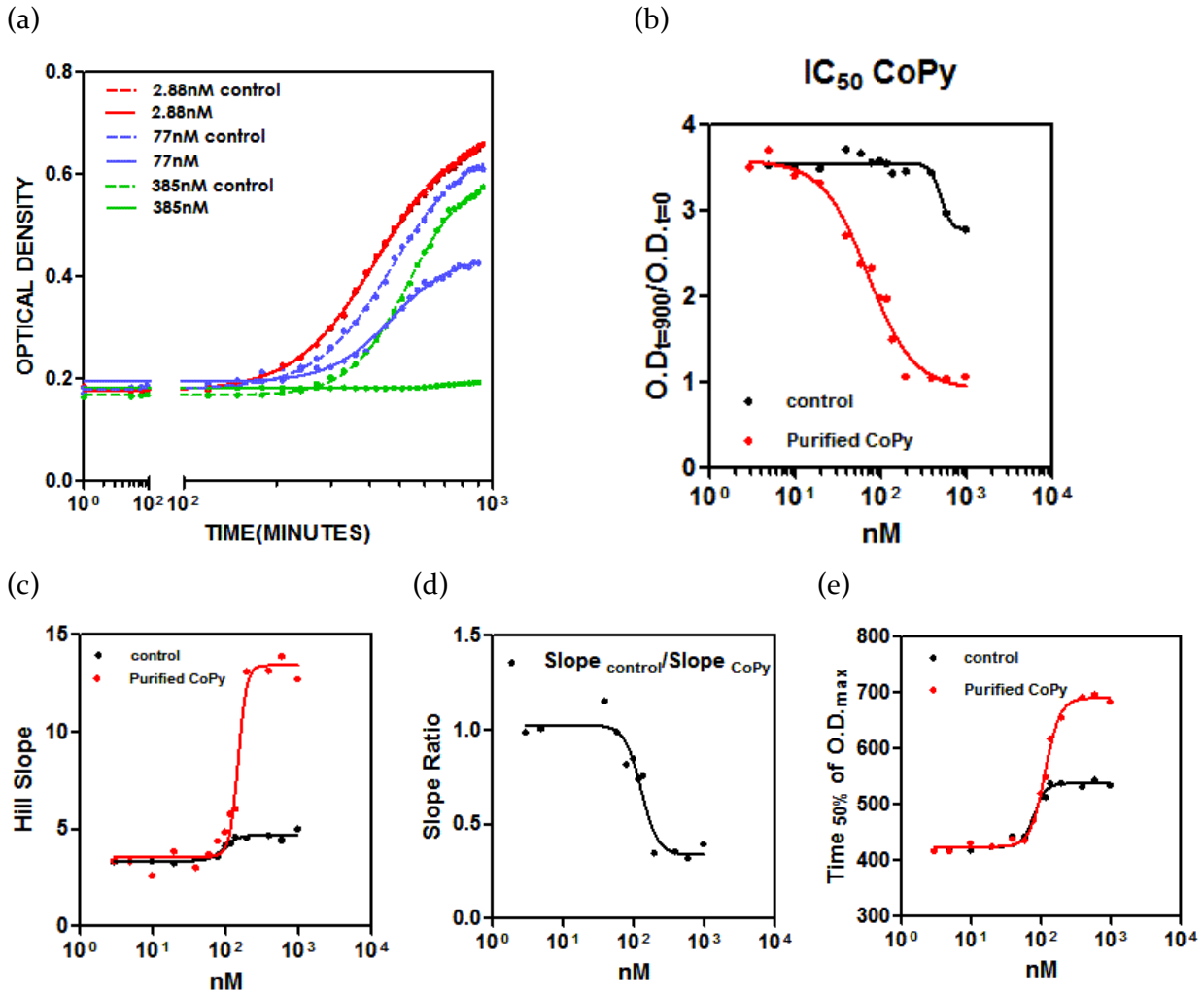

Figure 9: Analysis of the growth curves of PAO1 under different concentrations of purified CoPy. (a) Three representative dosage response curves for 2.88 nM, 77 nM and 385 nM purified CoPy along with their respective controls. (b) Half Maximal Inhibitory Concentration (IC50) curve (c) The HillSlope of various dosage response curves calculated by non-linear regression analysis. (d) Ratio of the HillSlope of control vs purified CoPy. (e) Time to reach 50% of difference between maximum and minimum Optical Density of any growth curve with and without purified CoPy. This curve demonstrates that purified CoPy caused a difference of around 200 minutes in the time it took PAO1 to reach its 50% maximum.

Figure 9 (c) clearly demonstrates that the HillSlope increased significantly with higher concentration of purified CoPy. In other words, it shows that there is a significant reduction in the growth rate of PAO1 under higher concentrations of purified CoPy. **Figure 9 (d)** shows the ratio of the HillSlope of control curve to that of purified CoPy. **Figure 9 (e)** compares the time it took PAO1 to reach 50% of its maximum O.D. under exogenous CoPy and control. This figure demonstrates that under CoPy, PAO1 takes at least 200 minutes more to grow than the control. **Figure 9 (c, d, e)** further confirms that 100 nM of purified CoPy is enough to inhibit growth of PAO1 by 50%.

Bacterial growth is often divided into three phases. In the first phase specific growth rate is zero resulting in a lag time (λ). In the second phase specific growth rate accelerates to a maximum (μ_m) and in the final phase the growth rate again decreases to zero reaching a maximum value at an asymptote (A). As shown in **Figure 10**, a sigmoidal curve is resulted when this growth curve is defined as the logarithm of the number of organisms plotted against time. This curve can be divided into three phases namely a lag phase defined by a lag time (λ), an exponential phase characterized by specific growth rate (μ_m) and a stationary phase described by an asymptote (A). In order to calculate these parameters the entire experimental data set is described by a growth model and then μ_m, λ and *A* are estimated from the model as follows [110]. As described above the PAO1 growth curves were curve fit with sigmoidal dosage response model. The equation for sigmoidal dosage response with variable slope is:

$$y = \text{Bottom} + \frac{\text{Top}-\text{Bottom}}{1+z} \qquad \text{where } Z = 10^{(\text{LogEC50}-t).\text{HillSlope}}$$

$$\frac{dy}{dt} = -\frac{\text{Top} - \text{Bottom}}{(1+z)^2} * \frac{dz}{dt}$$

Where $\frac{dz}{dt} = -\text{HillSlope} * \ln 10 * Z$

Hence $\frac{dy}{dt} = \frac{\text{Top}-\text{Bottom}}{(1+Z)^2} * (\text{HillSlope} * \ln 10) * Z$

$$\frac{d\left(\frac{dy}{dt}\right)}{dt} = (\text{Top} - \text{Bottom}) * \text{HillSlope} * \ln 10 * \left[\frac{1}{(1+z)^2} * \frac{dz}{dt} - \frac{2z}{(1+Z)^3} * \frac{dz}{dt}\right]$$

At the inflection point, where t=ti, the second derivative is equal to zero:

$$\frac{\mathrm{d}\left(\frac{\mathrm{dy}}{\mathrm{dt}}\right)}{\mathrm{dt}} = 0$$

» $\frac{1}{(1+z)^2} = 2 * \frac{z}{(1+z)^3}$

» $1 + \mathrm{z} = 2\mathrm{z}$

» $\mathrm{z}=1$

» $10^{(\mathrm{logEC50}-\mathrm{t})*\mathrm{HillSlope}}=1$

» $(\mathrm{LogEC50} - \mathrm{t}) * \mathrm{HillSlope} = 0$

» $\mathrm{ti} = \mathrm{LogEC_{50}}$

The expression of the maximum specific growth rate (μ_m) can be derived by calculating the first derivative at the inflection point.

$\mu_m = \left(\frac{\mathrm{dy}}{\mathrm{dt}}\right)$ at $\mathrm{t} = \mathrm{ti}$

» $\mu_m = \frac{(\mathrm{Top}-\mathrm{Bottom})*\mathrm{HillSlope}*\ln 10*z_{ti}}{(1+z_{ti})^2}$

» $\mu_m = (Top - Bottom) * HillSlope * 0.5756 \; as \; z_{ti} = 1$

Furthermore, the description of the tangent line through the inflection point is:

$$\frac{\mathrm{y} - \mathrm{y(ti)}}{\mathrm{t} - \mathrm{ti}} = \mu_m$$

» $y_t = y_{ti} + \mu_m t - \mu_m ti$

But $y_{ti} = \frac{Top+Bottom}{2}$

» $y_t = \frac{Top+Bottom}{2} + \mu_m * t - \mu_m * ti$

The lag time (λ) is defined as the t-axis intercept of the tangent through the inflection point (ti):

$$y_\lambda = 0$$

» $0 = \frac{Top+Bottom}{2} + \mu_m * \lambda - \mu_m * ti$

» $\lambda = ti - \frac{Top+Bottom}{2*\mu_m}$

» $\lambda = LogEC50 - \frac{Top+Bottom}{2*\mu_m} = \text{lag time}$

The asymptotic value is reached for *t* approaching infinity:

As $t \to \infty$, $y \to Top, \gg A = Top$

The values of λ, μ and A can be calculated by substituting the values of Top, Bottom, EC50 and HillSlope estimated from the analysis done in **Figure 9. Figure 10** (b) and (c) shows the change of growth rate (μ) and lag time (λ) of PAO1 with the concentration of CoPy. It is shown in **Figure 9** that 1000 nM purified CoPy is sufficient to completely inhibit growth of PAO1. In order to test the specificity of CoPy, seven different bacterial strains other than E. coli and PAO1 were grown with and without 1000 nM purified CoPy. The resulting growth curves were curve fitted and their HillSlope was compared as shown in **Figure 11 (b).** This result indicates that CoPy inhibits growth rate of PAO1 significantly more than that of the other strains and its inhibitory effects are fairly specific to PAO1. **Figure 11 (a)** and **(b)** show that CoPy completely inhibited growth of PAO1 while minimally affecting the growth of *E. coli* sentinels. *E. coli* and PAO-1 were incubated with purified CoPy on agar plug (see Chapter 6, Section 1.e for protocol) and observed for 10 hours under Zeiss microscope.

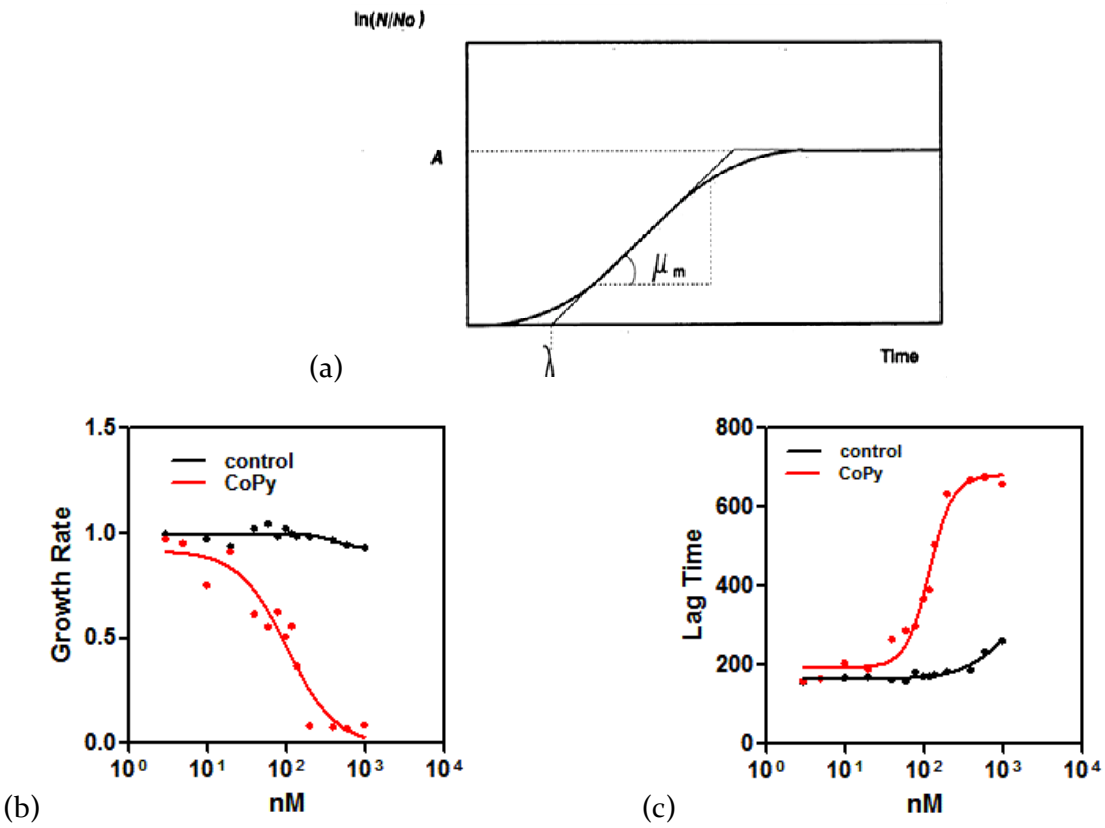

Figure 10: Deduction of μ_m, λ and *A* from PAO1 growth curves.
(a) A bacterial growth curve. This curve plot the logarithm of the relative population size [y=ln(N/No)] against time. Three parameters describe the three phases of the growth curve. The maximum specific growth rate, μ_m, is defined as the tangent at the inflection point. The lag time (λ) is defined as the x-axis intercept of this tangent and the asymptote [A= $\ln(N/N_o)$] is the maximum value reached [110]. (b) Specific growth rate of PAO1 with different concentrations of CoPy. (c) Lag time of different growth curves of PAO1 for different concentrations of CoPy.

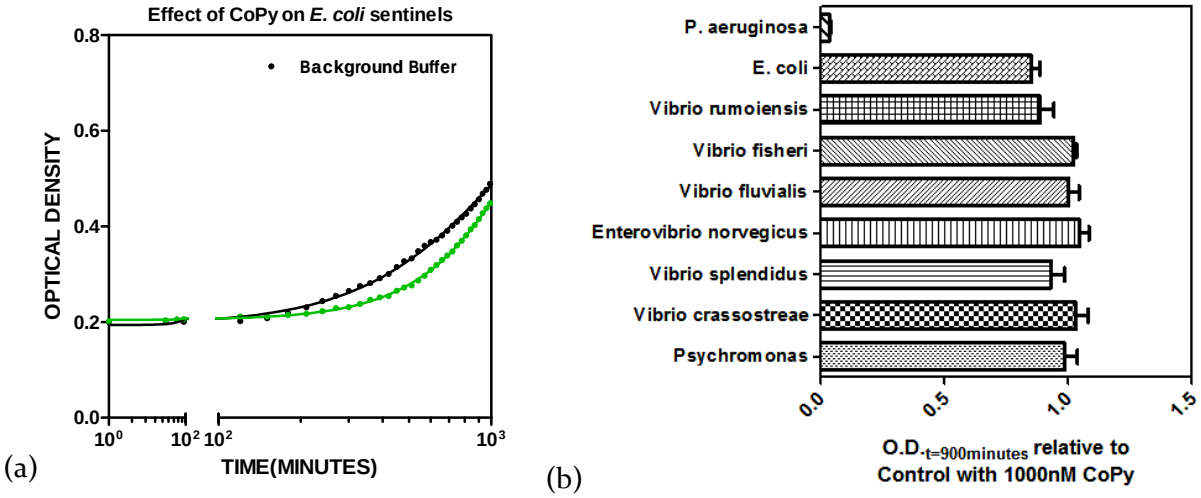

Figure 11: Specific activity of CoPy
(a) growth curve of *E. coli* incubated with 1000 nM CoPy (b) Comparison of the Optical Density at t=900 minutes of the growth curves relative to control for various strains under 1000 nM CoPy.

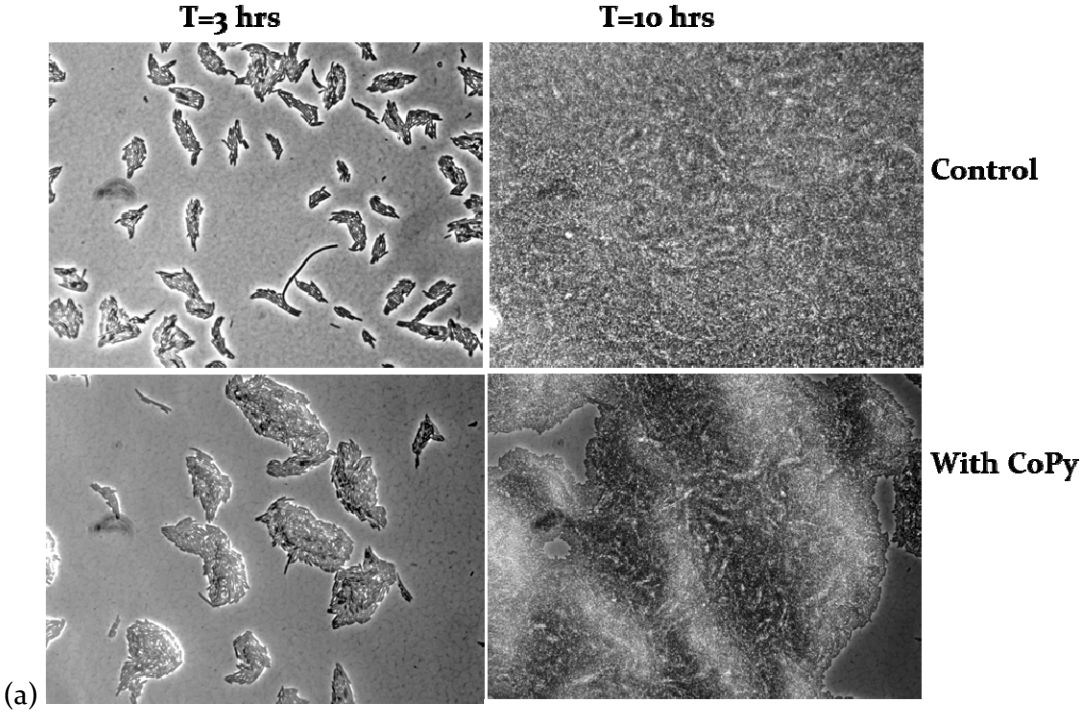

(a)

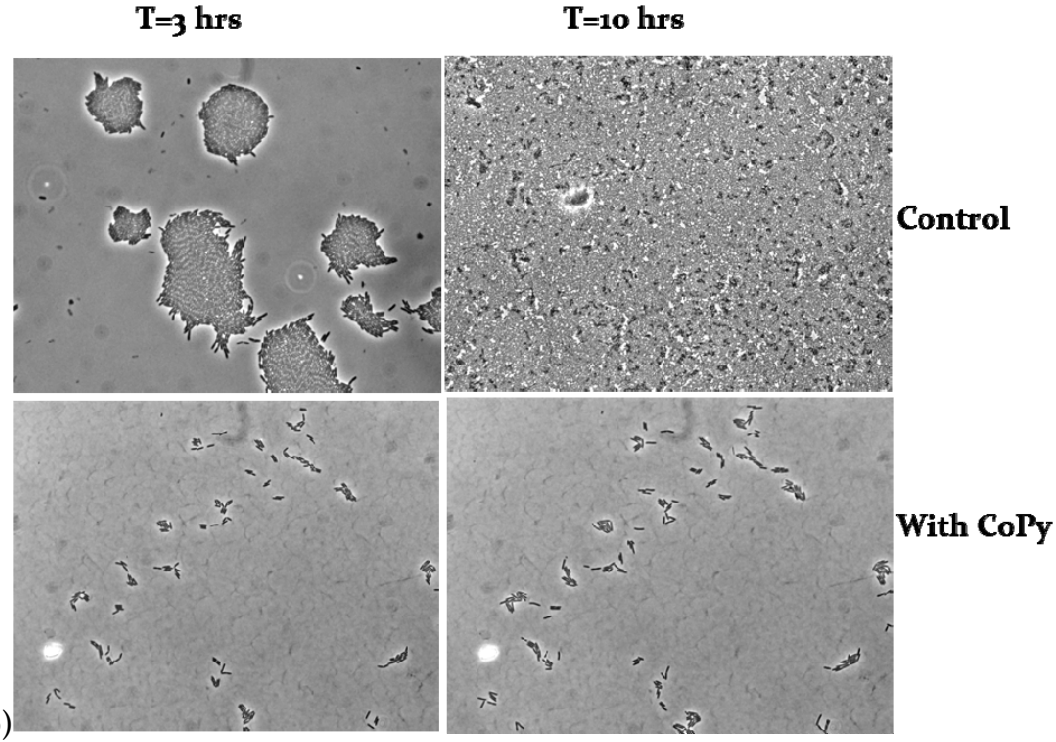

(b)

Figure 12: Microscopy images of the sentinels and pathogen with and without exogenous CoPy. (a) *E. coli* sentinels incubated with/without CoPy at T=3, 10 hrs. (b)PAO1 incubated with/without CoPy at T=3, 10 hrs.

Figure 12 shows that the sentinels' growth is unaffected by CoPy while PAO-1 growth is significantly reduced under CoPy. Cells were induced with CoPy at T=3 only after establishing that cells are growing in the experimental setup. This experiment supports the experiments done in a plate reader and once again demonstrates the specificity and efficacy of CoPy.

IV. Secretion of Pathogen specific Toxins

In section I it was showed that the sentinels can be engineered to specifically detect PAO1. From the results examined in section II it is evident that CoPy is an excellent candidate killer protein for the purpose of specifically destroying PAO1 without affecting the producing *E. coli* sentinels. In this section a suitable delivery mechanism to release CoPy into the extracellular medium is discussed. Once the sentinels detect the presence of pathogen they can release CoPy in one of two ways. Either the sentinels commit suicide and lyse themselves to release CoPy or they can secrete CoPy using a secretion tag without committing suicide.

a) Release of CoPy by the Sentinel Suicide

In [111] *E. coli* cells were engineered to self-lyse when induced with Acyl Homoserine Lactone (AHL). This was achieved by expressing the lysis protein E from *E. coli* bacteriophage ΦX174, referred to as the 'E-protein' in future discussions. 'E protein' inhibits cell wall synthesis by inhibiting the trans-membrane located MurNAc-pentapeptide translocase MraY. In a related study the lysis dynamics and recovery capabilities of these engineered cells were examined [112-116]. **Figure 13** shows images from a microscope experiment where cells were first allowed to grow, then directed to lyse by the addition of IPTG, and finally allowed to grow again by the addition of AHL. To achieve this *E. coli* cells were transformed a with a gene circuit where both IPTG induction and absence of AHL was required for expression of E protein, while the other three combinations of IPTG and AHL levels resulted in repression of E protein. The ability of a sub-population of engineered cells to recover from cell lysis will be important for maintaining a long-term viable population of sentinel/killer cells in future clinical and field deployment applications. The sentinels were engineered to respond to the presence of 3OC12HSL by expressing the E-protein. For this aim, the E protein was placed under the control of the Las system and is expressed in the presence of 3OC12HSL produced by PAO1. As shown in **Figure 13 (b)** cell density does not increase when induced by AHL because they are lysing by expressing E-protein.

(a)

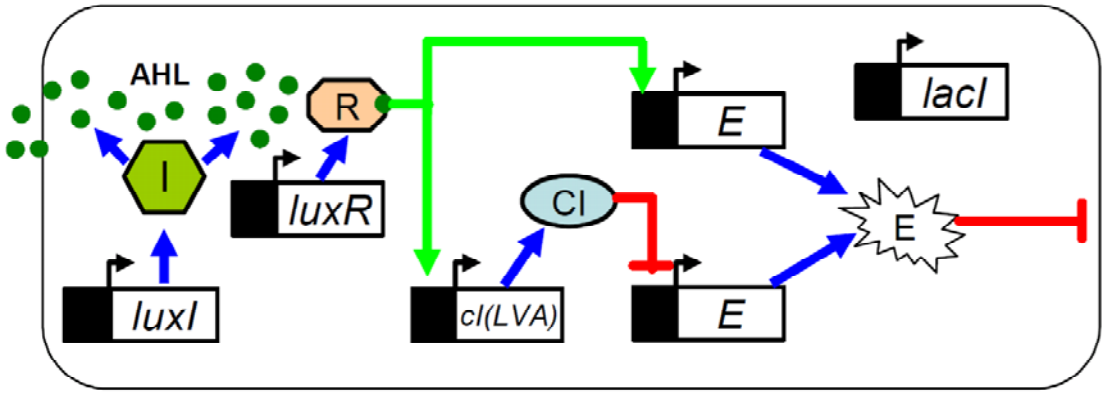

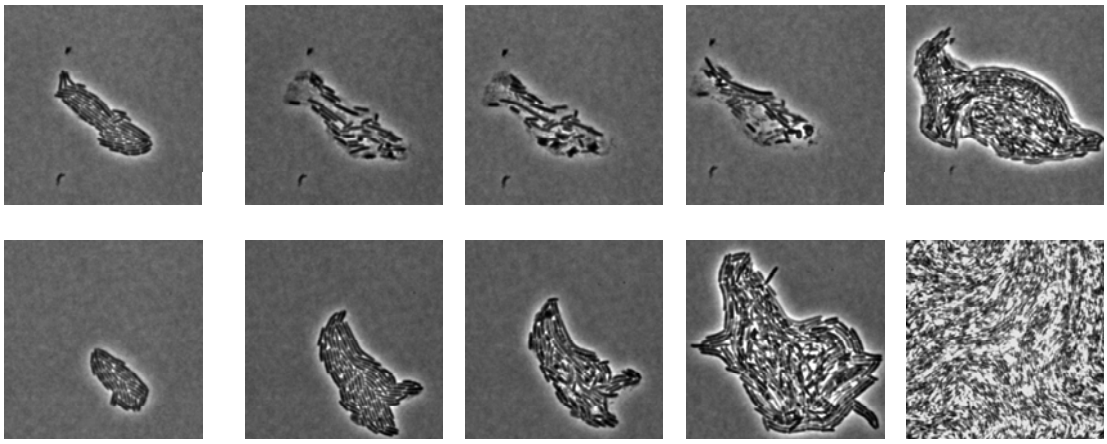

(b) 0 mins 56 mins 76 mins 200 mins 490 mins

Figure 13: Programmed cell lysis based on population density.
(a) Circuit for programmed cell lysis based on population density. Each cell synthesizes AHL that activates LuxR in neighboring cells. High or low AHL concentrations lead to cell lysis through expression of E protein. LacI, which represses production of both E proteins, is used to turn the system ON/OFF through the administration of IPTG. (b) A portion of the network for programmed cell death was tested in order to fine-tune expression levels of E protein based on IPTG and AHL induction and observation of the resulting cell lysis and ultimate recovery. The network did not include expression of LuxI or E from the lux promoter. Single cells with this sub-network were grown for 3 hours, then 1mM IPTG was added (indicated as 0 mins), and then 500 nM 3OC6HSL was added after 60 minutes. The top series of images show cells with a medium efficiency RBS controlling translation of E while the bottom series of images show cells with a weak RBS. Cells with the stronger RBS lyse more quickly and take longer to recover. The results shown here are representative of the observed behavior for approximately 10 microcolonies of each network variant.

(a)

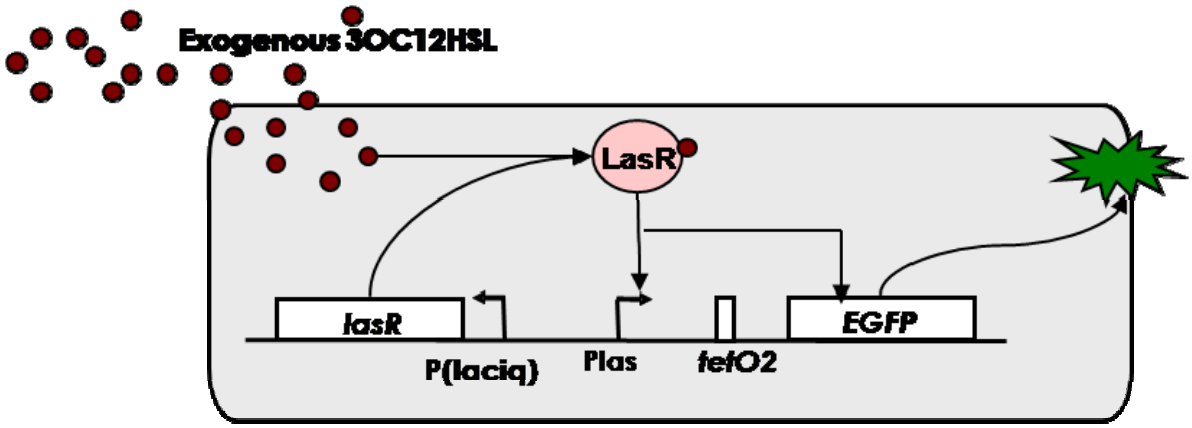

(b)

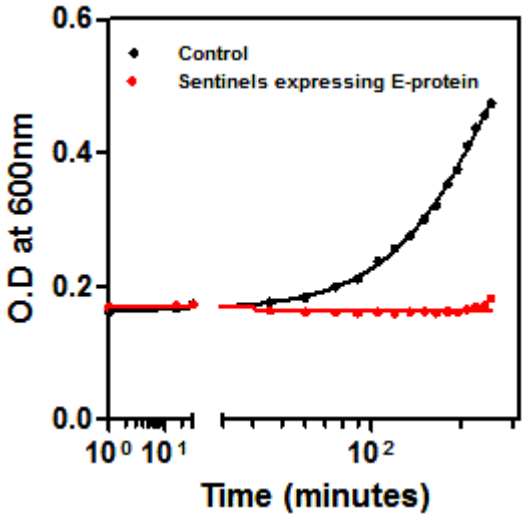

(c)

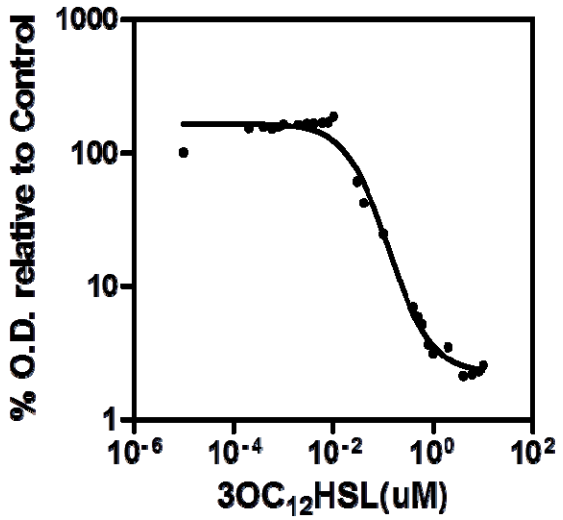

Figure 14: Characterization of death by 'E protein'.
(a) Circuit of cells expressing E protein when induced with 3OC12HSL (b) plate reader results showing that engineered cells with circuit shown in (a) die when induced with 10 uM 3OC12HSL (c) Characterization of E-protein lysis. 0.1 O.D. of cell culture was incubated in 30 different wells with 30 different conc. of 3OC12HSL of a 96 well plate for 3 hours at 37C. Following incubation an equal volume of the BacTiter-Glo reagent was added and the resulting luminescence was measured using a Luminometer after 5 minutes. The BacTiter-Glo Microbial Cell Viability Assay is an easy method for determining the number of viable microbial cells based on quantization of the ATP present. ATP is an indicator of metabolically active cells. The homogeneous assay procedure involves adding a single reagent (BacTiter-Glo Reagent from Promega) directly to bacterial cells cultured in medium and measuring luminescence. The luminescent signal is proportional to the amount of ATP present, which is directly proportional to the number of cells in the culture.

The circuit topology is given in **Figure 14 (a).** In **Figure 14 (c)** variation in the percentage of viable cells due to different concentrations of inducing AHL is reported which indicates that the amount of cells committing suicide varies with the concentration of AHL. From the experiments discussed above it is evident that the E protein is a good candidate delivery mechanism for CoPy but it presents some problems. It may be possible that the sentinels commit suicide before they produce enough CoPy to kill the pathogen and, since the sentinels are already dead, they cannot respond to surviving pathogen or new infection. Hence, sentinels capable of secreting CoPy may be better than the sentinels lysing themselves to release CoPy.

b) Secretion of CoPy

As discussed in Chapter 1 only type I, III, IV and VI secretion systems in *E. coli* are known to be capable of transporting proteins into the extracellular medium in one step. Out of these, Type-I secretion or the hemolysin pathway is one of the simplest secretion systems [76]. It is responsible for the translocation of a 107 kDa alpha-hemolysin protein (HlyA). It has been shown that the secretion signal for this pathway is located in the last 60 amino acids at the C-terminus of HlyA protein [117, 118]. These amino acids were fused to the C- terminus of CoPy and co-expressed with HlyB and HlyD (plasmid pVDL9.3 contains HlyB and HlyD which are needed for the secretion of HlyA). The resulting commassie blot is shown in **Figure 15**. Lane 9 represents the supernatant from cells expressing CoPy-HlyA along with HlyB and HlyD. From this figure it is evident that HlyA tag is unable to efficiently secrete CoPy. Hence another type of secretion system was tried. Another secretion system used by *E. coli* to transport proteins in the extracellular environment is the flagellar system. Flagellar export systems, related to but distinct from the pathogenesis-type systems, are prevalent in both gram-negative and gram-positive bacteria [119-122]. The bacterial flagellum is extensively studied in *Salmonella enterica serovar Typhimurium*, and comprises an engine and a propeller that are joined by a flexible hook [123-125]. The engine is composed of a basal body and a motor [119, 120, 122, 126-130]. The basal body is formed from an integral-membrane MS ring and a cytoplasmic-facing C ring. The flagellar rod is assembled in the center of the MS ring. P and L rings form the rod bushing. The motor of flagellar engine comprises rotor and stator protein complexes (MotA and MotB), which derive their energy from ion gradient and drive rotation. The flexible hook is composed of approximately 120 copies of FlgE protein assembled on L ring. This hook is connected to a rigid filament structure using junction proteins FlgK, FlgL and a filament-capping protein FliD.

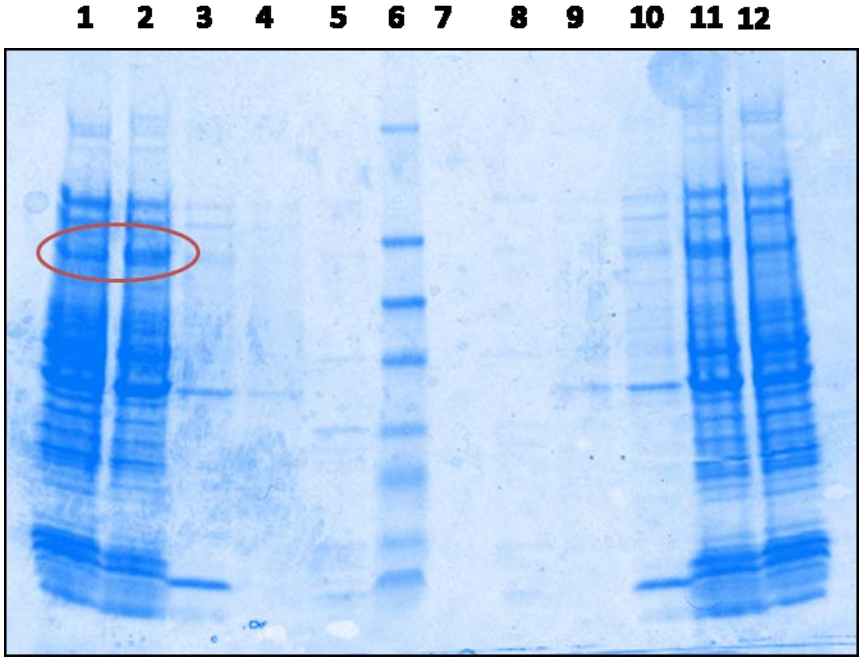

Figure 15: Validation of secretion using HlyA tag.
1)20 ul from 250 ul BL21(DE3) expressing HlyA-CoPy[O.D.—1.18] suspended in 50 ul of sample Buffer (2) 20 ul from 250 ul BL21(DE3) expressing HlyA-CoPy[O.D.—2.3] induced with 1 mM IPTG, incubated for 4 hours and suspended in 96ul of sample Buffer (3) 20 ul out of 10 ml spent cell lysate of BL21(DE3) expressing HlyA-CoPy[O.D.—2.3] induced with 1 mM IPTG used for purification after it is passed through the column packed with Nickel beads. (4) 20 ul out of 500 ul of concentrated supernatant of BL21 (DE3) expressing HlyA-CoPy [O.D.—2.3] induced with 1 mM IPTG and the cells are completely filtered out. (5) 20 ul out of 1ml purified HlyA-CoPy from 10 ml BL21 (DE3) expressing HlyA-CoPy [O.D.—2.3] induced with 1 mM IPTG when eluded with 150 mM immidazole. (6) Protein Ladder (7) empty lane (8) 20ul out of 1 ml purified [HlyA-CoPy+pVDL9.3] from 10 ml BL21 (DE3) expressing Hlya-CoPy [O.D.—1.632] induced with 1 mM IPTG when eluded with 150 mM immidazole. (9) 20 ul out of 500ul of concentrated supernatant of BL21 (DE3) expressing [HlyA-CoPy+pVDL9.3] [O.D.—1.632] induced with 1mM IPTG and the cells are completely filtered out. (10) 20 ul out of 10 ml spent cell lysate of BL21 (DE3) expressing [HlyA-CoPy+pVDL9.3] [O.D.—1.632] induced with 1mM IPTG used for purification after it is passed through the column packed with Nickel beads. (11) 20 ul from 250 ul BL21(DE3) expressing [HlyA-CoPy+pVDL9.3] [O.D.—1.632] induced with 1mM IPTG, incubated for 4 hours and suspended in 68 ul of sample Buffer (12) 20 ul from 500 ul BL21(DE3) expressing [HlyA-CoPy+pVDL9.3] [O.D.—0.88] suspended in 73 ul of sample Buffer.

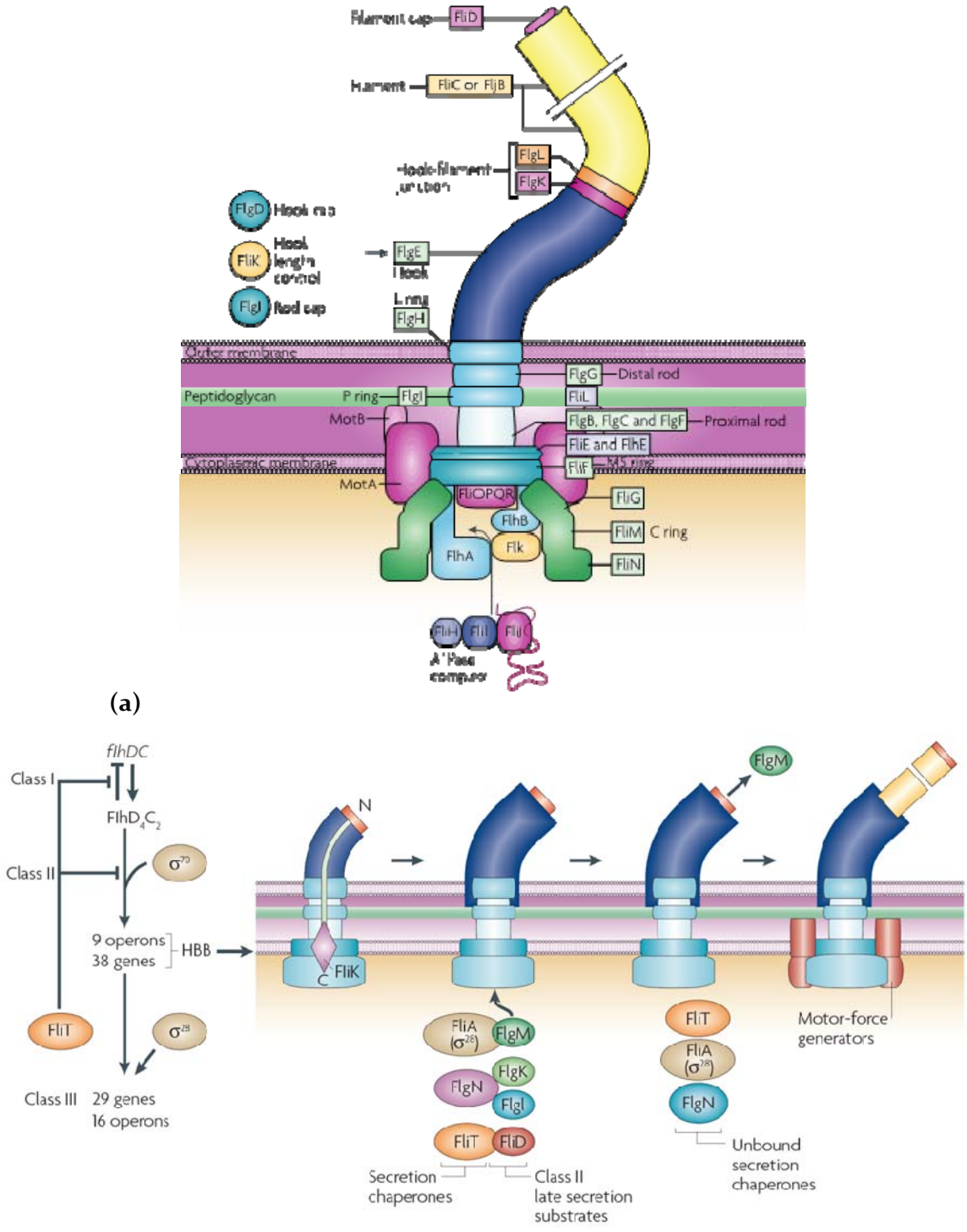

Figure 16: Flagellar assembly in gram-negative bacteria.
(a) Flagellar component for ***Salmonella enterica serovar Typhimurium***. (b) Coupling of flagellar gene regulation to flagellum assembly. This figure is adapted from [127, 131] and is used for illustrative purposes only.

This rigid filament structure is the flagellar propeller, which is a 20 nm thick, and 10-15 um long hollow tube and consists of as many as 20,000 units of a single protein, the flagellin (FliC or FljB in *Salmonella* species)[127, 131]. In the early stages of filament growth, 55-KDa flagellin subunits are delivered at a rate of several molecules per second which is equivalent to ~10,000 amino acids per second. The flagellar motor drives the rotation of this helical propeller and is the main cause of bacterial motility. In *S. typhimurium*, (as explained in the **Figure 16 (b)**) the flagellar master operon flhDC controls the fundamental decision of whether or not to produce flagella. The flhDC operon is expressed from a class I promoter. The FlhD and FlhC proteins form a heteromultimeric complex ($FlhD_4C_2$) that functions as a transcriptional activator to promote σ70-dependent transcription from the class II flagellar promoters. The class II promoters direct transcription of the genes that are needed for the structure and assembly of the flagellar motor structure, which is also known as the HBB. Upon HBB completion, class III promoters are transcribed by σ28 RNA polymerase, which is specific for flagellar class III promoters. Prior to HBB completion, σ28 RNA polymerase is inhibited by the anti-σ28 factor FlgM [125, 132-140]. Upon HBB completion, FlgM is secreted from the cell, presumably through the completed HBB structure, and σ28-dependent transcription ensues. In this way, genes such as the flagellin filament genes, the products of which are needed after HBB formation, are only transcribed when there is a functional motor onto which they can be assembled. *E. coli* has essentially a similar flagellar control.

In order to secrete CoPy using flagellar system, FlgM was fused to the N terminus of CoPy under the transcriptional control of Las promoter. This promoter is transcribed only in the presence of 3OC12HSL, which is produced by PAO1 and its quantity is correlated to the number of PAO1 present in the medium. Western blotting was performed to validate secretion of CoPy using FlgM. 1L of *E. coli* cells containing pLas-FlgM-CoPy were grown to an O.D. of 1 and then induced and incubated with 3OC12HSL for four hours. After this the cells were filtered using a 0.22 um filter and the resulting 1L supernatant was collected and concentrated using a Millipore Ultrafiltration Stirred Cell with a 10,000 NMWL membrane. 20 ul of this concentrated FlgM-CoPy was run on a SDS page gel. **Figure 17** shows a western blot of FlgM-CoPy that is secreted into the medium. This result demonstrates that the engineered sentinel/killer cells are able to secrete CoPy with the aid of FlgM in response to 3OC12HSL.

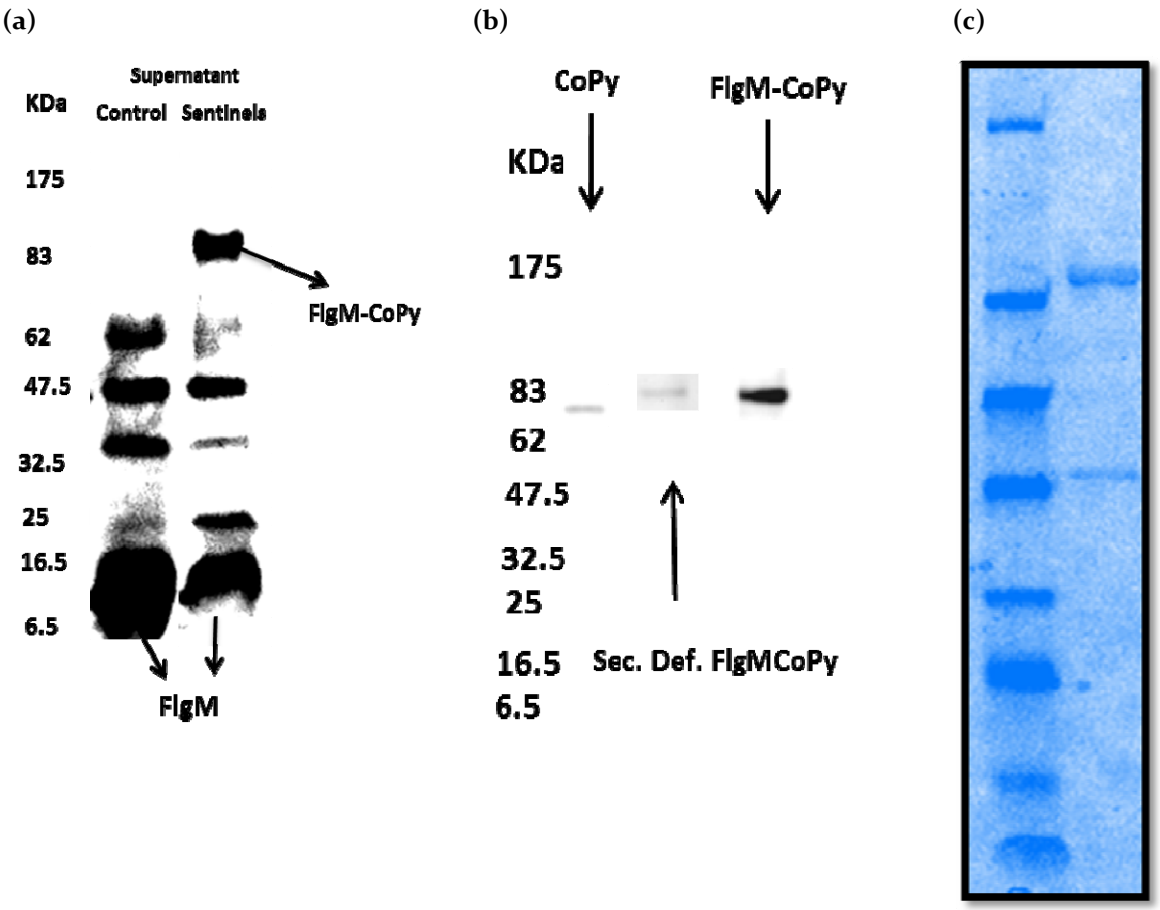

Figure 17: Secretion of CoPy using FlgM secretion tag.
(a) Western blot of the cells secreting FlgM-CoPy. It is evident that FlgMCoPy is only present in the concentrated supernatant from the sentinels. (b) Control to show that cells are exporting the FlgM-CoPy because of the FlgM secretion tag and not due to lysing. CoPy without a FlgM secretion tag gets exported at basal levels. By addition of FlgM secretion tag there is a marked increase in the amount of FlgM-CoPy in the supernatant. An *E. coli* strain deficient in hook basal body and flagellin genes (FlgM-, Fla-, FljB-) also exports FlgM-CoPy at basal levels. If the export of FlgM-CoPy was due to cell lysis only basal levels of FlgM-CoPy would be present in the supernatant. (c)Commassie Blot of the secreted, concentrated and purified CoPy.

Similar to CoPy the specific activity of the non-secreted FlgM-CoPy and the secreted FlgM-CoPy was verified**.** Analysis similar to **Figure 9** was done with the non-secreted and secreted FlgM-CoPy. **Figure 18 (a)** shows three representative dosage response growth curves of PAO1 under different amounts of purified non-secreted FlgM-CoPy. Half maximal Inhibitory Concentration (IC_{50}) of purified non-secreted FlgM-CoPy was calculated by plotting {(Optical $Density_{t=900minutes}$)/ (Optical $Density_{t=0}$)} under different concentrations as shown in **Figure 18 (b).** It indicates that 1000 nM purified non-secreted FlgM-CoPy is sufficient to inhibit 50% of PAO1. **Figure 18 (c)** compares the HillSlope of different dosage response curves with their control. This figure clearly demonstrates that the HillSlope increased significantly with higher concentration of purified non-secreted FlgM-CoPy. **Figure 18 (d)** shows the ratio of the HillSlope of the control curve to that of purified non-secreted FlgM-CoPy. **Figure 18 (e)** shows that similar to CoPy, non-secreted FlgM-CoPy slows down the growth of PAO1. **Figure 18 (c, d, e, f, g)** further confirms that 1000 nM of purified FlgM-CoPy is enough to inhibit growth of PAO1 by 50%. Comparison of **Figure 9** and **Figure 18** indicates that addition of secretion tag (FlgM) to CoPy has increased its IC50.

In order to do the analysis and characterization similar to **Figure 9**, the secreted FlgM-CoPy was purified using the protocol given in Chapter 6, section 1.a. Commassie blot of secreted, concentrated and purified FlgM-CoPy is shown in **Figure 17 (c). Figure 19** analyzes the dosage response curves of the secreted and purified FlgM-CoPy. Analysis similar to **Figure 9** and **Figure 18** was done with the secreted and purified FlgM-CoPy. **Figure 19 (b)** shows that the IC_{50} of secreted and purified FlgM-CoPy is only marginally different than the non-secreted and purified FlgM-CoPy. This conclusion is further supported by **Figure 19 (c, d, e, f, g).**

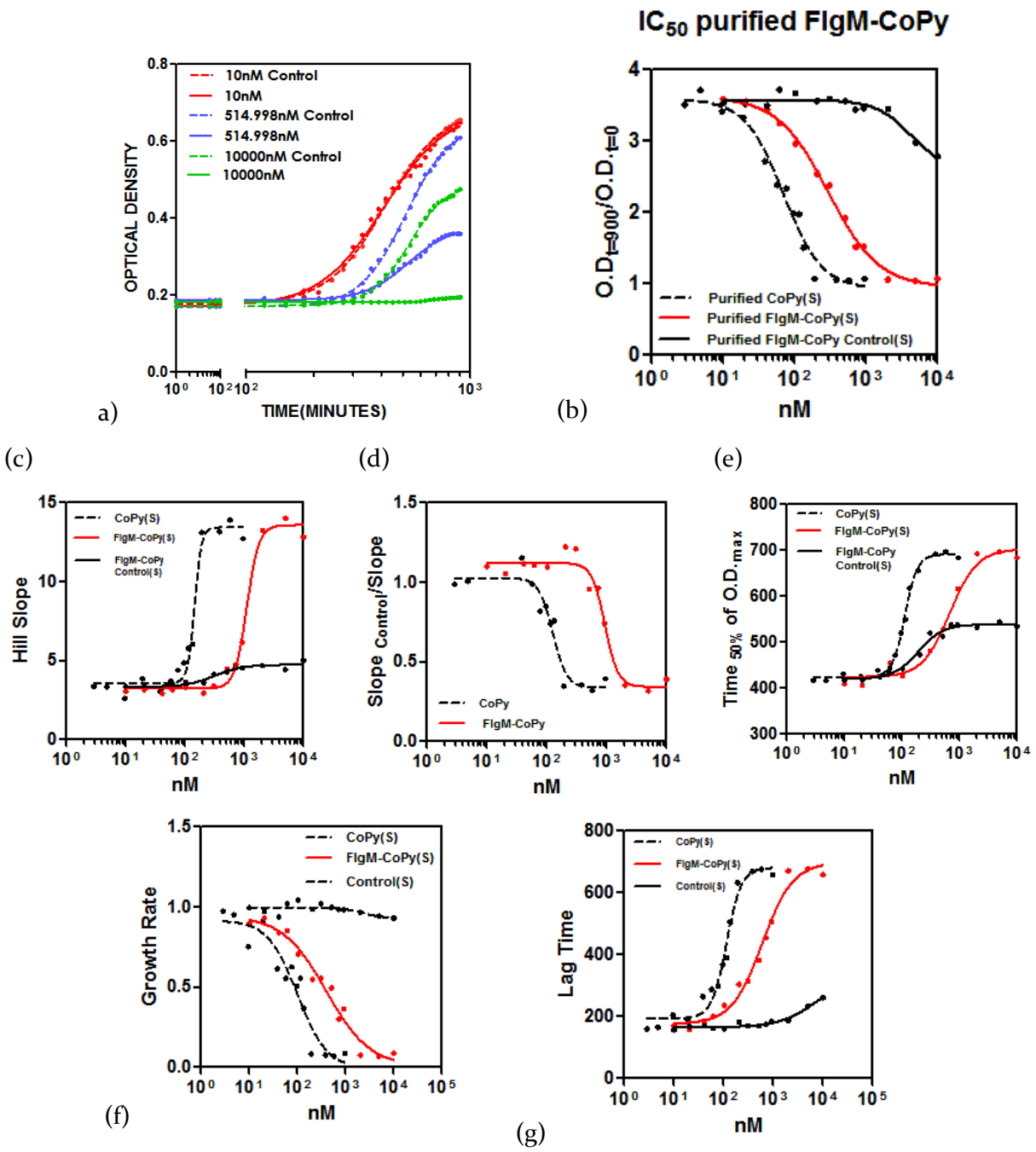

Figure 18: Detailed analysis of the growth curves of PAO1 under different concentrations of purified 'non-secreted' FlgM-CoPy.

(a) Three representative dosage response curves for 10 nM, 515 nM and 10,000 nM purified FlgM-CoPy along with their respective controls. (b) Half Maximal Inhibitory Concentration (IC50) curve (c) The HillSlope of various dosage response curves calculated by non-linear regression analysis. (d) Ratio of the HillSlope of control vs purified FlgM-CoPy. (e) Time to reach 50% of difference between maximum and minimum O.D. of any growth curve with and without purified FlgM-CoPy. This curve demonstrates that purified FlgM-CoPy caused a difference of around 200 minutes in the time it took PAO1 to reach its 50% maximum. (f) Specific growth rate of PAO1 with different concentrations of FlgM-CoPy. (g) Lag time of different growth curves of PAO1 for different concentrations of FlgM-CoPy. All the experiments were performed using a 96 well plate using Tecan Plate Reader.

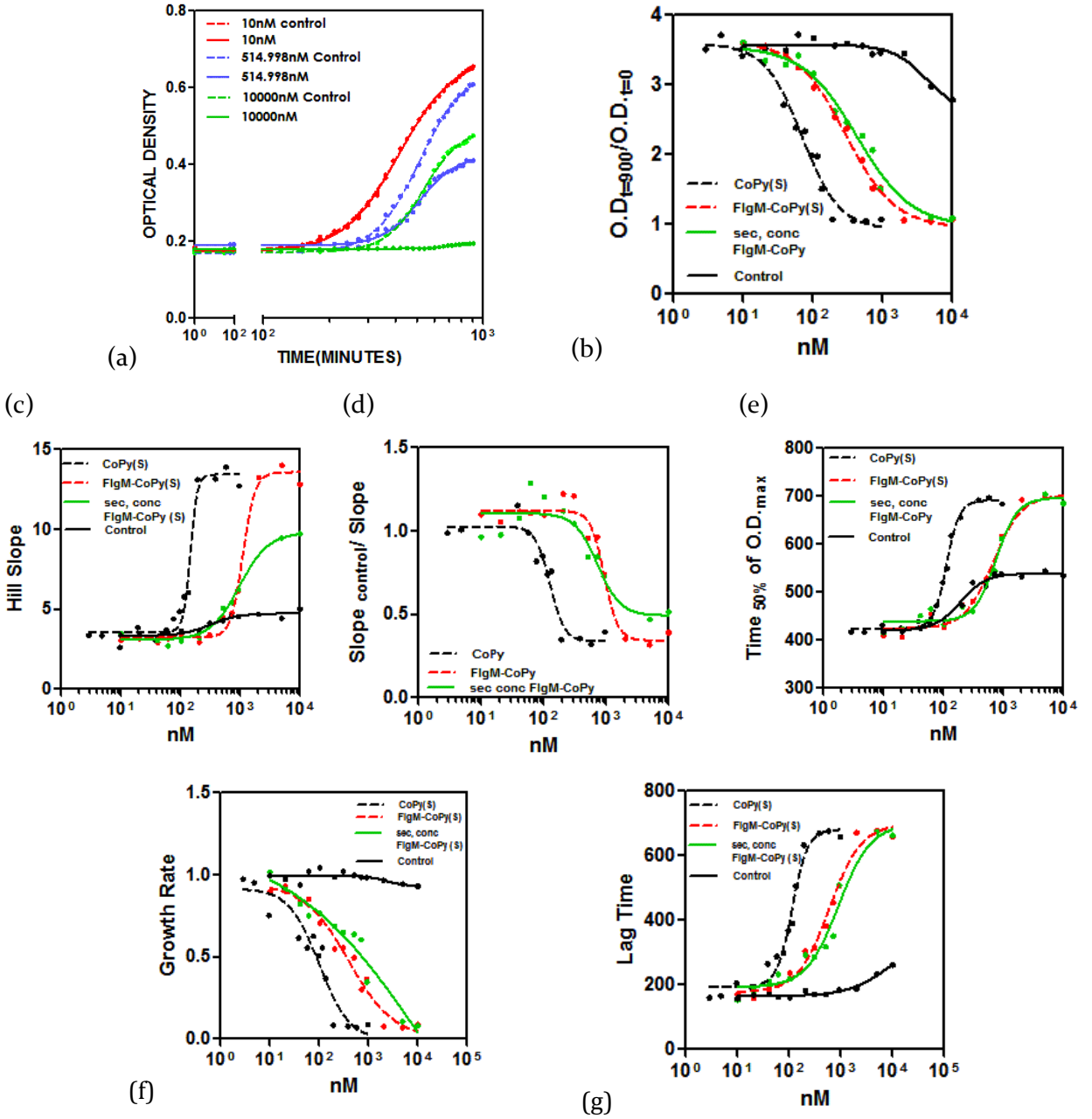

Figure 19: Detailed analysis of growth curves of PAO1 under different concentrations of secreted, concentrated and purified FlgM-CoPy.

(a) Three representative dosage response curves for 10 nM, 515 nM and 10000 nM secreted, concentrated and purified FlgM-CoPy along with their respective controls. (b) Half Maximal Inhibitory Concentration (IC50) curve (c) The HillSlope of various dosage response curves calculated by non-linear regression analysis. (d) Ratio of the HillSlope of control vs secreted, concentrated and purified FlgM-CoPy. (e) Time to reach 50% of difference between maximum and minimum Optical Density of any growth curve with and without purified secreted, concentrated and purified FlgM-CoPy. This curve demonstrates that secreted, concentrated and purified FlgM-CoPy caused a difference of around 200 minutes in the time it took PAO1 to reach its 50% maximum. This curve is similar to the purified and non-secreted FlgM-CoPy. (f) Specific growth rate of PAO1 with different concentrations of secreted FlgM-CoPy. (g) Lag time of different growth curves of PAO1 for different concentrations of secreted FlgM-CoPy. All the experiments were performed using a 96 well plate using Tecan Plate Reader.

V. Bacterial Sense and Destroy System Characterization

In the previous sections of this chapter separate modules of the bacterial 'Sense and Destroy' system are characterized. In this section all those modules are brought together and different parameters, which are important in connecting these individual modules, are closely studied. First, in order to couple these modules it is important to understand the relationship between colony forming units (CFU) and O.D. for each bacterium. This relationship will be used to calculate the number of sentinels needed to kill one PAO1 cell. CFU of bacteria is different than the O.D. measured by a UV spectrometer. Experimental validation of the relationship between O.D. and CFU was done for *E. coli* and PAO1 in order to accurately translate the density of the sentinels and the pathogen in various experiments. For this different dilutions of the cells at a particular density were plated and their respective colonies were counted the next day. The CFU at a specific density is shown in **Figure 20 (a)** and **(b).** From the figure it can be seen that approximately 1 O.D. of PAO1 corresponds to $2.8*10^9$ CFU and 1 O.D. of *E. coli* corresponds to $7*10^8$ CFU. This difference in the number of CFUs reflects the difference in sizes of *E. coli* and PAO1. Similarly a comparison of the growth rates of the sentinels and the pathogen was done and is shown in **Figure 20 (c).**

Next, secretion efficiency of the *'maximally induced'* sentinels at 10 uM 3OC12HSL was estimated as explained in **Figure 21**. 1 ml of secretion deficient *E. coli* sentinels were grown to an O.D.=1 and incubated with 10 uM exogenous 3OC12HSL. These cells were collected and non-secreted FlgM-CoPy was purified from them using His-Tag purification. Concentration of the pure non-secreted FlgM-CoPy was measured using a NanoDrop and the total amount of non-secreted FlgM-CoPy is 19.2 ug per 1 ml of O.D.= 1 sentinels. Similarly, the amount of secreted FlgM-CoPy was calculated by purifying secreted FlgM-CoPy from filter sterilized supernatant of the sentinels induced by 10 uM 3OC12HSL and at an O.D.=1. Again the concentration of purified and secreted FlgM-CoPy was measured using Nano-Drop and the total amount is 1.02 ug per 1 ml of O.D.=1 sentinels. Hence the approximate secretion efficiency of the *E. coli* sentinels is 5% as shown in the **Figure 21.**

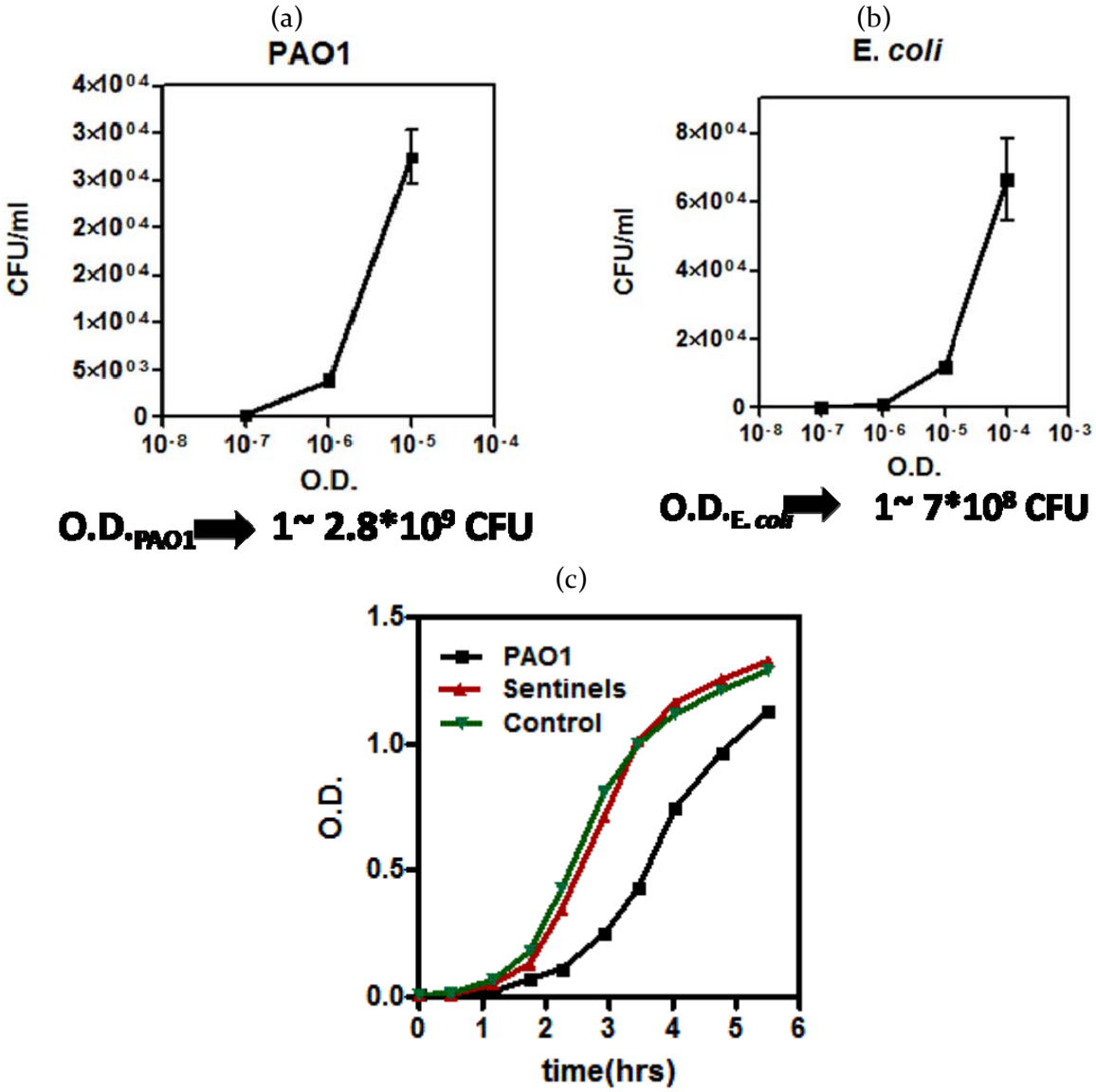

Figure 20: Relationship between the optical density and colony forming units (CFU).
(a) PAO1. (b) *E. coli*. (c) Comparison of the growth rates of PAO1, *E. coli* sentinels and *E. coli* control cells

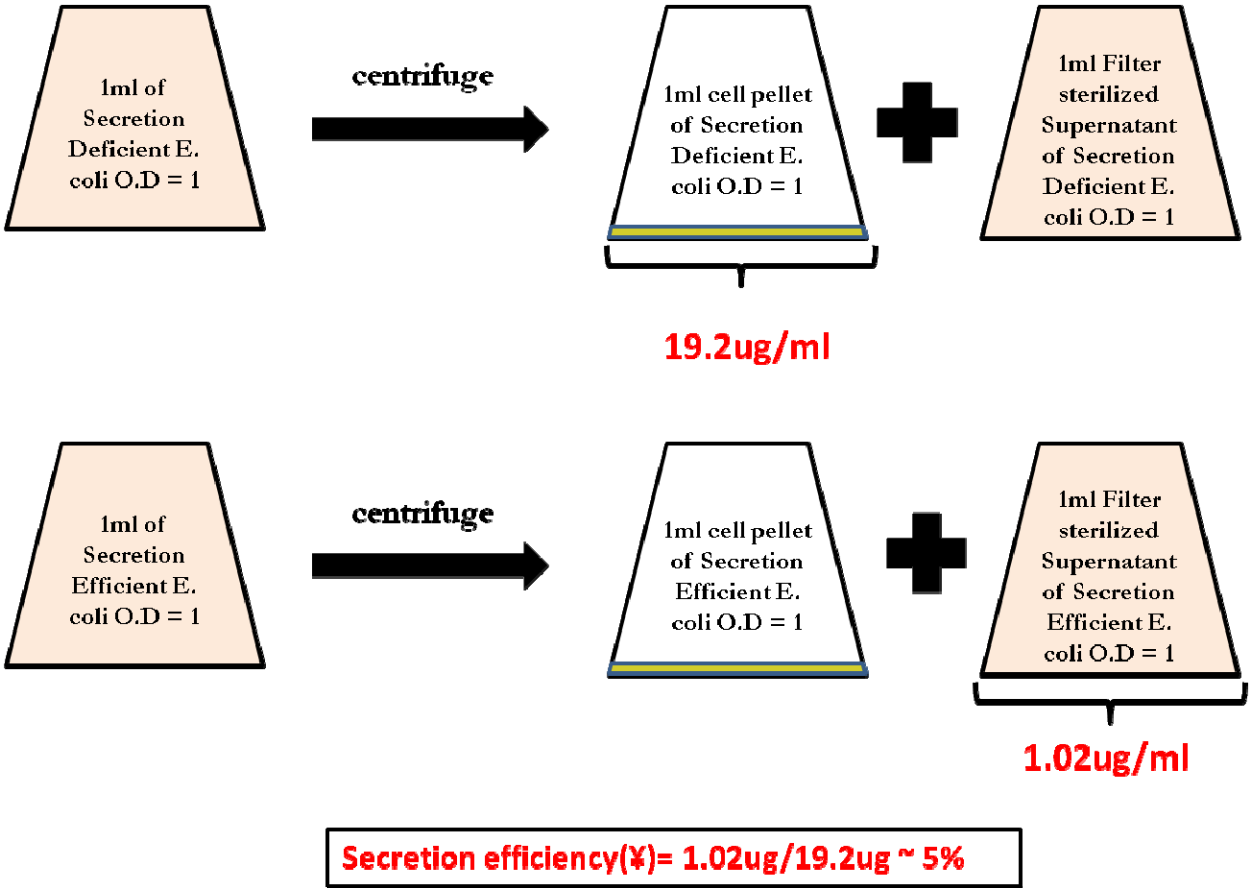

Figure 21: Secretion Efficiency of FlgM.
Experimental setup to calculate secretion efficiency of CoPy using FlgM secretion tag. Secretion efficiency is defined as the ratio of total amount of FlgM-CoPy secreted and the total amount of FlgM-CoPy produced. Approximate total amount of FlgM-CoPy produced in a secretion deficient strain is 19.2 ug/ml/O.D. of cells. Total amount of FlgM-CoPy secreted from the cells is calculated by purifying FlgM-CoPy from the supernatant of the cells expressing and secreting FlgM-CoPy. As shown above the secretion efficiency is 1.02/19.2~5%

Once all the basic elements were in place the following experiment was done to estimate the number of sentinels needed to kill one PAO1 cell. Schematic representation of the experimental setup is shown in **Figure 22**. 100 ml of PAO1 was grown to an O.D.=1. Then the PAO1 was removed from the cell culture by passing it through a sterile 0.22 um filter and collecting all the supernatant. This 100 ml of filter-sterilized supernatant has the Quorum Sensing (QS) molecules produced by PAO1. According to **Figure 5 (d)** O.D.=1 of PAO1 is sufficient to '*maximally induce'* the sentinels. Subsequently, sentinels were grown in this supernatant in order to characterize their response to these QS molecules. Since the sentinels secrete FlgM-CoPy in response to the QS signals from PAO1, the resulting cell culture will have all the secreted FlgM-CoPy from the sentinels. The sentinels were further removed from this cell culture and the supernatant was concentrated (400X) using a 10 KDa filter membrane (Centricon Plus-70 centrifugal units with 10,000 NMWL Ultracel PL-10 membrane from Millipore). This membrane retained all the proteins which are larger than 10 KDa. Final volume of the retentate was 250 uL and contains the FlgM-CoPy (84 KDa) secreted by the sentinels. The presence of FlgM-CoPy in the supernatant has already been verified earlier by Western Blot. In order to estimate the amount of FlgM-CoPy present in different volumes of the retentate, a Commassie Blot was developed for different dilutions of the retentate as shown in **Figure 23**. The row representing the secreted FlgM-CoPy is circled. The numbers above different columns in the figure represent the volume of the concentrated supernatant in that lane. It is evident that FlgM-CoPy is visible only for volumes greater than 5 ul of the concentrated supernatant, which is equivalent to 2 ml of the original supernatant.

Once it was verified that FlgM-CoPy is secreted in response to the pathogen, different amounts of PAO1 were grown in 50 ul of the concentrated supernatant per well in a 96 well plate. 50 ul of the concentrated supernatant is equivalent to the supernatant from 20 ml of '*maximally induced'* sentinels with an O.D.=1.26 or $17.6*10^9$ sentinels. In other words 50 uL of the concentrated supernatant contains all the FlgM-CoPy secreted by $17.6*10^9$ *'maximally induced'* sentinels. Therefore, the number of PAO1 and the sentinels effectively present in any well are known. The resulting growth curves for different ratios of the sentinels and PAO1 were analyzed similar to **Figure 9** and this analysis is shown in **Figure 24**. **Figure 24 (b)** shows that with a given secretion efficiency (discussed in **Figure 21**) at least 10^4 sentinals are needed to kill one PAO1. This ratio is further confirmed by **Figure 24(c, d, e)** which plots the HillSlope of all the dosage response curves.

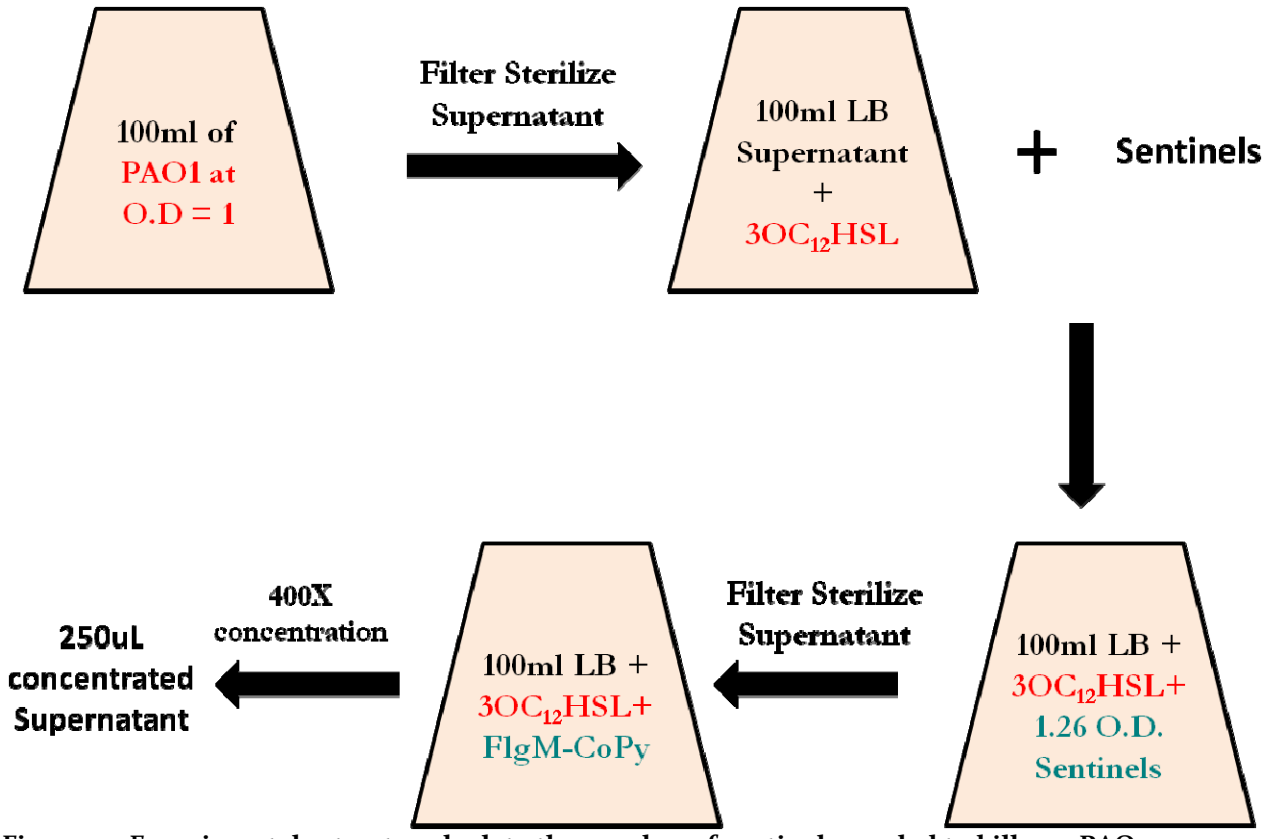

Figure 22: Experimental setup to calculate the number of sentinels needed to kill one PAO1.
Experimental setup to characterize the effect of secreted FlgM-CoPy in response to the quorum sensing molecules produced by PAO1 and to estimate the number of sentinels needed to kill one cell of PAO1.

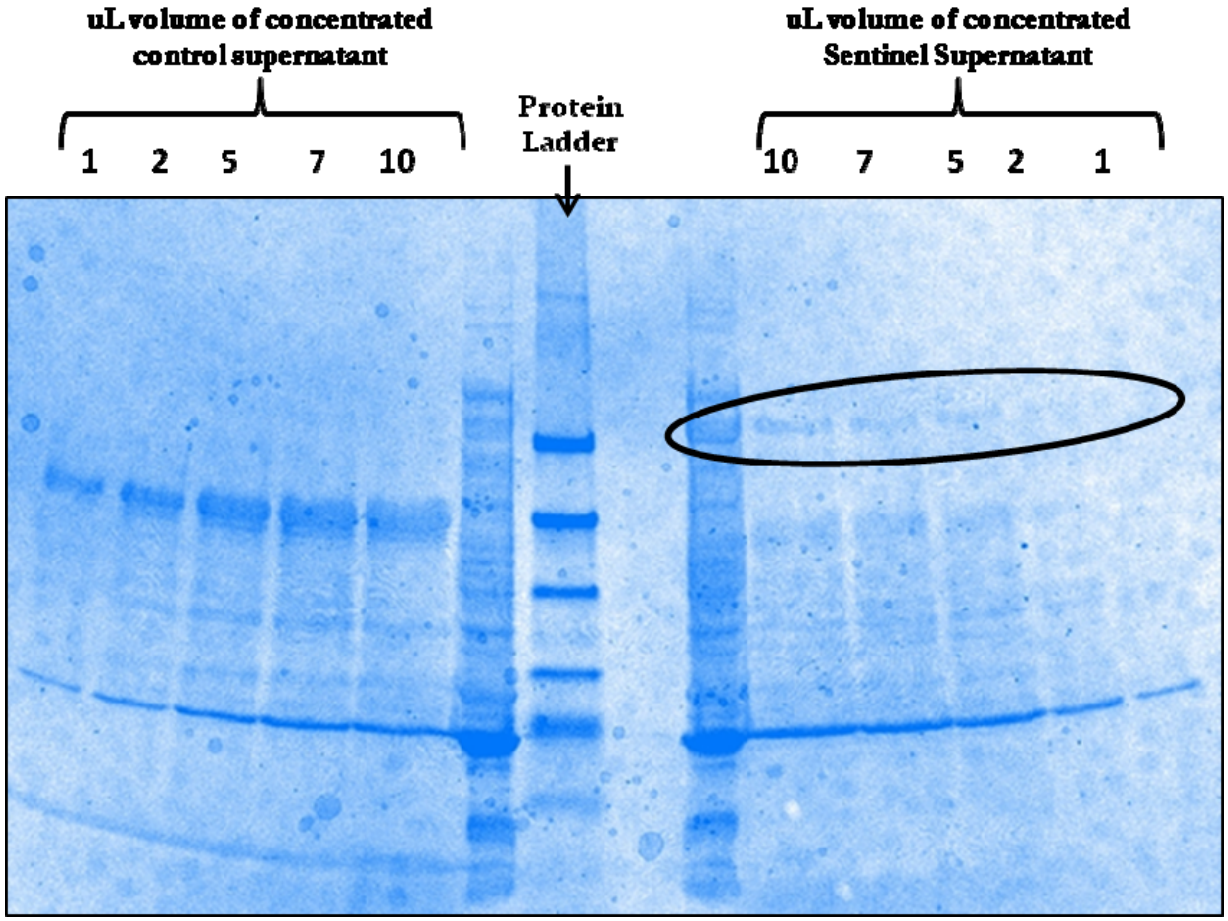

Figure 23: Commassie Blot of the concentrated supernatant obtained from the sentinels.
Every ml of the original supernatant is equivalent to 2.5 ul of the concentrated supernatant. (10) 10 ul out of 250 ul of the concentrated supernatant obtained from 100 ml of the sentinel/ control cells expressing FlgM-CoPy [O.D.—1.26]. (7) 7 ul out of 250 ul of the concentrated supernatant obtained from 100 ml of the sentinel/ control cells expressing FlgM-CoPy [O.D.—1.26]. (5) 5 ul out of 250 ul of the concentrated supernatant obtained from 100 ml of the sentinel/ control cells expressing FlgM-CoPy [O.D.—1.26]. (2) 2 ul out of 250 ul of the concentrated supernatant obtained from 100 ml of the sentinel/ control cells expressing FlgM-CoPy [O.D.—1.26]. (1) 1 ul out of 250 ul of the concentrated supernatant obtained from 100 ml of the sentinel/ control cells expressing FlgM-CoPy [O.D.—1.26].

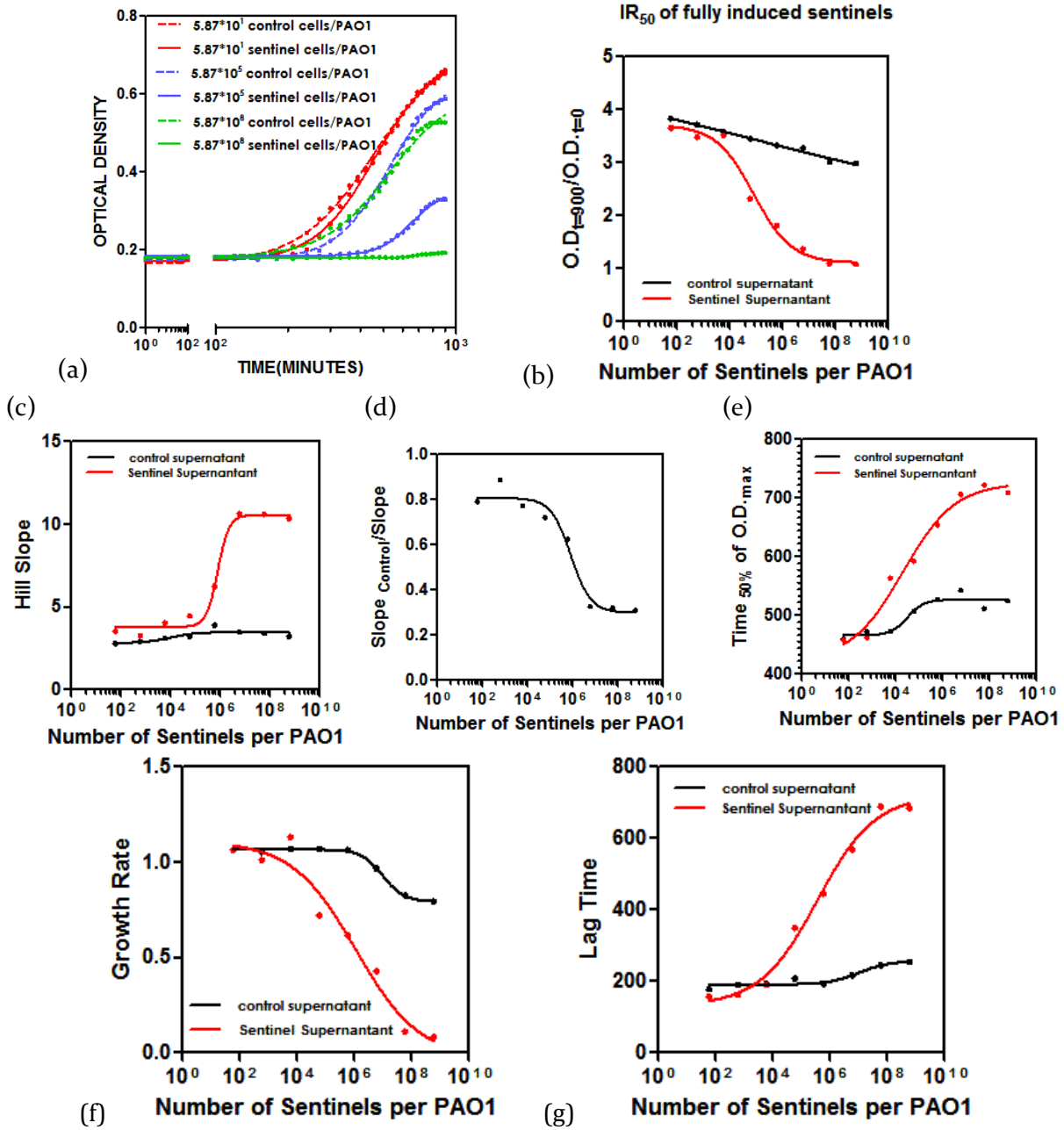

Figure 24: Analysis of the growth curves of PAO1 with the concentrated supernatant from '*maximally induced*' sentinels.

(a) Three representative dosage response curves representing different ratio of the sentinel/ control cells vs PAO1 (b) Half Maximal Inhibitory Concentration (IC50) curve for different ratios of the sentinel/ control cells vs PAO1 (c) The HillSlope of various dosage response curves calculated by non-linear regression analysis. (d) Ratio of the HillSlope of control vs sentinel supernatant. (e) Time to reach 50% of the difference between maximum and minimum optical density of any growth curve with and without the supernatant from *'maximally induced'* sentinels. This curve demonstrates that the supernatant from *'maximally induced'* sentinels caused a difference of around 200 minutes in the time it took PAO1 to reach its 50% maximum density. (f) Specific growth rate of PAO1 with different number of sentinels per PAO1. (g) Lag time of different growth curves of PAO1 with different number of sentinels per PAO1. All the experiments were performed using a 96 well plate using Tecan Plate Reader.

Information gathered from the characterization data discussed above can be used to fine-tune the sentinels' performance (e.g. detection, expression, secretion). The number of '*maximally induced'* sentinels required to kill one PAO1 cell was further verified by co-culturing the sentinels and PAO-1 in that ratio on a LB agar plate and observing them under a Zeiss microscope with 10X objective. This experimental setup is shown in **Figure 25**. 100 ul of constitutively red PAO1 of O.D.=0.001 was evenly spread on a 85 mm wide petri dish filled with 40 ml of LB agar. 10 ul of the constitutively green sentinels/control cells of O.D.=1 was pipetted on the agar surface which forms a 4 mm wide circle. The composition of the droplet is calculated in **Figure 25** and is about $3*10^7$ sentinels with 150 PAO1. This means that in the droplet there are approximately 10^5 sentinels for each PAO1 which is 10 times the minimum number of sentinels needed to kill each PAO1. In this experimental setup the sentinels are also '*maximally induced'* because of the QS signals produced by evenly spread PAO1 in the neighborhood. Therefore, killing of PAO1 by the sentinels should be observed in the immediate vicinity of the droplet where all the requirements are met. This droplet was observed under the microscope for 7 hours and the images at time T=0 and T=7 hrs are shown in **Figure 26**. The *E. coli* in the negative control are the cells which can detect PAO-1 but do not produce FlgM-CoPy in response. At T=7 hrs the concentration of PAO-1 (indicated by red fluorescence) is significantly lower, essentially undetectable, when the sentinels (green) are present as compared to when the control cells are present. In this Figure, the amount of green fluorescence (indicative of the number of sentinels) is also a little different than the control. My hypothesis for this observation is that producing FlgM-CoPy puts a lot of metabolic stress on the sentinels and hence their growth rate is slightly lower as was also shown in **Figure 11.**

The reason for co-culturing the sentinels and PAO1 in this fashion, as opposed to mixing them in the killing ratio and counting CFUs is because there is a mismatch between the number of PAO1 needed to '*maximally induce'* the sentinels and the amount of FlgM-CoPy secreted by the sentinels required to kill that many PAO1. According to **Figure 5** almost $1*10^9$ PAO1 are needed to '*maximally induce'* the sentinels. But according to **Figure 24 (b)** greater than $1*10^{13}$ sentinels will be needed to kill $1*10^9$ PAO1. Any number less than $1*10^9$ PAO1 is not enough to produce '*maximal induction'* but this number is very big to be reliably observed by counting CFU. The proposed experimental setup in **Figure 25** achieves both the conditions of '*maximal induction'* and killing ratio simultaneously and hence is able to demonstrate the 'Sense and Destroy' functionality.

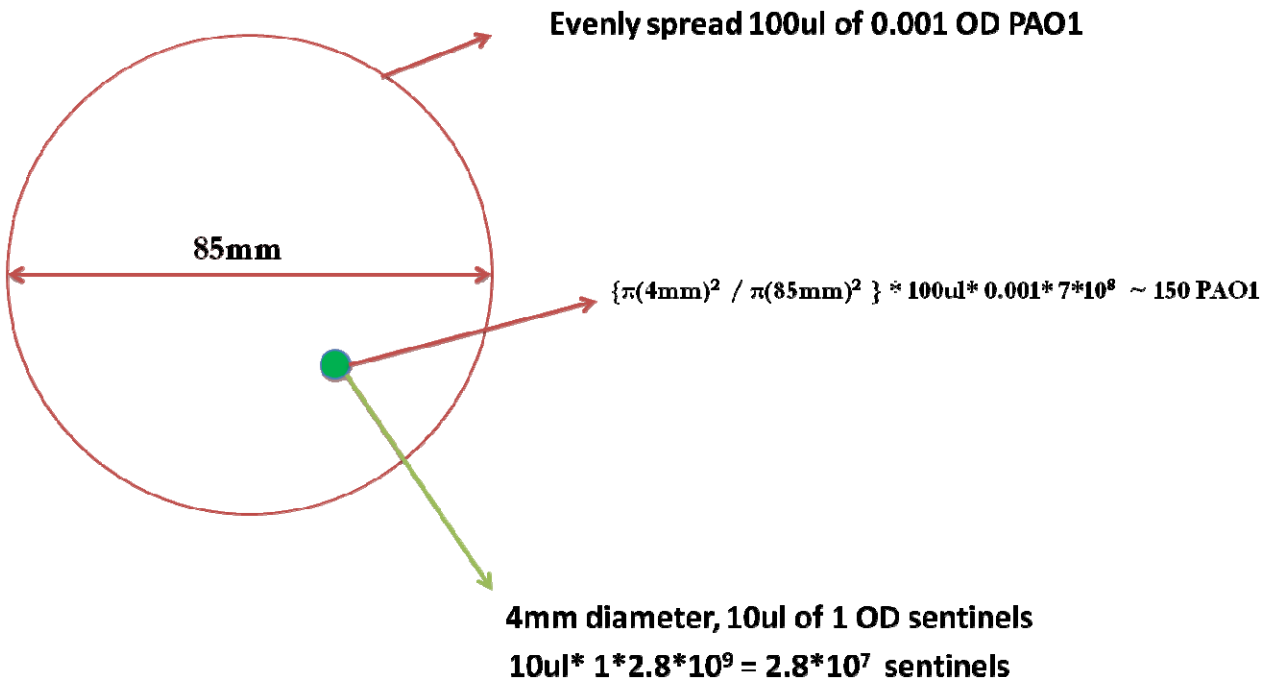

Figure 25: Experimental setup for co-culturing the sentinels and PAO1.
Droplet of sentinels over a bed of PAO1 is observed under 10X objective of Zeiss microscope. Diameter of the sentinel droplet is 4mm. Diameter of the entire plate is 85mm. Since PAO1 is evenly spread over the entire plate, an approximate number of *PAO1* present in the droplet area can be calculated by the following equation. (number of PAO1 per unit area of the plate) * (area of the droplet). As shown in the figure the number of PAO1 present in the sentinel droplet area is ~150. Similarly the number of sentinels present in the droplet can be calculated by knowing the volume and optical density of the droplet. CFU of *E. coli* in 1 O.D. can be approximated from **Figure 20**. Using these numbers the number of sentinels in the droplet is almost $3*10^7$. These numbers makes the ratio of sentinels per PAO1 cell in the droplet area greater than 10^4 and hence according to **Figure 24** killing should be observed.

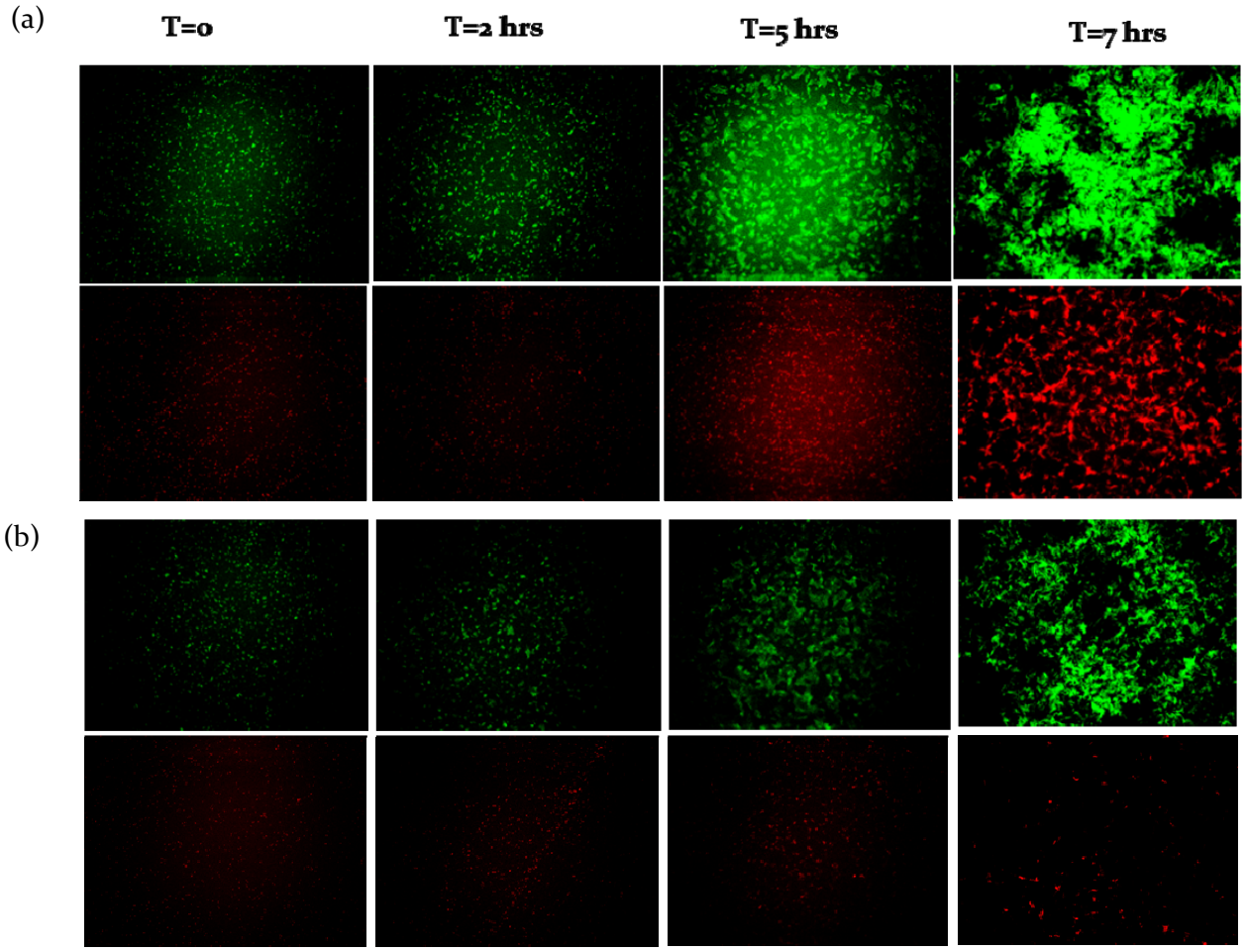

Figure 26: Microscopy images of Sentinel droplet on a bed of PAO1.
(a) T=0, 2, 5, 7 hrs images of the control droplet on PAO1 bed. (b) T=0, 2, 5, 7 hrs images of the sentinel droplet on PAO1 bed. PAO1 is constitutively red and *E. coli* sentinels and control cells are constitutively green. This figure shows that PAO1 is almost completely killed when incubated with the sentinels whereas it grows when incubated with the control cells.

.

VI. Probiotic Chassis for Bacterial 'Sense and Destroy'

In 1917, Alfred Nissle isolated an anaerobic probiotic strain of *E. coli* (*Escherichia coli* Nissle 1917 (EcN)) from the faeces of a World War I soldier who did not develop enterocolitis during a severe outbreak of shigellosis [141, 142]. Since then this strain has been used as a natural remedy against acute cases of infectious intestinal diseases. EcN has exhibited a number of fitness factors against enteric pathogens (e.g. microcins, adhesins, and proteases) and lacks prominent virulence factors (e.g., hemolysin, P-fimbrial adhesions etc.) [143]. This coupled with the demonstration of probiotic properties in several animal models for experimental colitis makes this strain a promising choice for the 'Sense and Destroy' sentinel chassis.

Therefore after successful laboratory results for the 'Sense and Destroy' in the lab strain of *E. coli*, I transferred the experimental system into *E. coli* Nissle which frequently inhabit the human urinary tract. PAO1 is one of the biggest causes of urinary tract infections and engineered *E. coli* sentinels can provide an alternate treatment strategy against these infections. In **Figure 27**, expression and secretion of FlgM-CoPy from *E. coli* Nissle is compared to the laboratory strain of *E. coli*, MG1655. This figure demonstrates that the secretion of FlgM-CoPy is similar and the system performance should not be affected by the change of chassis. Therefore it is possible to transfer the system from the laboratory strain of *E. coli* to a probiotic strain of bacteria for a more realistic application [144]. In the future more rigorous experiments are needed towards this direction.

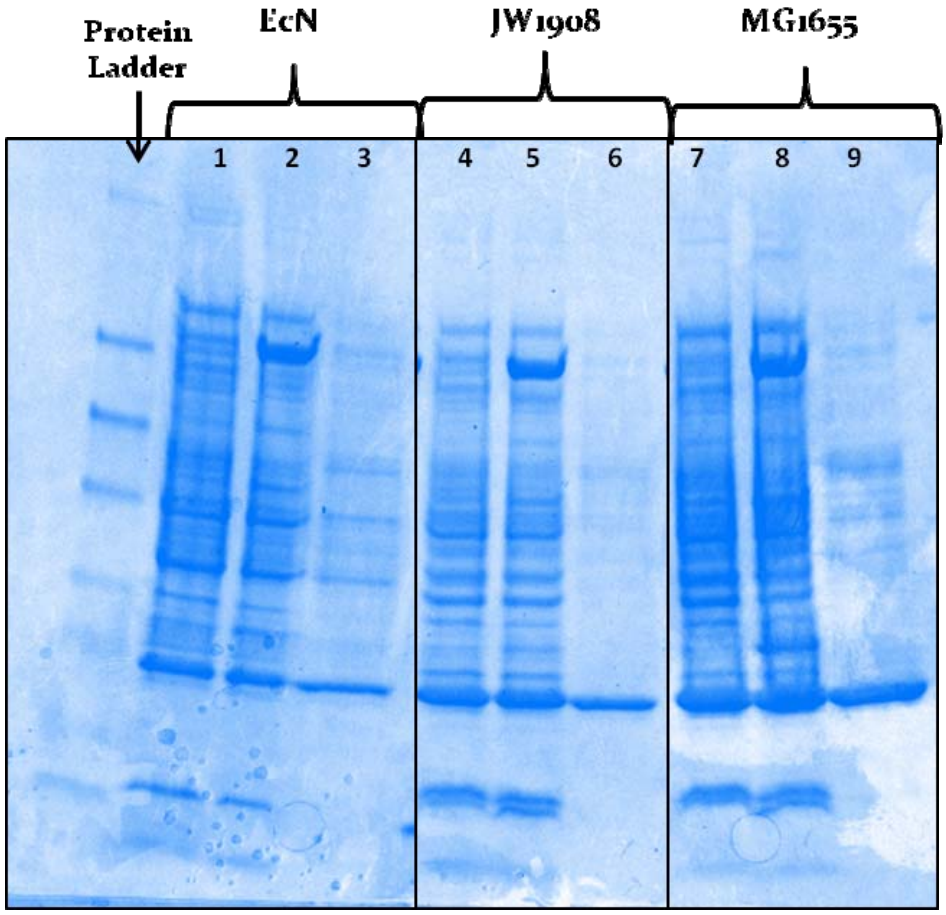

Figure 27: Comparison of the protein expression profile from three different *E. coli* strains.
(1) 20 ul from 250 ul uninduced EcN cells with FlgM-CoPy [O***.D.*—1.0]** suspended in 41 ul of sample Buffer (2) 20 ul from 25 oul EcN cells with FlgM-CoPy [O.D.—2.4] induced and incubated with 10 uM 3OC12HSL for 4 hours and suspended in 100 ul of sample Buffer (3) 20 ul out of 250 ul of concentrated supernatant of EcN cells with FlgM-CoPy [O.D.—2.4] induced and incubated with 10 uM 3OC12HSL for 4 hours and the cells are completely filtered out. (4) 20 ul from 250 ul uninduced JW1908 cells with FlgM-CoPy [O.D.—1.0] suspended in 41 ul of sample Buffer (5) 20 ul from 250 ul JW1908 cells with FlgM-CoPy [O.D.—1.77] induced and incubated with 10 uM 3OC12HSL for 4 hours and suspended in 74 ul of sample Buffer (6) 20 ul out of 250 ul of concentrated supernatant of JW1908 cells with FlgM-CoPy [O.D.—1.77] induced and incubated with 10 uM 3OC12HSL for 4 hours and the cells are completely filtered out. (7) 20 ul from 250 ul uninduced MG1655 cells with FlgM-CoPy [O.D.—1.0] suspended in 41 ul of sample Buffer (8) 20 ul from 250 ul MG1655 cells with FlgM-CoPy [O.D.—2.4] induced and incubated with 10 uM 3OC12HSL for 4 hours and suspended in 100 ul of sample Buffer (9) 20 ul out of 250 ul of concentrated supernatant of MG1655 cells with FlgM-CoPy [O.D.—2.4] induced and incubated with 10 uM 3OC12HSL for 4 hours and the cells are completely filtered out.

VII. Summary and Discussion

In this chapter I elaborated a mechanism to construct a bacterial 'Sense and Destroy' system and discussed experimental results and their analysis. In the future, different constituents can be used to make this system more effective in any given setting and against different pathogens. In the current study, I used Quorum Sensing to detect PAO1. The sensitivity of the pathogen detection can be further increased by using a signal amplifier. As discussed, the specificity and sensitivity of detection can also be enhanced by using directed evolution of the transcription factors [145]. Another way to improve pathogen specificity is to build an AND gate of all the signals produced by PAO1. For example a two input AND gate that turns on only when both the QS molecules, 3OC12HSL and C4HSL, produced by PAO1 are present will significantly lower the false detection rate.

I elaborated a novel method of engineering proteins in order for the sentinels to precisely kill the pathogen. This approach resulted in a chimeric protein, CoPy that specifically kills PAO1 while leaving the *E. coli* sentinels relatively intact. Different growth curves of PAO1 under different concentrations of CoPy were curve fitted with sigmoidal dosage response equation and EC50 and HillSlope corresponding to each curve was calculated. For each curve, HillSlope represents the growth rate and EC50 represents the time to reach 50% of the difference between maximum and minimum optical density. As shown in **Figure 10 (a)**, each growth curve is a sum of three phases i.e. lag phase , exponential phase and stationary phase [110]. The first phase is the lag phase where the bacteria are adapting to the growth conditions and synthesizing RNA but not dividing. As shown in **Figure 10 (b)** the length of this phase increases with higher concentrations of CoPy because CoPy is toxic to PAO1. In the exponential phase bacteria start to double and the growth rate of PAO1 will depend on the concentration of CoPy and its killing potency. As shown in **Figure 10 (c)** and **Figure 9 (c)** higher concentrations of CoPy correspond to lower growth rate and higher values of HillSlope.

HillSlope is smaller for steeper curves and higher for shallow curves. EC50 is higher for growth curves under higher concentrations of CoPy because it takes PAO1 longer to reach 50% of the difference between maximum and minimum optical density. As shown in **Figure 9** (a & c), the HillSlope of PAO1 growth curve with 2.88 nM CoPy is ~3 and the $\text{HillSlope}_{\text{control}}/\text{HillSlope}_{\text{CoPy}}$ is ~1. Whereas the HillSlope is ~13 for the PAO1 growth curve under 1000 nM of CoPy and the $\text{HillSlope}_{\text{control}}/\text{HillSlope}_{\text{CoPy}}$ is ~ 0.23. For 1000 nM CoPy, the optical density of PAO1 changed

from $O.D._{min}$=0.18 to $O.D._{max}$=0.2 and the growth curve is almost a straight line parallel to x axis. As shown in **Figure 9** (b) the growth rate for 1000 nM CoPy is near zero. Hence the minimum value of $HillSlope_{control}/HillSlope_{CoPy}$ attained in this experiment is 0.23.

Subsequently, I explained and tested two mechanisms to release the engineered pathogen specific toxin into the extracellular medium. First, by self-lysis where the sentinels release large amounts of toxin by exploding themselves and committing suicide. Alternately, sentinels can use a secretion tag to transport the toxin into the extracellular milieu without lysing. An approach similar to self-lysis was recently published by another group [146] where the authors were able to demonstrate that the growth of *P. aeruginosa* ln7 co-cultured with the engineered *E. coli* in the ratio 1:4 was inhibited by 90%. Even though simpler, this modus operandi has certain disadvantages. First, the toxin used in this system is only effective against *P. aeruginosa* ln7 but ineffective against 70% *Pseudomonas* strains which are naturally resistant to the toxin used in their system. Whereas the system described in this thesis is effective against all strains of *Pseudomonas* infections. Second, in this design the sentinels commit suicide to release the toxin and hence they cannot adapt if the pathogen survives. The entire amount of the toxin will be released in one burst and therefore the sentinels cannot release the toxin continuously until the pathogen dies. These sentinels are ineffective against a pathogen which becomes resistant to the toxin. Therefore I believe that an approach where the sentinels secrete the toxin instead of lysing themselves is more sophisticated and appropriate in the long run since they can be engineered to adapt to the resistant pathogen. Hence I focused my efforts to program the sentinels to secrete the toxin to kill the pathogen.

Secretion of recombinant proteins is very important for many biotech applications and several groups have worked on this problem for quite some time [67, 68, 147-149]. Most of the available techniques only allow secretion of the proteins in the periplasmic space of *E. coli*. As I discussed in the Introduction only type I, III, IV and VI secretion systems are known to enable transport of proteins in the extracellular medium in one step. Out of these, type I system is known to secrete unfolded or inactive proteins therefore this mechanism is not useful for my system. Additionally the secretion tag for this system needs to be on the C-terminal of the transported protein. In my system the C-terminus of CoPy is the nuclease domain and hence this type of secretion system is not useful to the current version of the 'Sense and Destroy' system. The remaining three mechanisms are mainly used by pathogenic bacteria to translocate proteins from their cytoplasm to that of their eukaryotic hosts [71, 150, 151]. Type IV system is mostly

characterized for the transport of DNA [81, 82] whereas type VI secretion system is only recently identified and details of its mechanism are still emerging [73, 86]. Flagellar machinery is analogous to the type III secretion apparatus except that it is used by the bacteria to assemble flagella and secrete flagellar components in the medium [123, 126, 127]. Therefore, I employed flagellar system to secrete CoPy. FlgM is a Sigma (σ) factor used in the regulation of the bacterial flagellar machinery and is naturally secreted into the extracellular space [126, 132, 136, 152]. Hence FlgM was utilized as a candidate secretion tag.

It was demonstrated that FlgM is capable of transporting ~5% of the total CoPy produced in the cytoplasm. This efficiency is comparable to the secretion efficiency achieved using various other techniques [118]. It is possible that some of the FlgM-CoPy is trapped in inclusion bodies [118]. Secretion can be improved in future by testing this hypothesis and resolving it as shown in [118]. Secretion efficiency can be further increased by modifying the flagellar machinery involved in exporting native FlgM [128, 132, 135, 153-158]. There are several factors which affect the expression and secretion efficiency of recombinant proteins from *E. coli*. Presence of recombinant proteins in the extracellular medium can be improved by approaching the problem from two sides. One approach is to optimize the expression of recombinant proteins and another approach is to increase secretion. Gene expression dynamics are controlled by the half-life of mRNA which can vary from seconds to maximally 20 minutes in E. coli at 37C [159, 160]. Two exonucleases RNase II and PNPase and the endonuclease RNase E are responsible for the degradation of mRNAs. Strains containing a mutation in the gene encoding RNaseE (*rne*131 mutation) are available for the enhancement of mRNA stability in recombinant expression systems (Invitrogen BL21 star strain) [161]. Non-optimal codon bias of the recombinant protein can cause transient pauses in translation at the non-optimal codons [162]. This problem can either be solved by codon-optimization or simultaneous expression of gene encoding the tRNA cognate to the problematic codons [163]. Expression of recombinant proteins induces a metabolic burden on the host which results in the down regulation of the hosts housekeeping genes including components of the protein synthesis machinery [164]. If the recombinant protein deviates considerably then amino acid starvation can occur. This in turn will lead to extensive reprogramming of gene expression patterns and down regulation of the majority of genes involved in transcription, translation and amino acid biosynthesis [165]. Addition of the appropriate amino acids can alleviate this stress. This stress also leads to increase *in vivo* proteolysis of the recombinant protein. Use of protease deficient host strains, heat shock deficient strains, chaperone co-

expression and protease inhibitor co-expression [166] can circumvent this problem. Non uniform expression in a population of cells can be another reason for low quantities of FlgM-CoPy in the supernatant. The expression dynamics were verified by looking at the expression of downstream GFP in the absence and presence of the inducer (**Figure 51**) with FACS. This figure shows that all the cells are expressing GFP and hence FlgM-CoPy with the presence of the inducer.

Besides improving gene expression, another avenue to increase the amount of recombinant proteins in the extracellular medium is by improving the secretion process. Protein folding is an important consideration in improving that process. For example Sec transport machinery requires proteins to be unfolded before export. [70]. Therefore the rate of folding or unfolding will affect the efficiency of the export. Rate of folding and unfolding will depend on the number of disulfide bonds in a protein. Pore size of the secretion machinery is another critical factor. It should be large enough to allow proteins which may have secondary characteristics such as alpha-helices to pass through. The more complex the protein structure is the less competent it is for export. Another problem is the formation of inclusion bodies in the cytosol and periplasm when using strong promoters to express the recombinant proteins. Aggregation of recombinant proteins can be minimized by optimizing temperature, expression rate, host metabolism and target protein engineering [117, 167]. Two *E. coli* mutant strains, C41 (DE3) and C43 (DE3), allow over-expression of some globular and membrane proteins unable to express at high-levels in the parent strain BL21 (DE3) [168]. Directed evolution of the secretion apparatus can give hypersecretion mutants. For example it was shown that certain mutation in HlyA protein caused increased secretion from type one secretion system [169]. Similarly, efficiency of FlgM secretion was improved in *fliS* and *fliT* mutants [132]. However, a deletion of FliC, D, S, T genes did not result in increase of FlgM-CoPy secretion as shown in **Figure 50**. Another hyper FlgM secretion mutant is sigma28* (H14D) which can be tested in the future for its efficiency. These examples demonstrate that some secretion efficiency may be improved by genome engineering approaches. The effect of fusing FlgM to CoPy on CoPy's potency was characterized by comparing the killing efficiency of non-secreted FlgM-CoPy to CoPy. Similar comparison was done between non-secreted FlgM-CoPy and the secreted FlgM-CoPy. This analysis revealed that adding a secretion tag to CoPy makes it less potent while the process of secretion itself has only minimal effect on FlgM-CoPy's potency.

Once I verified the individual components of the 'Sense and Destroy' system, the entire system was characterized by co-culturing PAO1 and engineered sentinels in a liquid medium in

different ratios as shown in supplementary **Figure 52 (a).** CFU of PAO1 and *E. coli* were counted the next day. As shown in **Figure 52 (b),** there is no significant difference in the growth of PAO1 with or without the engineered *E. coli*. This experiment was repeated in the presence of maximally inducing amounts of exogenous 3OC12HSL. As shown in **Figure 52** (c), there is still no significant difference in the growth of PAO1 with or without engineered *E. coli*. Therefore the hypothesis is that the concentration of FlgM-CoPy per PAO1 cell in the liquid medium is not sufficient to observe the desired killing effect. To clearly understand the dynamics of PAO1 killing, the number of sentinels needed to kill one PAO1 was calculated. For this, different amounts of PAO1 were grown in the same amount of filter sterilized supernatant collected from '*maximally induced*' sentinels and the growth of PAO1 was monitored. The resulting growth curves were evaluated and their growth functions were established by curve fitting with sigmoidal dosage response equations. This demonstrated that at least 10,000 '*maximally induced*' sentinels are needed to kill one PAO1. At the same time, one PAO1 cell is not enough to '*maximally induce*' the 10,000 sentinels required to produce enough FlgM-CoPy. It is evident from this analysis that in order to lower the number of sentinels needed to kill one PAO1, the secretion efficiency and the pathogen detection limit needs to be increased so that the sentinels can start secreting larger amounts of CoPy before PAO1 reaches high densities.

I have discussed some of the possible ways to increase the secretion. A tenfold increase in secretion will reduce the number of sentinels needed to kill one PAO1 to 1000 [132]. The potency of FlgM-CoPy was tenfold less than CoPy which is the cost the sentinels pay to secrete CoPy. FlgM is 100 aa long and its size could be one of the factors affecting the killing efficacy [132]. The minimum length of FlgM needed to secrete CoPy can be found by various deletion studies which can increase the potency. A further tenfold increase in killing efficacy will reduce the number of sentinels needed to kill one PAO1 to 100. The sentinels can be made more sensitive to PAO1 by integrating a signal amplifier and may allow even fewer sentinels to kill one PAO1. Since the number of sentinels needed to kill one PAO1 cell is very high, it was difficult to co-culture them in liquid in the ratio of 10,000:1 and accurately study the killing dynamics by counting colony forming units (CFU) the following day because the sentinels outnumbered PAO1 in any dilution. In **Figure 52** I have demonstrated that there was no change in the number of CFU's of PAO1 when co-cultured with the sentinels in a liquid culture. This indicated that probably the observed death of PAO1 is a concentration based killing. The concentration of FlgM-CoPy seen by individual PAO1 in a 96 well plate is much higher than the concentration achieved in a turbulent liquid

culture. To verify this hypothesis the 'Sense and Destroy' functionality was visually demonstrated by locally observing a droplet of the sentinels over a bed of PAO1 on a semi-solid agar plate with a microscope. The semi-solid environment is an approximation of the bacterial micro-environments in the gastrointestinal tract [170]. In a semi-solid environment the diffusion of FlgM-CoPy is much reduced compared to the liquid medium and local concentration of FlgM-CoPy per PAO1 cell will be much higher than the average concentration of FlgM-CoPy for all PAO1 cells. Furthermore in this experiment the number of sentinels per PAO1 in the local environment of the droplet is in excess of 10,000. Therefore the killing of PAO1 was observed in a semi-solid environment.

In the Introduction, I discussed several ways through which pathogenic bacteria can gain resistance to various antibiotics. I argued that suitable prevention and drug administration techniques are equally useful to curb bacterial resistance besides the discovery of new antibiotic compounds. Bacteria can gain resistance against 'Sense and destroy' system by mutations in the QS molecule or the receptor of CoPy. However it is shown that QS molecules are essential for the virulence of PAO1 and a non-functional quorum sensing will result in diminished virulence. Similarly the receptors of CoPy are used for transport of essential nutrients for example vitamin B12 and iron and colicin resistance comes at a cost. It was shown that the resistant strains grow slower than the sensitive ancestors [171]. Using a combination of bacteriocins that work by different mechanisms would theoretically reduce the emergence of resistance. Another widespread mechanism by which bacteria can gain resistance is by horizontal gene transfer. Even though this process cannot be completely prevented, its occurrence can be reduced by several barriers. Chromosomal integration of the 'Sense and Destroy' circuit, instead of on a plasmid, will reduce plasmid based transfer. Furthermore, an effective barrier against conjugative transfer can be created by surface exclusion [172-174]. Detailed analysis showed that surface exclusion works at two levels: TraT changes the outer surface of the cell and reduces its receptiveness to the F pilus about 10-fold, TraS sits in the inner membrane and prevents DNA entry by about 100-fold [172, 175, 176]. Additionally, a synthetic circuit can be engineered to contain several rare gene sequences which will promote their degradation in foreign host [174, 177].

The lessons learnt from the experiments described above can be used in the future to engineer an improved 'Sense and Destroy' system. It was shown recently that PAO1 switches to C4HSL as the Quorum Sensing molecule at very high densities [178]. Since the sentinels are designed to detect only 3OC12HSL they will stop responding to PAO1 at high densities. To get

around this problem an OR gate can be implemented using a dual promoter system which is activated in the presence of either 3OC12HSL or C4HSL. Recently it was published that wild type PAO1 can outcompete other gram-negative bacteria growing in the same milieu by injecting a toxin [84]. PAO1 are immune to this toxin because they simultaneously produce an anti-toxin against it. This issue can be resolved by having the sentinels express the antitoxin as well. However this phenomenon was not observed as *E. coli* sentinels grew at the same rate with and without PAO1 as shown in **Figure 53**. In order to achieve a perfect pathogen 'Sense and Destroy' system it is pertinent to understand the gene expression profile of *E. coli* cells when co-cultured with the pathogen. New insights obtained from studying this data will lead to a more robust system design.

CHAPTER 3 -GENETICALLY PROGRAMMABLE MAMMALIAN SENSE AND DESTROY

I. Introduction

One of the most important functions of human skin is to act as a barrier between internal organs and the external environment by blocking foreign bacteria. This barrier is destroyed in burn patients. Depending on the depth and extent of damage to the skin, burns can be either superficial or full-thickness. Full thickness or third degree burns are very serious and will heal only at the edges by scarring, unless skin grafting is done. Unfortunately people with large burns lack any healthy skin to act as grafts. To make matters worse, skin grafts from foreign sources are rejected far too often. To get around this problem surgeons use artificial skin products made of scaffolds of collagen, which encourage growth of new dermis. More recently, doctors embeded collagen scaffolds with skin cells to help skin grow. The latest advances in tissue engineering [179, 180] allowed scientists to harvest patients' own skin cells including skin stem cells and spray them directly over the wound. Besides the difficulty in growing new skin in severely burnt victims the underlying vascular system is also destroyed. As shown in **Figure 28 (a)** this prevents any antibiotics from reaching the site of injury thus making it difficult to treat the life threatening bacterial infections. It could take up to a week or two before the damaged blood vessels can grow and reconnect to the new dermis and allow access to the infection fighting machinery of the immune system. Hence infecting bacteria can easily reopen the wound and destroy a graft. Currently, doctors prevent this by continually wrapping the wounds by antibacterial bandages [181]. The bacterial 'Sense and Destroy' system discussed in the previous chapter has enormous benefits but its implementation is limited in areas on the human body already populated with bacteria. For instance it fails to provide solution to blood or tissue borne infections where sterility is the key for infections in severely burnt victims. A goal for my research is to use the scientific insights obtained from the bacterial 'Sense and Destroy' system to genetically program mammalian cells [49, 182-185] that will detect and destroy PAO1 (major cause of hospital infections) in the absence of a healthy immune system. These cells can be embedded in smart bandages where they can play their traditional role of healing the wound while simultaneously protecting the victims from incoming infections.

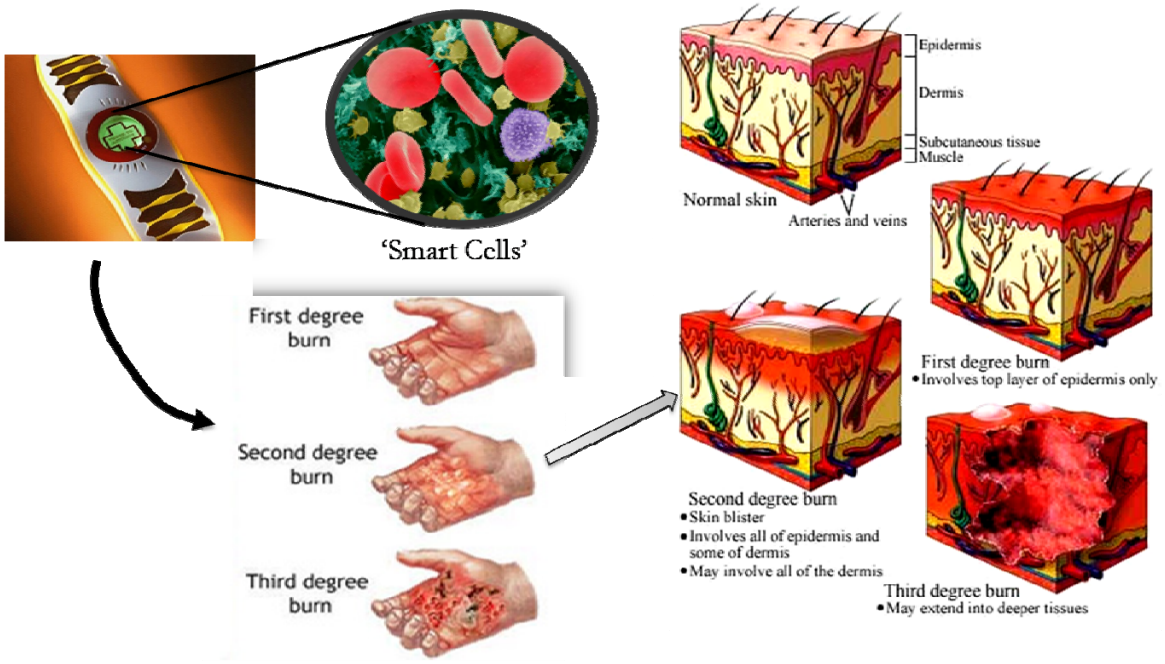

(a)

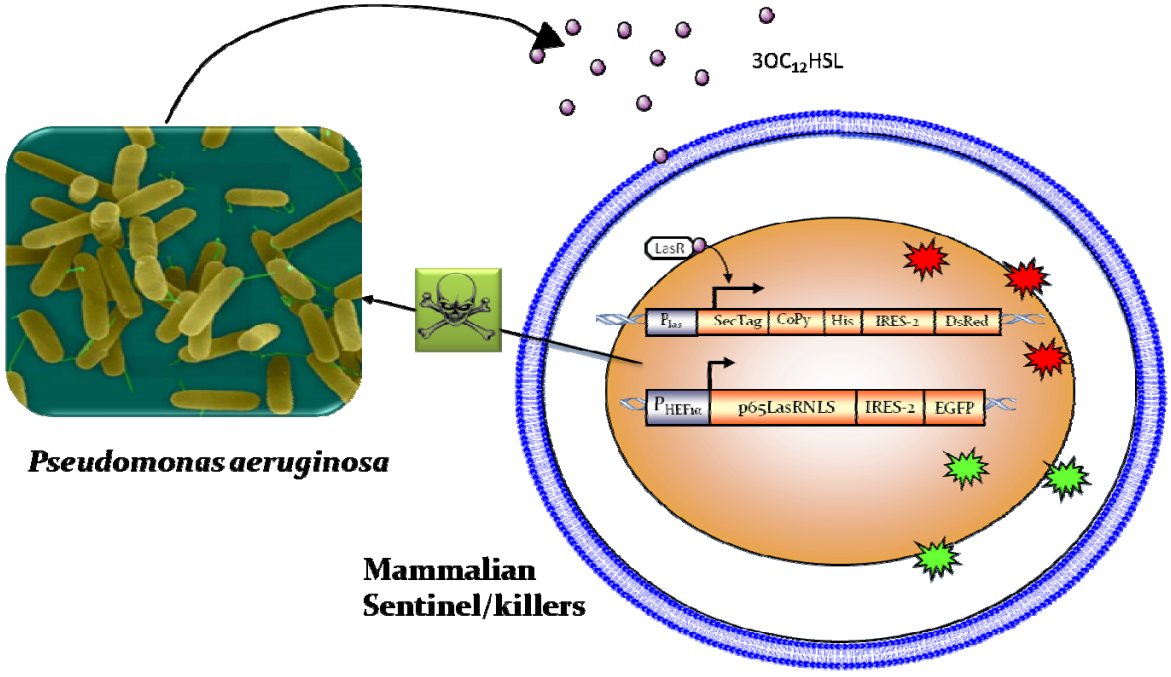

(b)

Figure 28: Mammalian 'Sense and Destroy' System.
(a) Smart Bandage employing the mammalian 'Sense and Destroy' system (image is taken from Battelle.org news listing) (b) Genetic composition of the mammalian 'Sense and Destroy' System. Similar to the bacterial 'Sense and Destroy' system, mammalian sentinels detect PAO1 using Quorum Sensing molecules produced by the pathogen and secrete a pathogen specific toxin. As a first attempt, mammalian codon optimized version of CoPy (discussed in chapter 2) was used.

Figure 28 (b) shows detailed architecture of the mammalian 'Sense and Destroy' system. Similar to its bacterial counterpart, mammalian cells detect the QS molecule produced by PAO1 and secrete a codon optimized CoPy to specifically kill PAO1. In the following sections I discuss the experimental progress made towards implementing a 'Sense and Destroy' system in mammalian cells.

II. Mammalian Sensors of PAO1

A PAO1 sensing module was constructed as a first step towards engineering a mammalian 'Sense and destroy' system. In previous efforts [8], mammalian cells were engineered to respond to 3OC6HSL. The design of a module that responds to 3OC12HSL produced by PAO1 is shown in **Figure 29 (a)** and is similar to the one that detects 3OC6HSL. A mammalian codon-optimized version of the bacterial LasR fused with p65 activation domain and a Nuclear Localization Signal (NLS) was used as a transcriptional regulator. Additionally a hybrid promoter was constructed with seven las boxes obtained from the las promoter in bacteria. The dosage response of the resulting mammalian sensor to 3OC12HSL was measured using the circuit in **Figure 30 (b)** and is shown in **Figure 30 (d).** Mean fluorescence levels of the 3OC12HSL sensor are almost 5 fold lower compared to that of the 3OC6HSL sensor shown in **Figure 30 (c).** Also, engineered mammalian sensors are not as sensitive as their bacterial counterparts. The bacterial sensors are able to respond to even 1 nM of the signal whereas mammalian sensors need 1 μM or higher of 3OC6HSL/ 3OC12HSL to elicit a comparable response. In Chapter 2, it was discussed that concentrations greater than 1 uM are toxic to mammalian cells. It was also found that AHLs are more rapidly degraded in mammalian cells by esterases and lactonases such as those of the paraoxonase (PON) gene family in the humans which has three members, PON1, PON2, and PON3 [186-188]. 3OC6HSL has a half-life of about 2 hours in mammalian cells. 3OC12HSL has an even higher degradation rate. These issues can be resolved in the future by building a 3OC12HSL signal amplification circuit. This circuit will be similar to a 3OC6HSL signal amplification circuit [8] that was discussed in Chapter 1. **Figure 29 (b)** depicts the design of a transcriptional cascade that amplifies weak 3OC12HSL signals. rtTA is a strong activator of transcription and requires only a few molecules of itself and DOX to maximally activate the TRE promoter. Hence through this design even small amount of 3OC12HSL will lead to changes in rtTA which in turn will translate into amplified EGFP response. Effect of various DOX concentrations on both the steady state and dynamic response can be further explored.

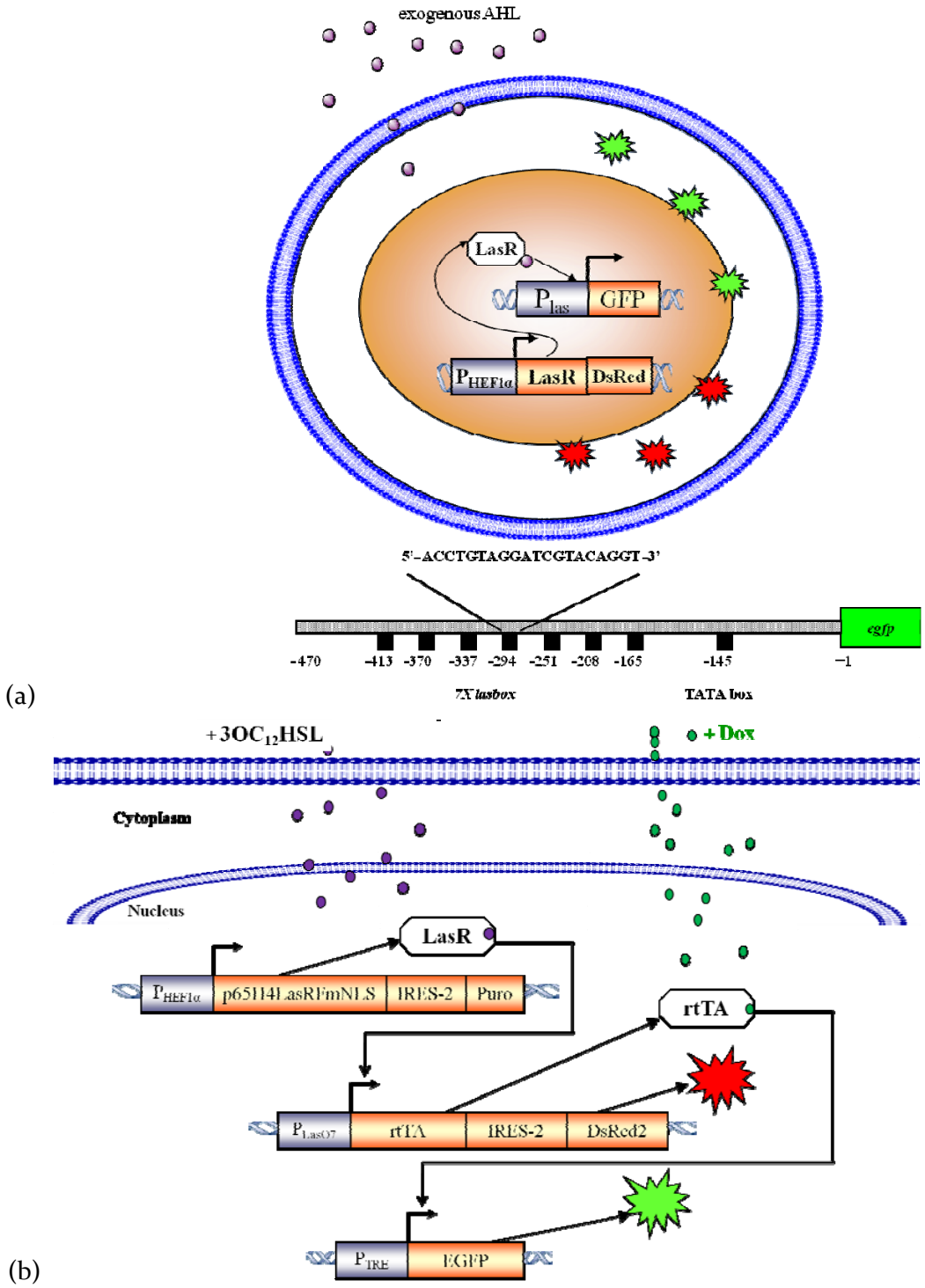

Figure 29: Circuit design of a 3OC12HSL mammalian sensor.
(a) The synthetic mammalian promoter plasO7 is based on the minimal CMV promoter and contains seven repeats of the las operator. Positions are shown relative to EGFP start codon. (b) Mammalian AHL signal amplifier circuit.

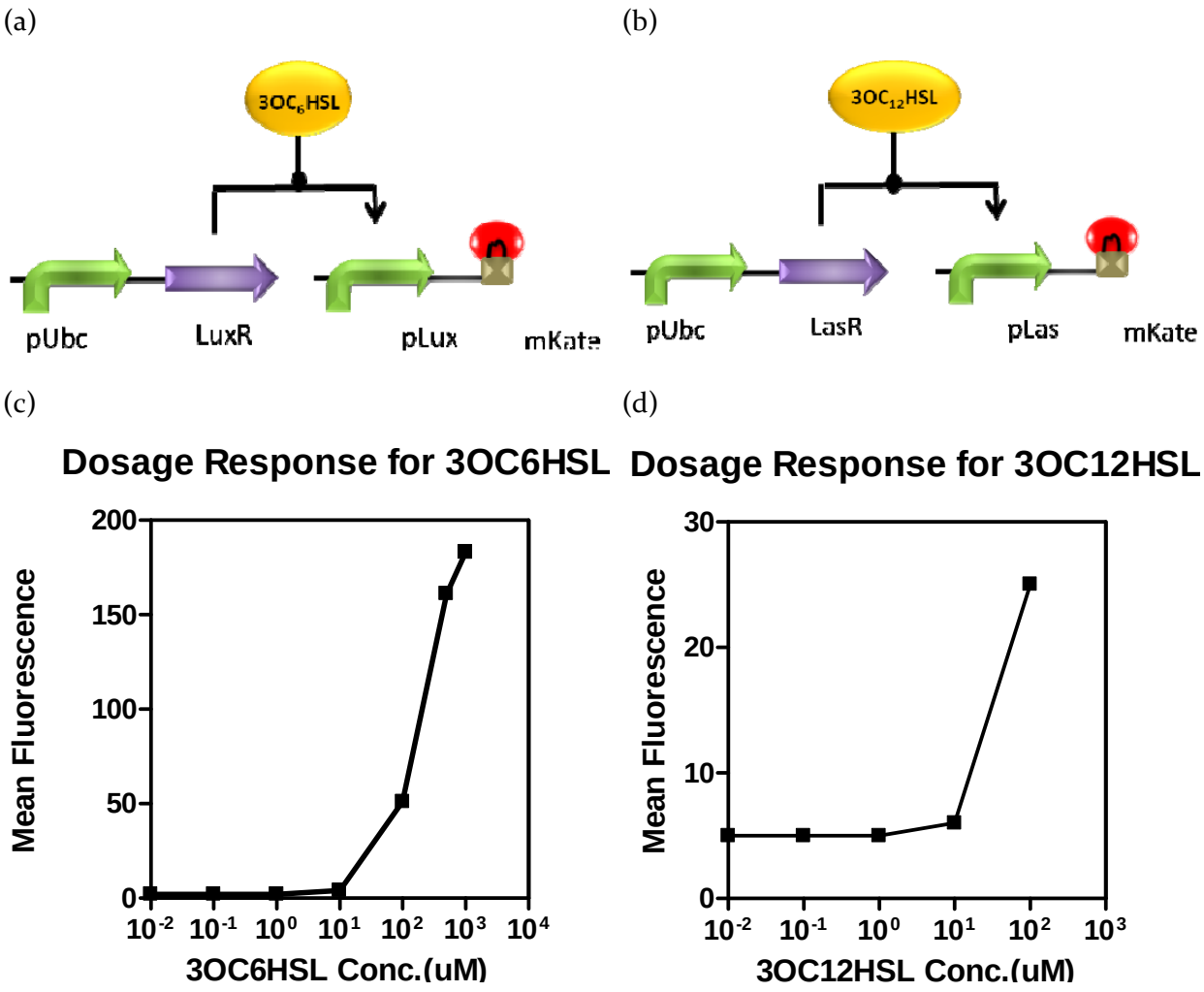

Figure 30: Mammalian sensors.
(a) Full circuit for the characterization of pLuxO7. (b) Dosage response of pLux w.r.t different concentrations of 3OC6HSL. (c) Full circuit for the characterization of pLasO7. (d) Dosage response of pLasO7 for different concentrations of 3OC12HSL.

(a)

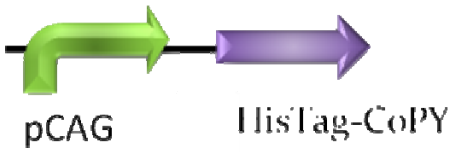

(b)

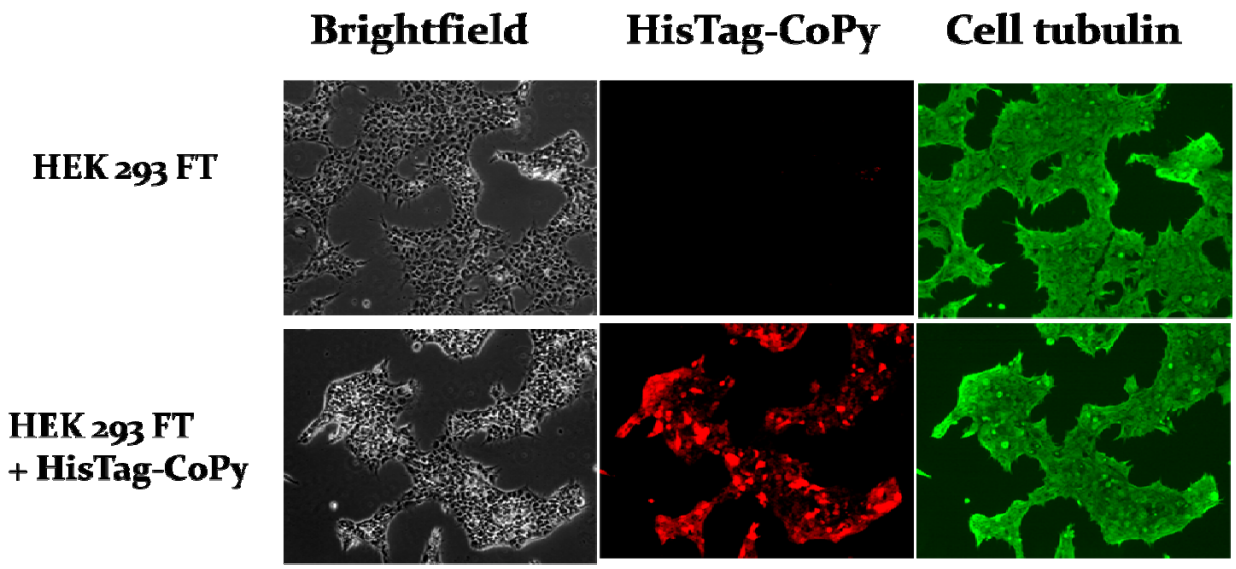

Figure 31: Mammalian cells constitutively expressing CoPy.
(a) Circuit for the constitutive expression of HisTag-CoPy. (b) Immunostaining of mammalian cells (HEK293 FT) expressing constitutive CoPy. Negative control is HEK293 FT cells which do not express CoPy. Green indicates positive immunostaining of cell tubulin. Red indicates constitutive HisTag-CoPy. BF-Brightfield Images. This result shows that mammalian cells are successfully engineered to express codon optimized CoPy.

III. Mammalian Killing Module

As shown in **Figure 28**, the mammalian sentinels should produce CoPy after they detect PAO1. For this purpose the bacterial version of CoPy was codon optimized and cloned under a strong constitutive promoter pCAG in mammalian cells as shown in **Figure 31 (a & b).** Immunostaining was done to demonstrate that the CoPy is successfully expressed and the results are shown in **Figure 31 (c)**. There is a HisTag at the N terminus of CoPy for the purpose of antibody binding. Two different fluorophores were used to differentiate between the cells and CoPy. Green is indicative of beta-tubulin of HEK293 cells and red suggests HisTag-CoPy. These cells were viewed with Zeiss microscope under 10X objective and are presented in **Figure 31 (c).** This result shows that the mammalian cells are successfully engineered to express codon optimized CoPy. In the future this CoPy will be purified and its potency against PAO1 will be validated.

IV. Mammalian Protein Secretion

The mammalian sentinels need to secrete pathogen specific toxins into the extracellular medium to kill PAO1. For this purpose some candidate secretion tags were discussed in Chapter 1. I constructed plasmids which constitutively express tagged CoPy. In the future these secretion tags can be characterized for their secretion efficiency and the best tag will be used to export a pathogen specific toxin into the medium.

V. Summary and Discussion

I used the scientific and analytical insights obtained from implementing a prokaryotic 'Sense and Destroy' system to establish the foundation for a mammalian 'Sense and Destroy' system. The Las promoter from bacteria was modified to program mammalian sentinels that respond specifically to 3OC12HSL produced by PAO1. It was found that high concentrations of 3OC12HSL are toxic to mammalian cells. In the future this problem can be addressed by integrating a signal amplifier into the system. This device will allow the mammalian sentinels to respond to minute quantities of 3OC12HSL. The mammalian sentinels were subsequently engineered to respond to 3OC12HSL by expressing optimized CoPy. The next step in the direction

of building a mammalian 'Sense and Destroy' system is to enable mammalian sentinels to secrete CoPy in response to 3OC12HSL.

In the current study, two secretion tags viz., *SS* and *SecPen* were tested in order to secrete CoPy. Further work is needed to efficiently transport CoPy into the extracellular medium. Secretion of hetrologous proteins from mammalian cells remains a difficult research problem and is very important for the success of this system. CoPy is a large protein (700aa, 84 kDa) and hence will be difficult to secrete. Therefore a library of various secretion tags should be tested and characterized for their secretion efficiency and the best candidate should eventually be used. Different cell types other than HEK293 FT, for example CHO (Chinese Hamster Ovary) cells can be employed as the mammalian sentinels since it is known that some cell types are naturally more efficient in secreting recombinant proteins [189, 190]. In addition to secretion, the toxicity of CoPy to mammalian cells remains to be verified. A possible solution to this problem can be to find a smaller protein that is easier to secrete and is specifically toxic to PAO1 but not to the mammalian sentinels. Once the secretion is observed, PAO-1 killing can be assayed by using both the supernatant and the cell lysates of the mammalian sentinels as demonstrated in case of the bacterial 'Sense and Destroy' system. Mammalian cells exhibit a severe immune response to the bacterial LPS (Lipo polysaccharide) and hence it will be difficult to co-culture the mammalian sentinels with PAO1 to characterize killing dynamics. It is possible that just expressing CoPy or any specific toxin against PAO1 is enough to improve survival of the mammalian sentinels [180].

CHAPTER 4 -ADAPTIVE RESPONSE--DELAYED, MASSIVE RELEASE OF MULTIPLE LYSINS AND CELL SUICIDE

I. Introduction

Antibiotics are one of the most important inventions of the 20th century. They have single-handedly contributed to the largest increase in life expectancy. Unfortunately their overuse is threatening to undo most of the progress made in the last century [13]. According to several statistics, infectious pathogens are becoming increasingly resistant to even the most potent of antibiotics available [10, 13, 191]. **Figure 32 (a)** shows an upward trend of the antibiotic resistance for three of the most common infectious pathogens. Furthermore there are hardly any antibiotics in the pipeline and even fewer pass FDA approval process as shown in **Figure 32 (b)** [10]. In this thesis, I propose a synthetic bacterial/mammalian system that explicitly detects PAO1 and secretes a toxin that specifically kills it. This strategy is better than antibiotics because the sentinels have the capability to respond before the pathogen reaches its disease causing density. Incomplete elimination of a pathogen with a given antibiotic is the main culprit for breeding antibiotic resistance as the surviving bacterium gets a chance to mutate and become resistant [12, 191, 192]. In my approach, the pathogen detection is highly sensitive and therefore the sentinels can kill the pathogen before it reaches its disease causing density, potentially causing significantly less harmful side-effects. Hence this approach can potentially help limit the chances of developing antibiotic resistance as it has recently been shown that in certain cases combination therapies can be more effective than independent therapy [38]. In this chapter, I will discuss how the sentinels can be further programmed to adapt if the pathogen develops resistance. The genetic code of this strategy is given in **Figure 32 (c).** In this strategy, sentinels respond to 3OC12HSL in two phases. As the first phase response, sentinels secrete FlgM-CoPy as soon as they detect AHL. After this, they wait for *'n'* hours (which can be optimized based on system parameters) and if they still detect AHL then it is an indication that the pathogen has survived. In response, the sentinels launch the second phase attack by producing another toxin (CDAP-4) and releasing it into the extracellular medium by lysing themselves through E/GFP lysis protein.

(a)

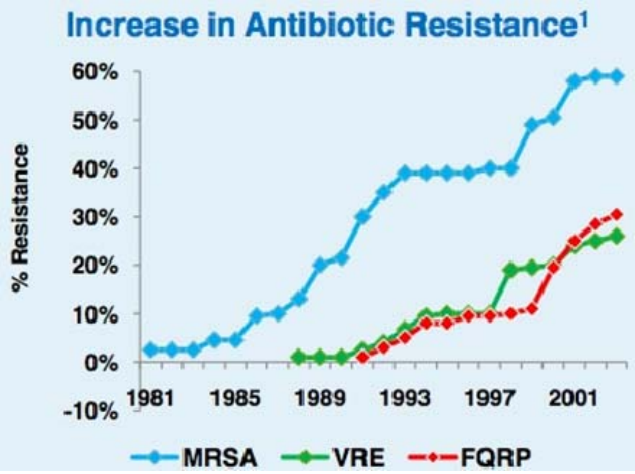

(b)

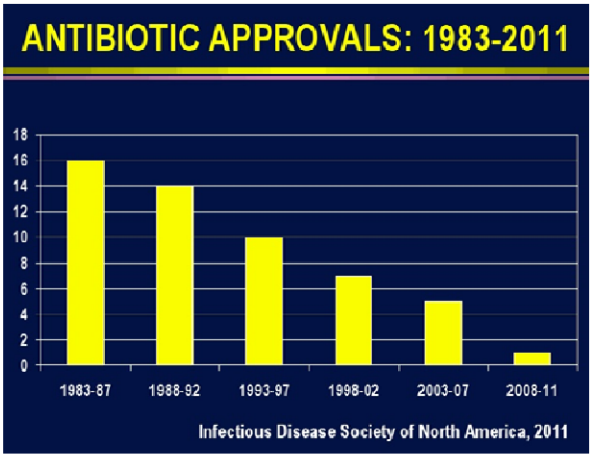

(c)

adaptive response()

```
if detect(3OC12HSL)
{
        secrete(FlgM-CoPy)
        delay(n hrs)
        if detect(3OC12HSL)
        {
                % 2nd line of defense
                produce(CDAP-4)
                % self lysis
                produce(E/GFP)
        }
}
```

(d)

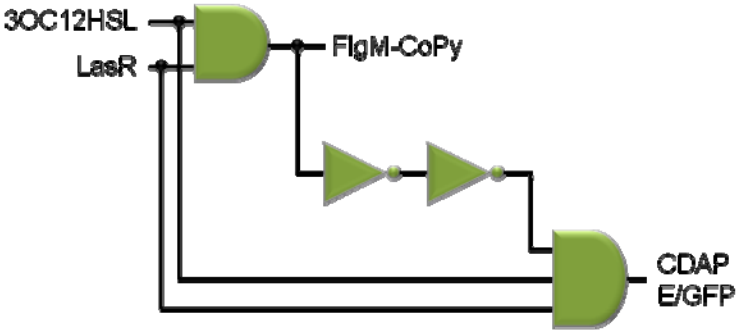

Figure 32: Adaptive 'Sense and Destroy' system.
(a) Increasing incidence of antibiotic resistant infections. MRSA- methicillin-resistant *Staphylococcus aureus*, VRE-Vancomycin resistant *enterococci*, FQRP-Fluoroquinolone-resistant *Pseudomonas aeruginosa*. Source: Centers for Disease Control and Prevention. (b) Decline in the FDA approvals of new antibiotic agents. (c) Genetic code of the adaptive 'Sense and Destroy' system (d) The combinatorial circuit obtained by using digital logic design principles for the adaptive 'Sense and Destroy' System. In the first phase FlgM-CoPy is expressed when both LasR and 3OC12HSL are present and can be represented by a two input AND gate. If 3OC12HSL is still present after a delay (introduced by 'not gates' and represented by small triangles with little bubbles after them) then the sentinels respond by expressing another toxin CDAP and lysis protein E/GFP. This functionality can be represented by a three input AND gate.

II. Bacterial Adaptive Response System

I partially implemented the adaptive response circuit in bacteria and mammalian cells. Progress made towards implementing an adaptive response system in bacteria is discussed in this section, and the advances attained for a mammalian adaptive response system are reviewed in the next section. It has already been elucidated through the implementation of 'Sense and Destroy' system that the expression of FlgM-CoPy can be programmed on the conditional presence of LasR and 3OC12HSL. According to **Figure 32 (d),** the sentinels wait for *n* hours before they 'realize' that the pathogen has survived the first stage attack. Then the sentinels employ the second stage attack. An optimized 'waiting period' can be introduced by synthetic cascades consisting of repressors (i.e. genetic logic inverters) connected in series [49, 53, 58, 59, 193, 194]. This second stage attack will involve the sentinels bursting (using E-protein discussed in Chapter 2 Section III (a)), and releasing large quantities of a broader spectrum toxin into the medium to kill any remaining pathogen. In some ways, the sentinels monitor the population of PAO1 through the adaptive response circuit and attempt to control it by releasing toxins in two stages. In a preliminary study [111] a synthetic network was demonstrated where each cell synthesizes AHL that activates LuxR in neighboring cells. High or low AHL concentrations lead to cell lysis through the expression of ccdb protein and thus population density is maintained constant for intermediate AHL concentrations. The width of the survival band can be optimized by fine tuning hybrid las/cI-OR promoter.

For the second phase one of the broad spectrum toxins used in this study is CDAP-4. CDAP-4 is a small 20 amino acid antimicrobial peptide derived from chemokine CCL13. CCL13 is highly expressed in the human lung, kidney and colon tissues as part of its immune response. CDAP-4 operates on a charge interaction model, which is somewhat non-specific for gram-negative bacteria [195]. CDAP-4 was expressed in *E. coli*, purified, and its effects were assayed on *E. coli* and PAO1. As shown in **Figure 33 (a),** CDAP-4 is able to destroy PAO-1. At higher concentration CDAP-4 is also toxic to *E. coli*. It is imperative to note that CDAP-4 only operates when it is external to the cell but is non-toxic in the cytoplasm (verified experimentally; data shown in **Figure 49**). For the second line of defense, CoPy and CDAP-4 will be co-expressed with the lysis protein E from *E. coli* bacteriophage ΦX174. E protein inhibits the transmembrane MurNAC pentapeptide translocase MraY and causes *E. coli* to burst open thus releasing all its contents into the extracellular medium.

(a)

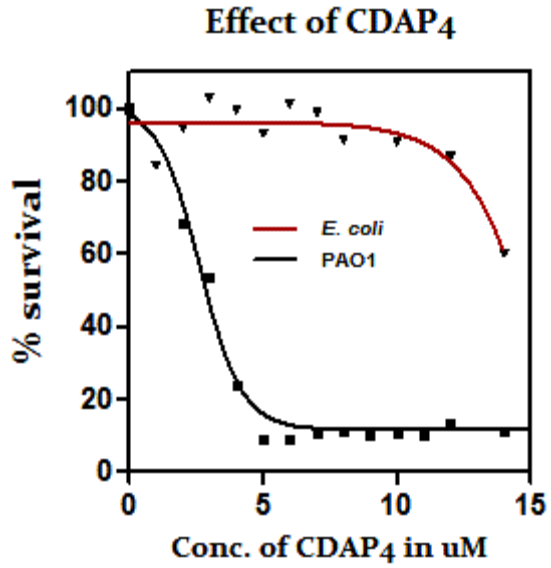

(b)

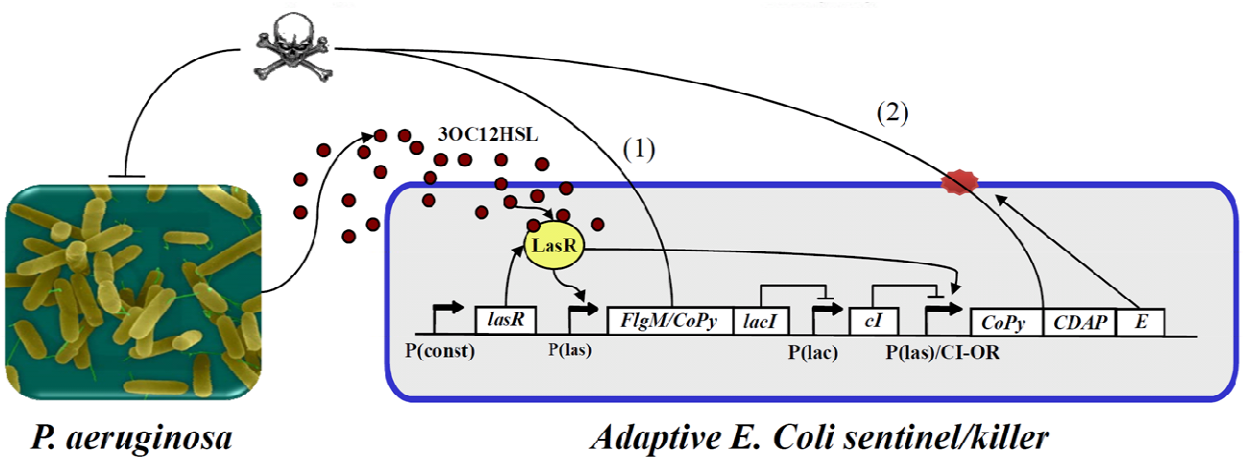

Figure 33: Characterization of CDAP4.
(a) Experimental results with CDAP-4 killing of *E. coli* and PAO1, showing effective, but somewhat non-specific killing. (b) Genetic circuit for the adaptive bacterial 'Sense and Destroy' system. The first line of attack (secretion of FlgM/CoPy) and the second line of attack (expression of CoPy, CDAP-4, and cell lysis via E protein) are indicated by (1) and (2) respectively.

In the future, all the modules discussed above can be optimized to engineer an adaptive response strategy as depicted in **Figure 33 (b)**. Cascades can be modified and fine-tuned so that the second line of attack on the pathogen will be produced after a certain time interval if the initial attack fails. The desired delay as well as the killing dynamics of the sentinels will be evaluated using simulations. The three-stage cascade [59] can be modified such that LasR replaces TetR, the las promoter regulates LacI and FlgM/CoPy expression, EYFP is replaced with CoPy, CDAP-4, and the E protein, and is controlled by a hybrid las promoter that is repressed by cI **(Figure 33 (b)).** The expected behavior of this circuit will be as follows: First, initial detection of 3OC12HSL results in the expression of LacI and FlgM/CoPy (which is secreted). Second, LacI accumulation results in the repression and decay of cI. Third, if 3OC12HSL levels persist to be high, cI decay allows LasR/3OC12HSL to activate the expression of CoPy, CDAP-4, and E protein. This second line of defense occurs only if the initial line of defense was ineffective in killing PAO-1 (and therefore there was no corresponding reduction in 3OC12HSL levels). The combination of high CoPy / CDAP-4 expression in the sentinel/killer cells coupled with effective release of the proteins through cell lysis will provide a formidable second line of defense, albeit at the cost of killing the sentinels.

III. Mammalian Adaptive Response Sense and Destroy

I designed a mammalian version similar to the bacterial adaptive 'Sense and Destroy' system. **Figure 34** shows the architecture of an adaptive mammalian 'Sense and Destroy' System. Its function can be explained in three steps. First, initial detection of 3OC6HSL/3OC12HSL results in expression of CoPy, TetR and micro-RNA 5 (mirff5). Second, TetR and mirff5 accumulation results in the repression and decay of LacI and mirff4. Third, if 3OC6HSL/3OC12HSL levels persist to be high, LacI and mirff4 decay allows LuxR-3OC6HSL/LasR-3OC12HSL to activate the expression of CDAP-4 and EYFP as a second phase attack to kill PAO1.

To build the adaptive mammalian 'Sense and Destroy' system, its individual components were characterized first. All characterization data was generated using HEK293 FT cells that are transfected (protocol is explained in Chapter 6, Section I(i)) with the relevant construct and their fluorescence measured using FACS. **Figure 30 (b)** and **(d)** show the dosage response curves of pLux and pLas promoters to varying concentrations of 3OC6HSL and 3OC12HSL respectively. With 3OC6HSL there is an almost 20 fold difference between the 'ON' and 'OFF' states whereas

the difference with 3OC12HSL is about 5 fold. As described earlier this difference can be increased by using a signal amplifier.

Repressor elements in the circuit were tested individually as well. TetR was cloned under a Rheo promoter which is activated by RSL ligand **(Figure 35 (a)).** Rheo itself is constitutively expressed from pUbc. Strength of the Rheo promoter is measured by the amount of EBFP present in the cells, which in turn can be titrated by RSL ligand in the medium. Rheo promoter (UAS5X) controls expression of TetR. TetR represses tetO2 operator in the promoter Hefıa-tetO2 and hence levels of mKate directly correlate with the amount of repression. As shown in **Figure 35 (b**) mKate levels start to go down as EBFP levels increase and in turn are indicative of TetR getting expressed and repressing pHelfa-tetO2. Similarly, repression by LacI and micro-RNA FF4 was measured by cloning them under TRE-tight which is a DOX inducible promoter **(Figure 35 (c)).** Like Rheo, rTTa3 was expressed constitutively from pHefıa. DOX bound to rTTa3 controls the expression of LacI and mirff4. LacI represses pHefıa-LacOid, and mirff4 represses 4xff4. As expected, increased LacI expression with increasing DOX levels reduces EYFP fluorescence by almost 15 fold **(Figure 35 (d))** and is an accurate measure of the repression achieved by LacI and mirff4. In this case, mKate is constitutively expressed so that during FACS it can be used to select cells that were successfully transfected.

Next LacI-mirff4 was tested under Lux promoter, which is inducible, by 3OC6HSL (**Figure 36 (a)**). This circuit is similar to **Figure 35 (c)** except that the inducer is 3OC6HSL. In **Figure 36 (a)** levels of mKate reflect the amount of LacI-mirff4 in the system. There is an inverse relationship between mKate and EYFP since mKate levels reflect the amount of LacI-mirff4 present in the medium and EYFP reflect the amount of repression achieved. More mKate means high LacI-mirff4, which in turn mean high repression and consequently less EYFP. This is clearly seen in **Figure 36 (b).** It shows how levels of mKate and EYFP change with different concentrations of 3OC6HSL and decline of EYFP corresponds to the rise of mKate. This inverse relationship between mKate and EYFP is more clearly depicted in **Figure 36 (c).**

Once individual components were tested, steady state response of the entire mammalian adaptive response circuit **(Figure 37 (a))** without CoPy and CDAP-4 was tested under different induction levels of 3OC6HSL. As expected a rise in mKate levels corresponds to a rise in TetR, which in turn is responsible for the repression of tetO2 and hence results in lower EBFP and LacI levels. Lower LacI and mirff4 levels in turn relieve LacI repression of pLux-LacOid. LuxR and 3OC6HSL simultaneously activate pLux-LacOid.

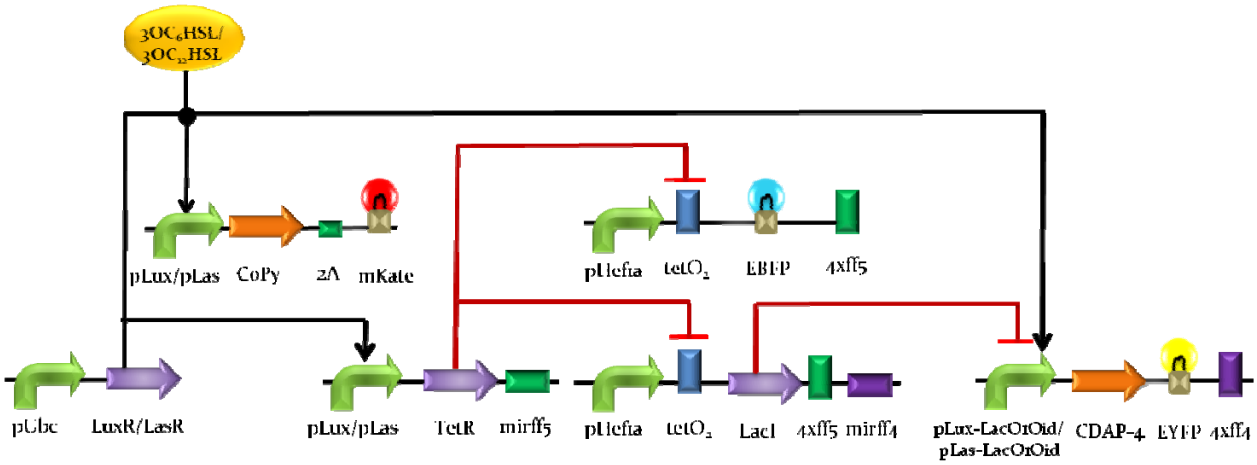

Figure 34: Architecture of the adaptive mammalian 'Sense and Destroy' system.
Promoter pLux works with 3OC6HSL and pLas works with 3OC12HSL. LuxR/LasR is constitutively expressed from the promoter pUbc. CoPy and CDAP-4 are two toxins.

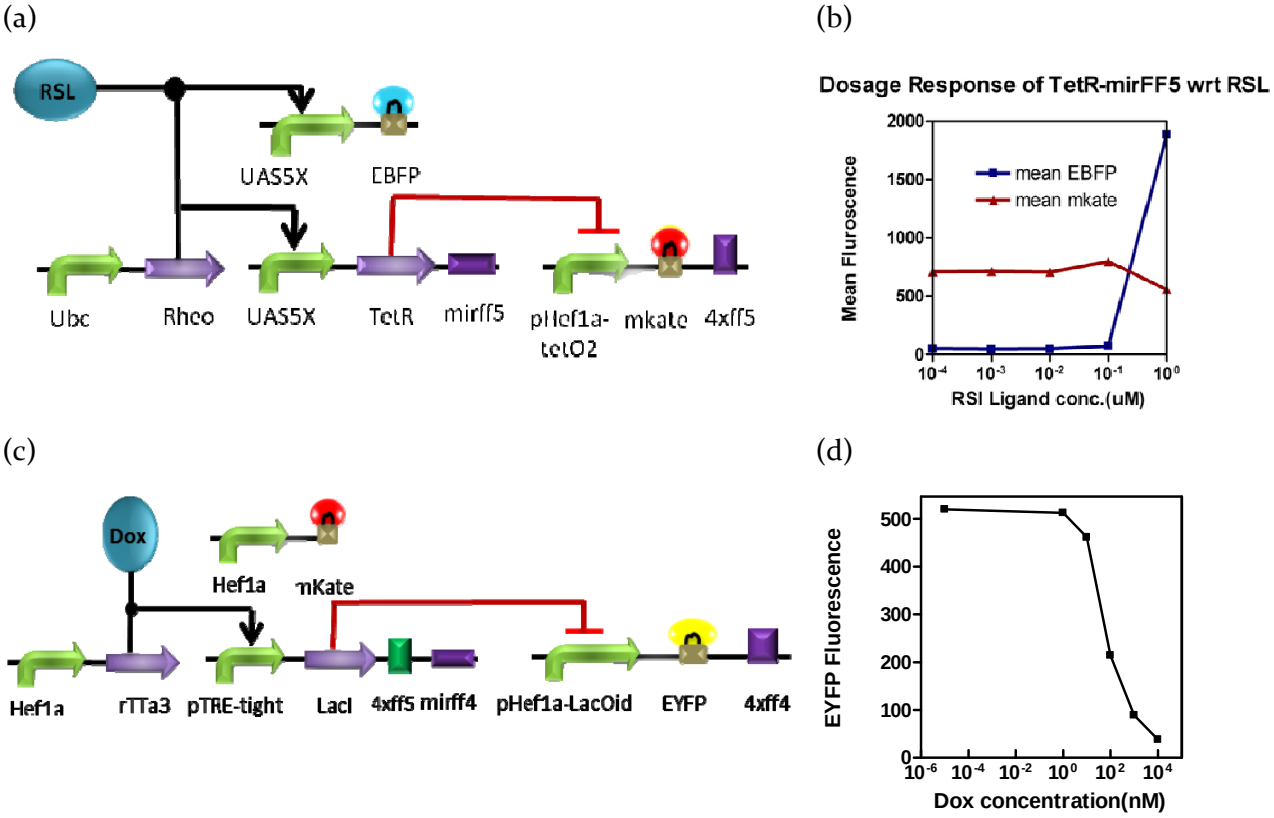

Figure 35: Characterization of TetR and LacI repressors.
(a) Circuit for the characterization of TetR-mirff5 (b) Dosage response of TetR-mirff5 w.r.t different concentrations of RSL ligand. (c) Full circuit for the characterization of LacI-mirff4. (d) Dosage response of LacI-mirff5 w.r.t different concentrations of DOX.

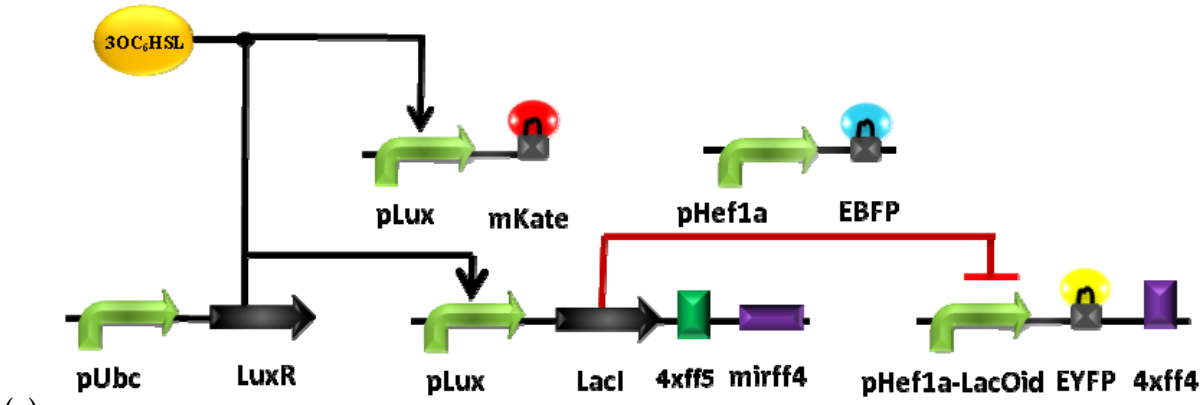

(a)

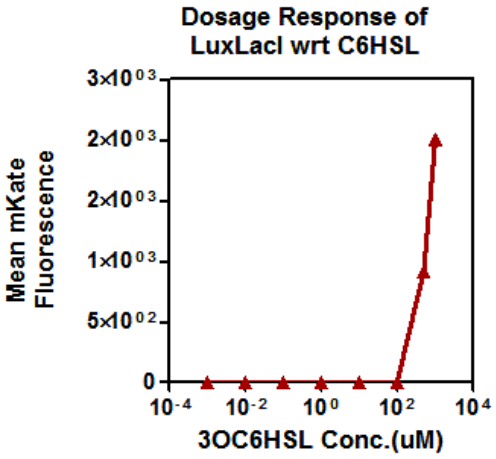

(b)

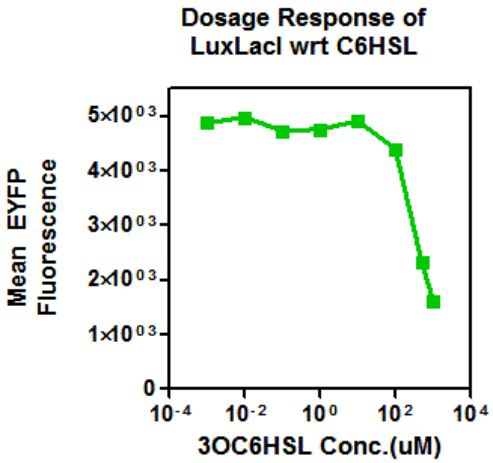

(c)

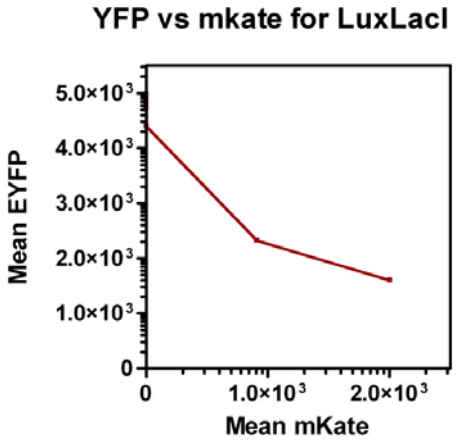

(d)

Figure 36 : Characterization of 3OC6HSL inducible LacI-mirff4.
(a) Circuit design. (b) Dosage response of pLux w.r.t different concentrations of 3OC6HSL as shown by mean fluorescence levels of mKate. (c) Dosage response of pHefıa-LacOid w.r.t different concentrations of 3OC6HSL as shown by mean fluorescence levels of EYFP. (d) The relationship between EYFP and mKate.

As the repression from LacI is relieved, activation of pLux takes over and EYFP fluorescence increases albeit with a delay as observed in **Figure 37 (b).** This delay is a combination of pLux activation and LacI repression dynamics along with the length of a repression cascade achieved by TetR and LacI. A computational simulation of the entire system will help explore the best possible parameters needed to optimize the delay. Modeling of the effect of various components on this delay is done in the next section. A 3OC12HSL inducible adaptive mammalian response system **(Figure 38 (a))** similar to 3OC6HSL inducible system was further engineered and a similar characterization response **(Figure 38 (b))** was observed. It was also noted that 3OC12HSL is toxic to the cells and hence high enough induction levels were unachievable to observe a rise in EYFP levels during the time frame of the experiment.

After steady state results of the 3OC6HSL/3OC12HSL inducible cascade, dynamic response of the 3OC6HSL inducible system **(Figure 37 (a))** was characterized by observing the system for 24 hours. **Figure 38 (c)** shows that activation of mKate (which in turn reflects the level of TetR) by 3OC6HSL after 12 hours. EBFP levels were higher before TetR gets expressed due to AHL induction. Once TetR starts to repress tetO2, EBFP levels go down after 18 hours. It is expected that EYFP levels will go up if the system is observed for more time.

As part of the adaptive response strategy discussed in **Figure 34** the mammalian sentinels will release CDAP4 as a broad spectrum toxin if PAO1 survives the first stage attack. Its potency was characterized in **Figure 33 (a)**. For this, a codon optimized CDAP4 was expressed in mammalian cells and its expression was verified through immunostaining as shown in **Figure 39**. To differentiate between the cells and HisTagged CDAP4, the fixed cells were incubated with two primary antibodies. One is against the HisTag-CDAP-4 and the other is against the beta-tubulin. Green represents beta-tubulin and red represents CDAP-4. In the future codon optimized CoPy and CDAP4 can be integrated into the mammalian adaptive response system.

(a)

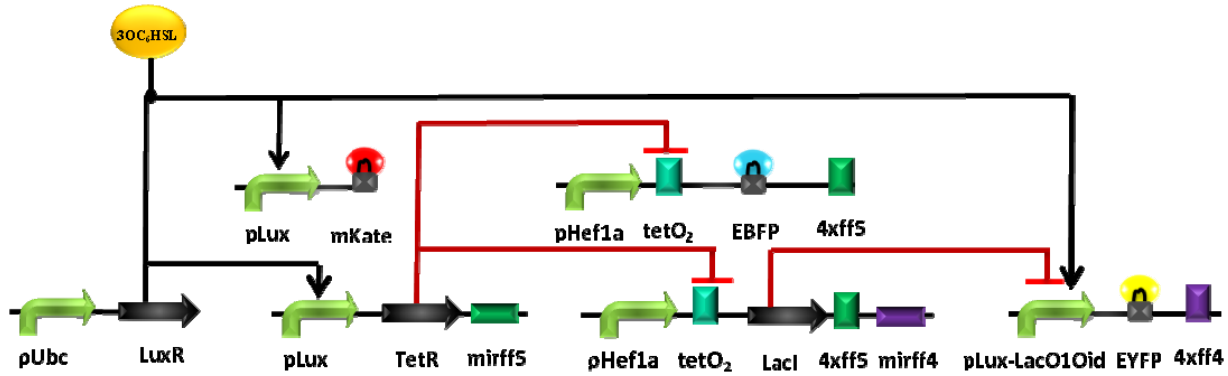

(b)

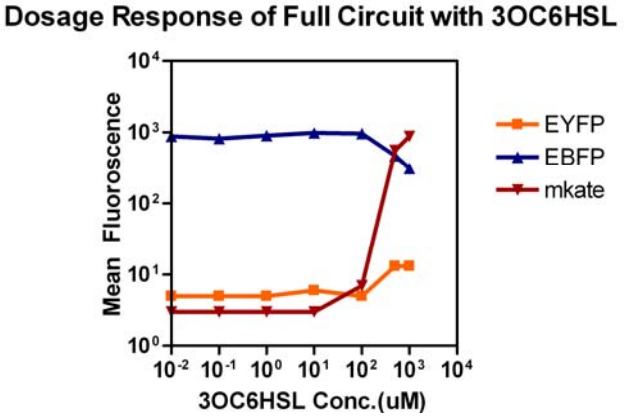

(c)

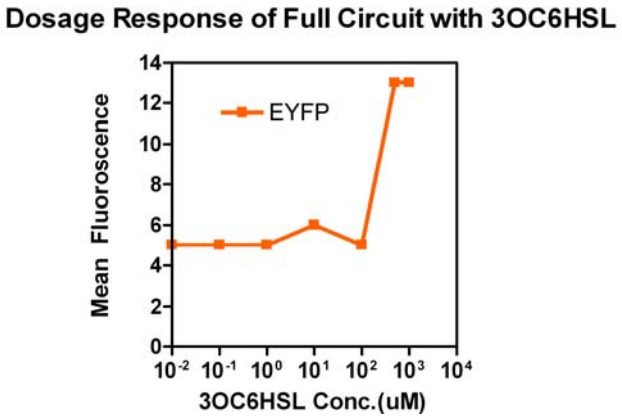

Figure 37: Steady state response of the 3OC6HSL inducible adaptive response system.
(a) Full circuit design. (b) Steady state dosage response of the full circuit to different concentrations of 3OC6HSL. (c) A closer look at EYFP fluorescence which is indicative of the adaptive response.

(a)

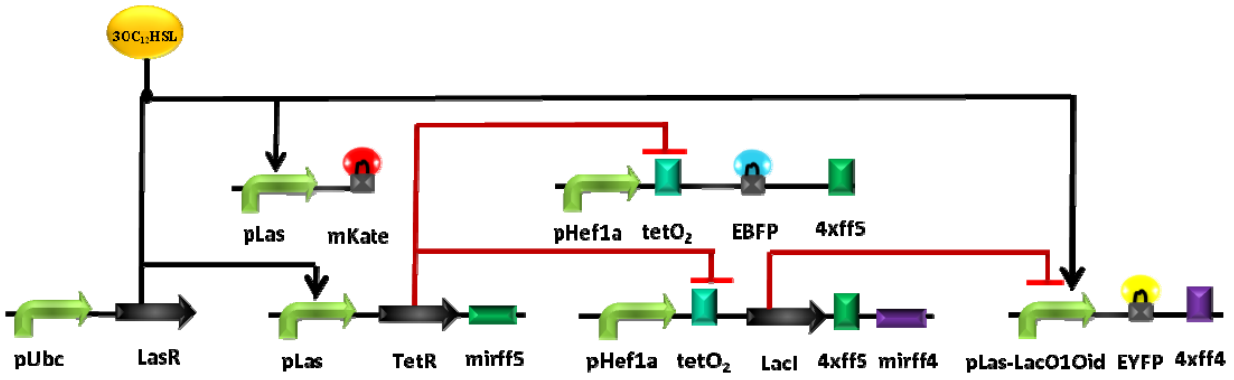

(b)

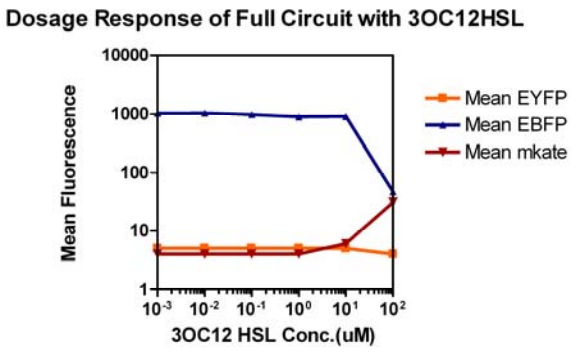

(c)

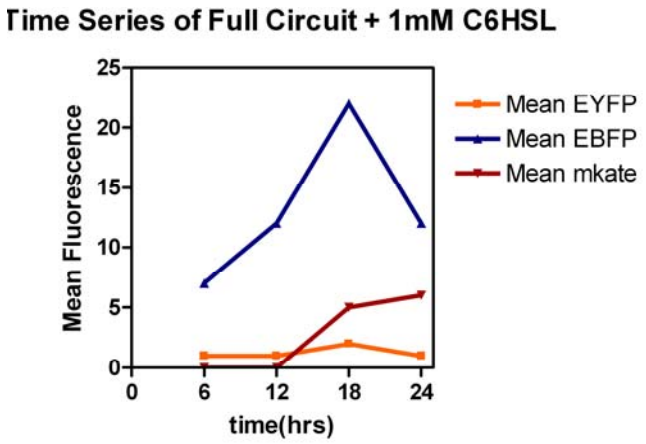

Figure 2: Steady state response of the 3OC12HSL inducible and dynamic response of 3OC6HSL inducible adaptive response system.
(a) Full circuit design of 3OC12HSL inducible adaptive response system (b) Steady State dosage response of the full circuit to different concentrations of 3OC12HSL. (c) Temporal response of the 3OC6HSL inducible adaptive response system for 24 hours.

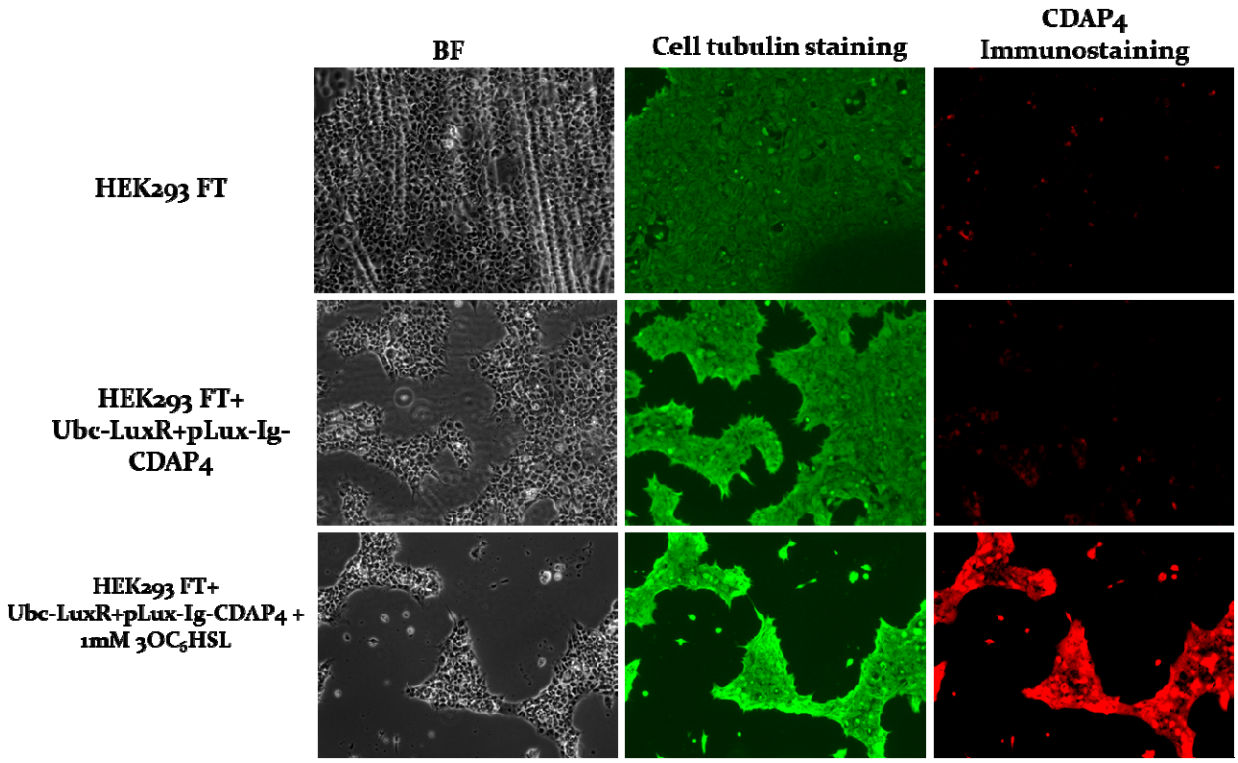

Figure 39: Expression of CDAP4 in mammalian cells.
Immunostaining of CDAP4. All three channel images are shown. BF-Brightfield, Green- beta tubulin and Red-CDAP4. This figure demonstrates that CDAP4 can be successfully expressed in HEK 293FT cells.

IV. Modeling of Adaptive Response

To better understand the dynamics of the two-phase adaptive response circuit, a kinetic mass action model of the system was constructed and analyzed **(Figure 40 (a)).** In this circuit, LuxR is constitutively produced, and, upon AHL induction, binds the pLux promoter to activate production of mKate and TetR. TetR suppresses LacI production and since LacI was repressing eGFP production initially, production of TetR eventually supports eGFP production. Upon AHL induction, this double negative pathway creates a delay in production of eGFP. Hence, mKate fluorescence defines the first phase response, and eGFP fluorescence defines the second phase.

Central to the model is the delay incurred by transcription and translation in the double negative pathway. **Figure 40 (b)** shows all the species and different interconnecting parameters used to model the response of the circuit given in **Figure 40 (a).** The various parameters used in the MATLAB code are given in Chapter 6, Section II. Using the model discussed above, simulation results in **Figure 41 (a)** show that in response to a step impulse of AHL, mKate is initially produced, and eGFP is produced after a delay. If the pathogen becomes resistant to the first phase attack, represented by red, then the input AHL response can be approximated by a step function. In reality eGFP represents the second phase of a two-phase response which is produced after a time delay. In **Figure 41 (b)**, the duration of AHL induction is varied. In response to short AHL induction, only mKate is produced. This is the case when pathogen dies in the first phase. If the pathogen survives the first attack then theoretically the duration of AHL pulse will increase. After a threshold, longer duration of AHL pulse triggers a second response represented by the production of eGFP. eGFP is produced in greater quantities as the duration of AHL pulse is increased, until eGFP reaches a steady state amount. In addition to optimizing the start time of the second phase attack, the magnitude of response and the delay incurred can be varied by tuning the strength of the promoters that drive TetR and LacI production.

Increasing the strength of the promoter that drives LacI production increases the delay between mKate and eGFP production **(Figure 42 (a)).** Similarly increasing the strength of pLux promoter increases the amplitude of fluorescence outputs **(Figure 42 (b)).** This model validates the two phase response of the circuit and suggests how promoter engineering can fine-tune the response dynamics.

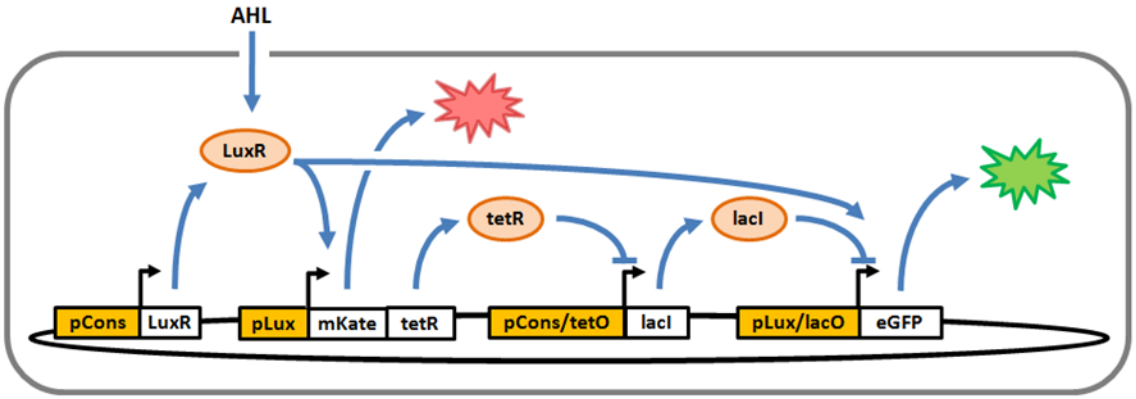

(a)

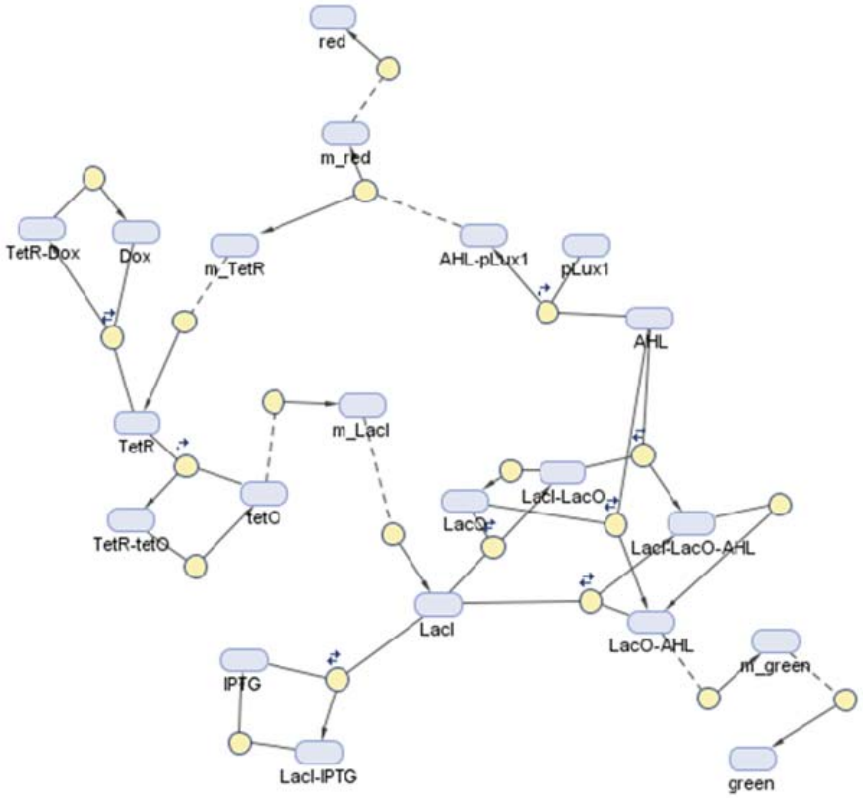

(b)

Figure 40: Modeling the dynamics of the two-phase adaptive response circuit.
(a) Circuit diagram of the modeled system. Input is AHL, and outputs are mKate and eGFP fluorescence. (b) Different species involved in the model. Nodes showing m_X represents the rate of formation of mRNA of X. Initial values of these nodes are given in Chapter 6, Section.II.

(a)

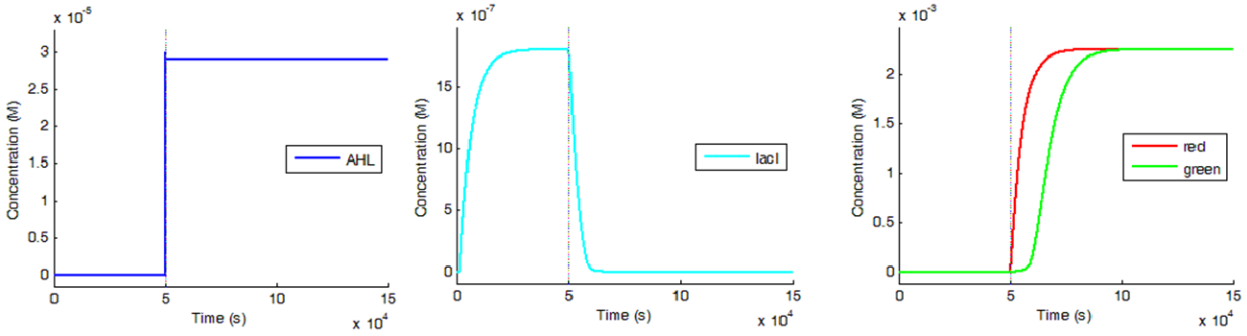

(b)

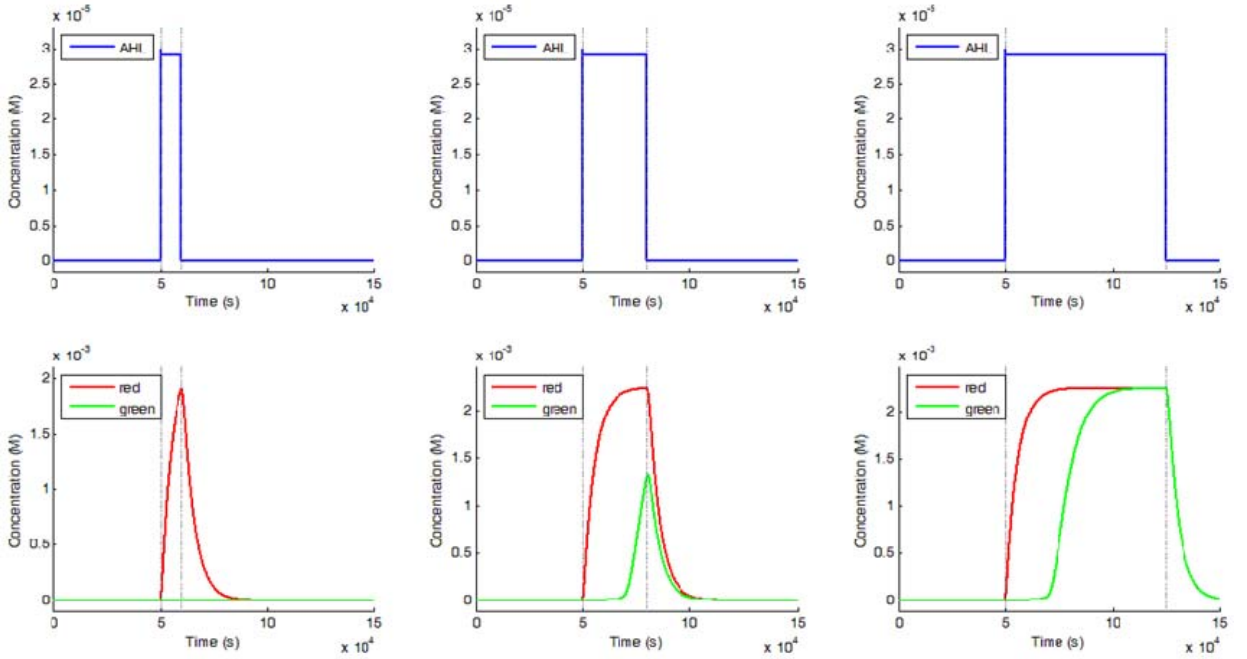

Figure 41: Response of two phase adaptive system to different input duration.
(a) Two phase response of the circuit to a step input. (b) Response of the system to AHL pulses of varying time duration. AHL pulses are shown in blue and their corresponding responses are shown below in red and green.

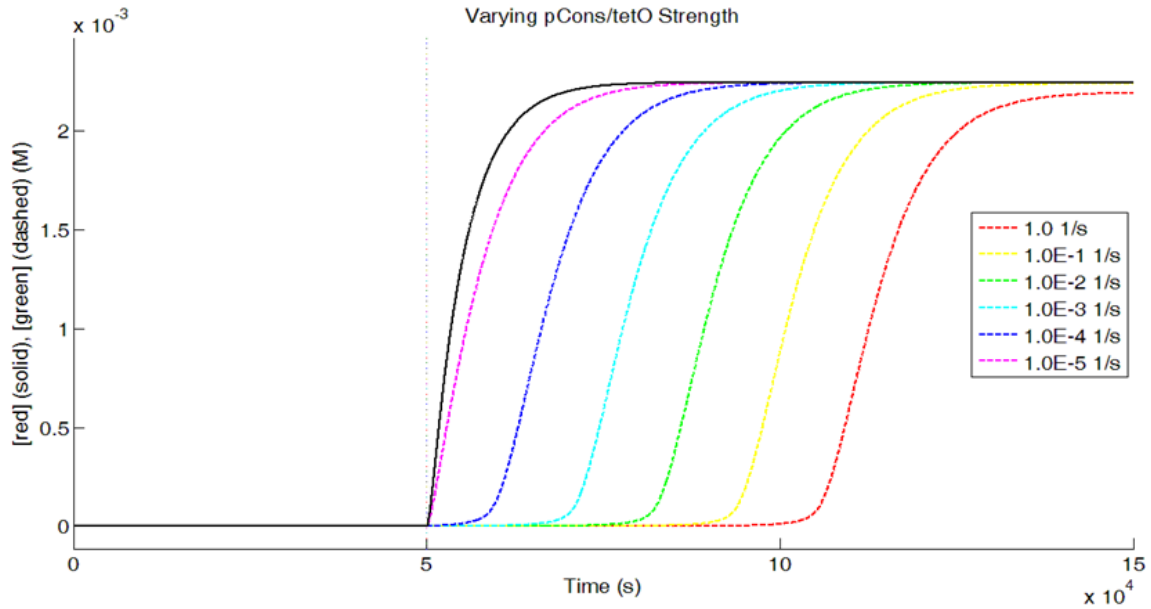

(a)

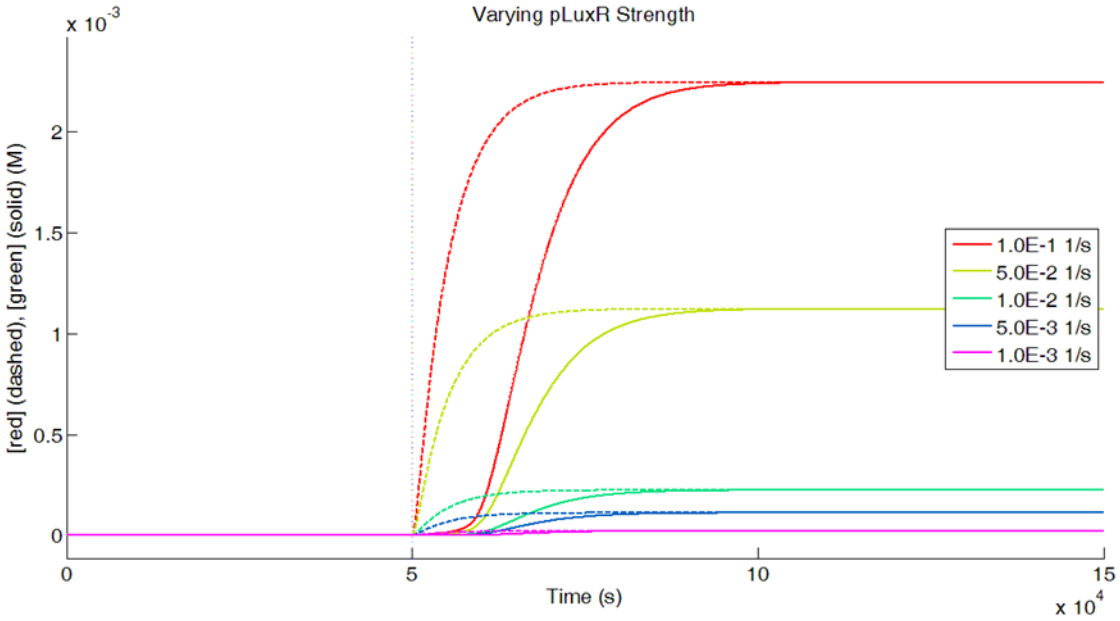

(b)

Figure 42: Modeling of the delay between two phases of adaptive response.
(a) Varying the strength of pCons/tetO promoter changes the delay between the first and second wave outputs. The dynamics of mKate production (black solid line) remain unchanged, but increasing pCons/tetO promoter strength delays eGFP production (colored dashed lies). (b) Varying the strength of pLux promoters changes the output amplitudes. mKate production dynamics are shown by dashed lines, and corresponding eGFP production dynamics are shown by solid lines.

V. Summary and Discussion

In this chapter, I proposed additions to the design of bacterial/mammalian 'Sense and Destroy' system that can potentially allow the sentinels to adapt to the resistant pathogen. Adaptable sentinels will use a two pronged approach to kill the pathogen. The first phase will be similar to the 'Sense and Destroy' system. After this, the adaptable sentinels examine the efficacy of the first phase by continuously monitoring the levels of AHL present in the medium for a predetermined amount of time. If the levels of AHL do not diminish, which is indicative of the surviving pathogen, the sentinels then launch the second phase attack. This involves releasing large amounts of another toxin besides CoPy. This design is based on by the assumption that the surviving pathogen will keep using the same QS molecule. This system design is not possible for sentinels that commit suicide in order to release the first phase toxin [146].

In **Figure 19** (g) it was shown that due to FlgM-CoPy there is a delay of ~500 minutes in the growth of PAO1. This time is an indication that any remaining PAO1 in the media after this time interval survived the first phase attack. The adaptive response sentinels can be engineered to launch the second phase attack after 500 minutes. The time between the two stages can be programmed by the integration of synthetic cascades [59] between them. I demonstrated and characterized a tunable cascade in mammalian cells. Furthermore the mammalian adaptive 'Sense and Destroy' system was modeled and simulated to understand the dynamics of various species for a stable and predictable performance. Besides CoPy, a second toxin CDAP-4 was expressed and validated in bacterial and mammalian cells and can be used for the second stage attack. Secretion and killing efficiency of the first phase response will be an important design consideration in the system architecture of the adaptive response system. The delay between two phases will depend on the length of the cascade and different characteristics of various elements of the cascade. The potency of the second stage toxin will be important for the overall efficacy of the system against the pathogen.

CHAPTER 5 – CONCLUSIONS AND FUTURE WORK

I. Conclusions

This thesis establishes a proof of principle for a preventative cell therapy in which genetically engineered *E. coli* cells explicitly detect a common human pathogen, *Psuedomonas Aeruginosa* (PAO1) and respond by producing and secreting a novel, pathogen specific engineered toxin. Using fundamental principles of Synthetic Biology, I established that an advanced synthetic system with potentially numerous applications can be designed and engineered. This project also showed that such a system can be further tuned to different chassis and modified for diverse outputs. This was exhibited by transferring the bacterial 'Sense and Destroy' into probiotic bacteria and mammalian cells. Additionally I proposed an adaptive 'Sense and Destroy' system as a possible mechanism to address the growing problem of antibiotic resistance. Furthermore I presented two new designs of the bacterial 'Sense and Destroy' system against *Shigella* and *Vibrio cholera* in the Future Work section. In the following paragraphs I present my achievements and discuss the future challenges that lie ahead.

In Chapter 2 I genetically engineered bacterial cells to precisely detect *Psuedomonas aeruginosa* (PAO1) and respond by producing and secreting a novel, pathogen specific engineered toxin. Engineered *E. coli* sentinels detect $3OC_{12}HSL$, which is the main Quorum Sensing signal produced by PAO1. The sentinels were programmed to produce a chimeric toxin (CoPy) in response to $3OC_{12}HSL$. CoPy was engineered to specifically kill PAO1. Growth rates of seven different strains of bacteria were compared to *E. coli* and PAO1 under maximum killing concentration (1000 nM) of purified CoPy and are shown in the **Figure 11.** Dosage response curves of purified CoPy were characterized and half maximal Inhibitory Concentration (IC_{50}) of purified CoPy was calculated and is shown in the **Figure 9**. FlgM secretion tag was fused to the N terminus of CoPy and was used to transport CoPy into the extracellular medium. IC_{50} and dosage response curves of the secreted and non-secreted versions of purified FlgM-CoPy were analyzed and presented in the **Figure 18 and 19** respectively. After detailed characterization of differential detection and specific killing of PAO1, half maximal inhibitory ratio (IR_{50}) of the sentinels against PAO1 was calculated by growing different number of PAO1 in the filter sterilized supernatant of the '*maximally induced*' sentinels as shown in the **Figure 24 (b).** With the given system parameters, IR_{50} determines an approximate minimum number of the bacterial sentinels needed

to kill one PAO1. Furthermore the sentinels and PAO1 were co-cultured on semi-solid agar according to the IR_{50} and system dynamics were observed under a microscope as shown in the **Figure 26.** A suitable chassis needs to be selected to implement the 'Sense and Destroy' system in a real setting. Probiotic bacteria present a natural advantage over the laboratory strain of *E. coli.* I discussed using *E. coli* Nissle as a possible chassis and achieved comparable secretion of FlgM-CoPy from this strain with respect to the wild type strain of *E. coli*. *E. coli* Nissle has long been used in Europe as a natural remedy against many cases of Inflammatory Bowel Disease (IBD) and is currently marketed as Mutaflor by Ardeypharm GmbH, Herdecke in Germany. Additionally probiotic gram-positive bacteria such as lactobacillus can potentially be used as a host to the synthetic 'Sense and Destroy' circuit. Gram-positive bacteria will have advantage over gram-negative bacteria to secrete proteins since they only have one outer membrane. Furthermore gram-positive bacteria can harmlessly colonize the human intestines as it has been shown that 80% of the bacteria found in the gut are gram-positive [196]. Before *in vivo* testing, the 'Sense and Destroy' system can be studied in microfluidic lung models. These models can be used to closely monitor the dynamics of the sentinel and pathogen cell populations by live-dead staining. Spatiotemporal progression and the physical proximity requirement of the 'Sense and Destroy' system can also be understood by using these microfluidic devices. Additionally this data will be helpful to accurately optimize sentinels' response, timing and potency, to the pathogen relevant for clinical deployment.

In Chapter 3 I illustrated initial experimental progress made towards achieving a mammalian 'Sense and Destroy' system. I designed and programmed mammalian cells to detect 3OC12HSL produced by PAO1. In the future, the mammalian sentinels' response to PAO1 need to be characterized by co-culturing them with PAO1 as was done for the bacterial 'Sense and destroy' system. Furthermore, I discussed a theoretical design of a signal amplification module which will make the 3OC12HSL detection module significantly more sensitive. I demonstrated that the mammalian sentinels can constitutively express codon optimized CoPy as a possible mechanism to kill the invading pathogen. More research is required to successfully secrete CoPy into the extracellular medium.

In Chapter 4 I demonstrated that it is possible to engineer mammalian and bacterial cells that can respond to resistant pathogen using a biphasic strategy where the second phase attack can be programmed to take place after a specific time delay from the first phase attack. This adaptive response by the bacterial and mammalian 'Sense and Destroy' system was modeled and

simulated which will be helpful to understand the dynamics of an adaptive response. It will be further useful to decide parameters which are necessary for stable and predictable system performance. Expressions of two different toxins, CDAP-4 and CoPy were verified. In the future these toxins will be integrated into the two phases of the adaptive response.

In this project I created a set of modular sentinel circuits in *E. coli* and mammalian cells for the detection and destruction of PAO1, and to equip sentinel circuits with sophisticated logic for an adaptive response to the presence of PAO1 via the deployment of different killing strategies. Detection and destruction strategies will depend on the target pathogen since the quorum sensing molecules and toxin are specific to the pathogen. In the following section I have suggested possible design modifications for the sentinels to detect and specifically destroy two highly pathogenic bacteria.

II. Future Work

I extended the concepts of the bacterial 'Sense and Destroy' system to design novel 'Sense and Destroy' system against *Shigella* and *V. cholera*.

a) *Shigella* Sense and Destroy

Shigella is a Gram-negative bacterium that is nonmotile, facultatively anaerobic shaped as non-spore-forming rods. It is the principal agent of bacillary dysentery also called shigellosis. Three Shigella groups out of four are the major disease-causing species: *S. flexneri* is the most frequently isolated species worldwide and accounts for 60% of cases in the developing world; *S. sonnei* causes 77% of cases in the developed world, compared to only 15% of cases in the developing world; and *S. dysenteriae* is usually the cause of epidemics of dysentery. The serotype 1 of *S. dysenteriae* (Sd1) is of particular concern due to its expression of the Shiga toxin (Stx). It is the cause of epidemic dysentery and can cause vicious outbreaks in confined populations. Stx inhibits protein synthesis in eukaryotic cells via inactivation of ribosomal RNA, leading to cell death. The toxin is cytotoxic, neurotoxic and enterotoxic. It targets glomerular epithelial cells, central nervous system and microvascular endothelial cells causing haemolytic-uremic syndrome (HUS) and seizures. Sd1 also causes a rapid increase in the cell membrane permeability of infected macrophages and destroys their mitochondrial function. A major obstacle to the control of Sd1 is its resistance to antimicrobial drugs. Therefore there is an urgent need to develop new anti-bacterial strategies.

In my thesis I proposed a programmable 'Sense and Destroy' system **(Figure 43),** where *E. coli* sentinels detect *Shigella* using its QS signal AI-3 along with its lambdoid phage and then specifically kill the pathogen without releasing the toxin out of the dead cells and thus reducing *Shigella* infection. It has been calculated that human gastrointestinal tract houses 10^{14} bacteria. The proximal small intestine has a relatively sparse gram-positive flora, consisting mainly of *lactobacilli* and *Enterococcus faecalis*. This region has about 10^5 - 10^7 bacteria per ml of fluid. The distal part of the small intestine contains greater numbers of bacteria (10^8/ml) and additional species, including coliforms (*E. coli* and relatives) and Bacteroides, in addition to lactobacilli and enterococci. Distal colon has 10^9-10^{12} bacteria and is the neighborhood of Shiga-Toxin producing *E. coli* and *Shigella* (the most common cause of bloody diarrhea). A non-pathogenic commensal strain of *E. coli* Nissle, which lives in the same environment, can be engineered to detect *Shigella* first by recognizing one of its QS signal. Sentinels will express high amount of transmembrane histidine kinase (HK) QseC to detect autoinducer AI-3. AI-3 is a known bacterial signal that binds the bacterial membrane receptor QseC and results in its auto-phosphorylation **(Figure 44).**

Shigella requires very low quantity of inoculum (10^2-10^3CFU) for clinical manifestations of Acute Gastrointestinal Infections [197] because it survives the stomach acid. Furthermore the QS response regulator QesC is very sensitive and even a small amount of signal activates full autophosphorylation for a quick response [198]. 100 nM of AI-3 has been shown to invoke a response from QseC in vivo. QseC then phosphorylates its response regulator QseB and results in expression of the *Shigella* and *Salmonella* virulence genes [199, 200]. AI-3 defective cells are unable to colonize and cause pathogenicity [201]. AI-3 is produced by several species of bacteria in the normal human GI microbial flora but many of them exist either in respiratory tract, urinary tract or distal colon. Therefore the sentinels themselves will carry a mutation in luxS gene making them defective in producing AI-3 [202] hence preventing crosstalk (luxS mutations are not lethal for the cell). Note that in principle AI-3 sensing is not needed for system operation but can be advantageous for the metabolic fitness of sentinels especially for future multi-input sense and destroy cells. AI-3 sensing also prepares the sentinels for the possibility of an attack. Most antibiotic therapies are ineffective because by the time symptoms of a particular disease appear it's already too late e.g. for *V. cholerae*. Instead these sentinels will launch an early response and destroy the pathogen even before the symptoms are present.

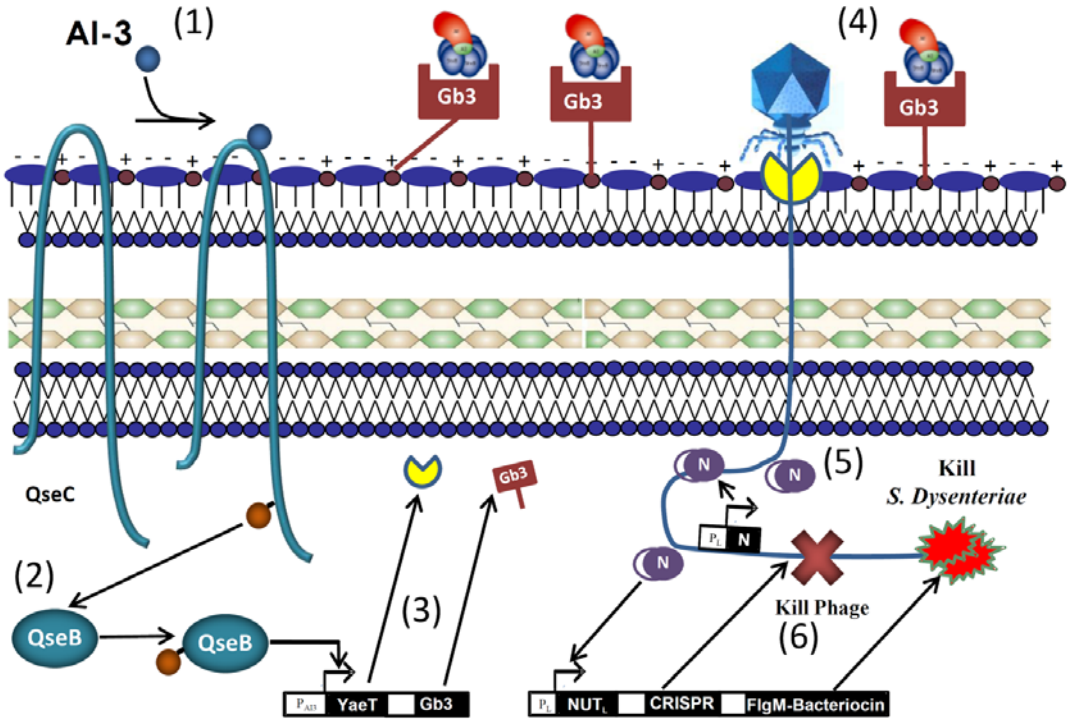

Figure 43 : System architecture of *Shigella dysenteriae* Sense and Destroy.
1) Sentinels detect AI-3. 2) QseB initiates transcription from PAI-3. 3) Transcribe and transport receptors for the Shiga toxin and Stx phage. 4) Phage binds to its specific receptor and inserts its DNA 5) Sentinels detect incoming phage 6) Inactivate the phage by CRISPRs and secrete *Shigella* specific colicin to kill the pathogen.

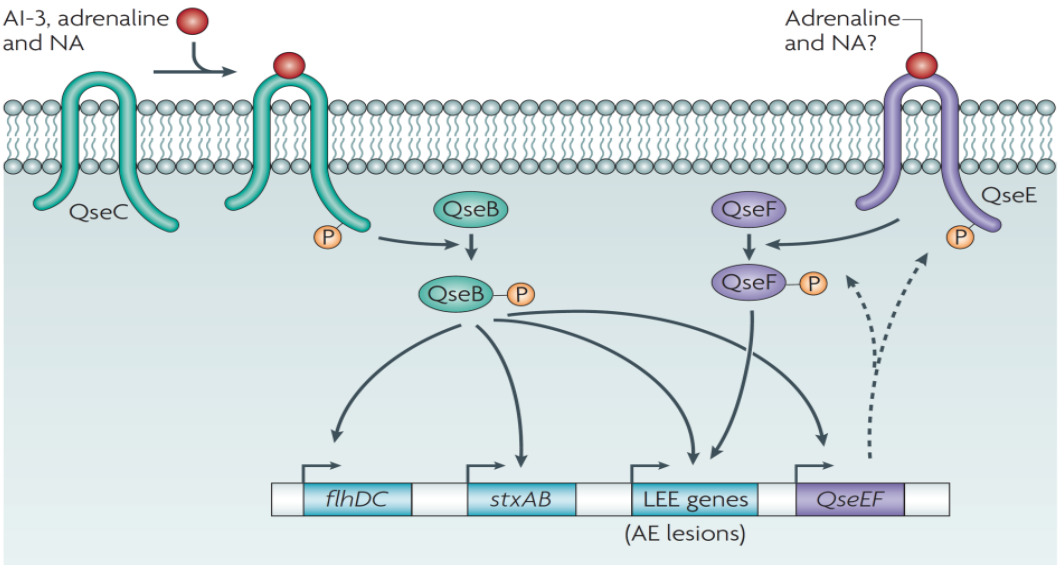

Figure 44 : AI-3 signaling in *Shigella* and *Salmonella*.
This figure is adapted from[199] for illustrative purpose.

Since AI-3 is not sufficient proof of *Shigella* existence, once sentinels detect AI-3 they will employ a two-pronged approach to more specifically detect and destroy the pathogen with minimum damage to enterocytes and neighboring gut flora.

First, sentinel killer cells express molecular mimics of Shiga toxin (Stx1/Stx2) receptors (Gb3) on the surface to sequester the toxin which 'may' be present, assuming the pathogen is there, into the lumen of intestine. The Stx family, a group of structurally and functionally related exotoxins, includes Stx from *Shigella dysenteriae* serotype 1 and the Shiga toxins that are produced by enterohaemorrhagic *Escherichia coli* (EHEC) strains. All the toxins in this family are now called 'Stx toxins'.These toxins can be Stx1 variants (Stx1 and Stx1c), Stx2 variants (Stx2, Stx2c, Stx2d, Stx2e, and Stx2f) or variants of both in a range of combinations. Gb3 (Saccharide structure: Gal (α1, 4) Gal (β1, 4) Glcβ1--) is the primary natural glycoconjugate receptor for Stx1/Stx2 on enterocytes, the main colonizing factor of *Shigella dysenteriae*. It is demonstrated [203, 204] that these receptors neutralize more than 98% of the cytotoxicity of each of the Stx types associated with human disease. This chimeric LPS will be incorporated into the outer membrane of sentinels. With a mutation in the waaO gene LPS core is truncated and terminates in Glc. Insertion of two *Neisseria* galactosyl-transferase genes (lgtC and lgtE) directs the addition of two Gal residues to the Glc acceptor, generating a chimeric LPS terminating in Gal (α1, 4) Gal (β1, 4) Glc, which is the Stx receptor. This in turn prevents Stx from binding similar glycolipid receptors on the surface of enterocytes and their characteristic attaching and effacing (A/E) histology.

Second, sentinels will express *Shigella* lambdoid phage specific receptor, YaeT,[205, 206] to absorb phage containing the virulence genes and Stx genes. The toxins in *S. dysenteriae* are encoded by diverse temperate lambdoid bacteriophages. These phages are highly mobile genetic elements that play an important part in horizontal gene transfer. Infection of *Escherichia coli* by Shiga toxin-encoding bacteriophages (Stx phages) was the pivotal event in the evolution of the deadly Shiga toxin-encoding *E. coli* (STEC), of which serotype O157:H7 is the most notorious. The number of different bacterial species and strains reported to produce Shiga toxin is now more than 500 after the first reported STEC infection outbreak in 1982. In my system incoming phage, along with AI-3, provides the sentinels sufficient proof of *Shigella* existence. After infection **(Figure 45 (a)),** phage repressor silences transcription of most of its genes [207-209]. Removal of repression leads to a cascade of regulatory events beginning with expression of N transcription antitermination protein.

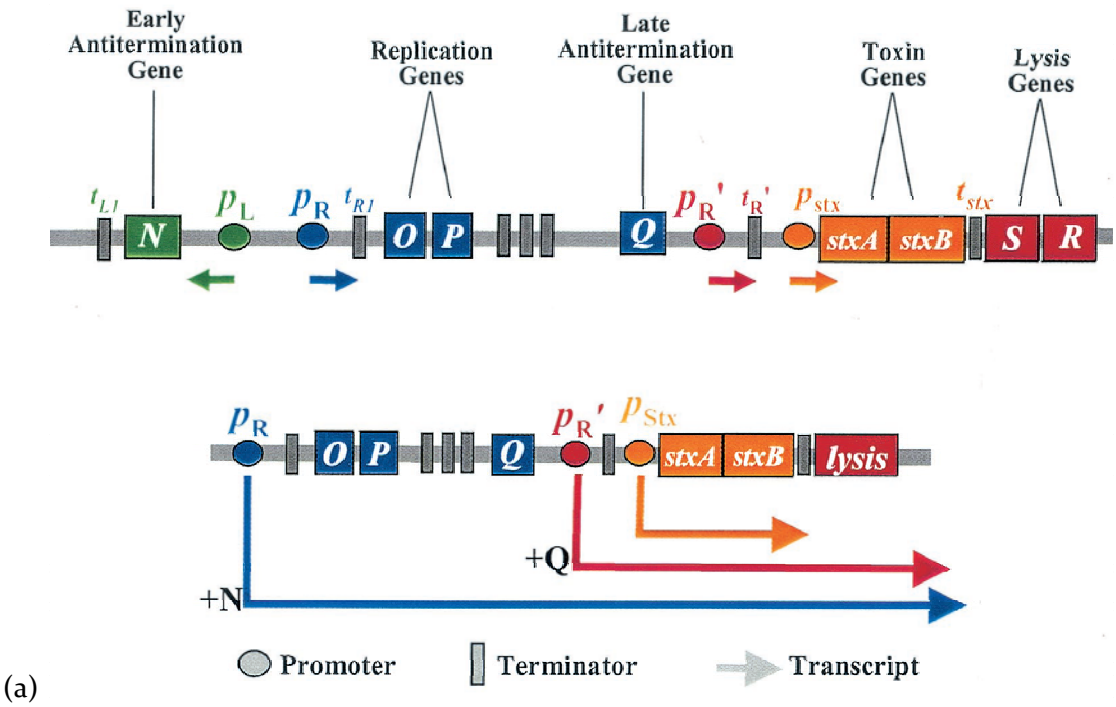

(a)

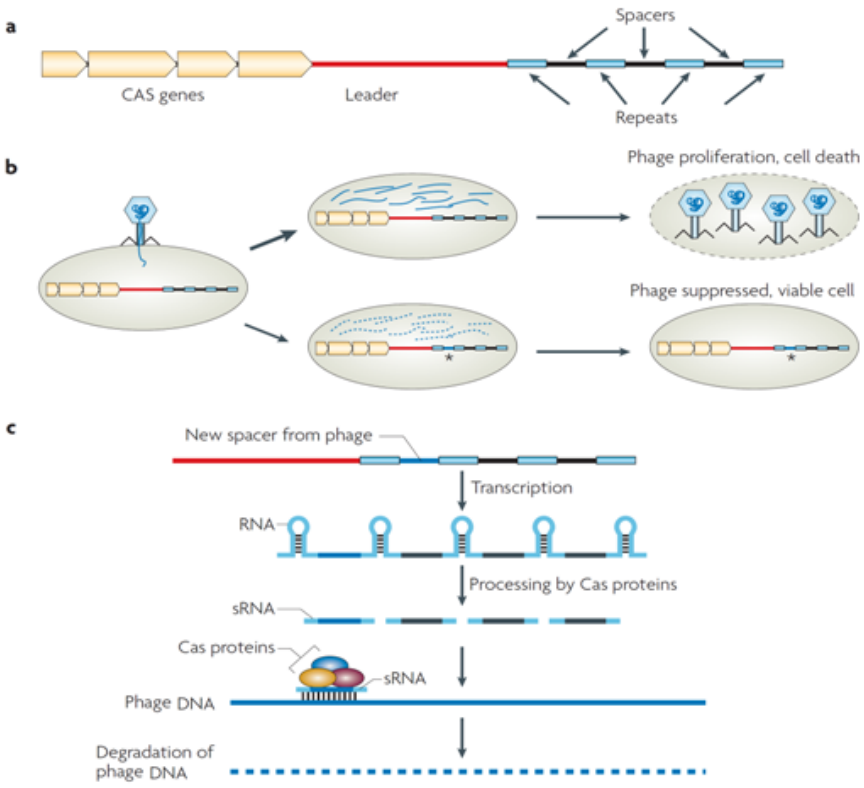

(b)

Figure 45: Mechanism of action of phages and CRISPR
(a) Organization and regulation of phage genes. This figure is adapted from [209] for illustrative purpose.
(b) Mechanism of action of CRISPR [210, 211]

Terminator read through mediated by the N protein results in expression of delayed early genes that encode products involved in replication, prophage excision and expression of late genes, which include Stx genes. Thus Stx expression by lambdoid prophages is a consequence of phage cycle. Sentinels sense the lytic phase of the incoming phage by having the same phage promoter P_L, activated by N protein, control phage and pathogen killing. Based on system performance a positive feedback regulator can be added on P_L after phage detection to maintain FlgM-Bacteriocin synthesis for a while till the pathogen is effectively destroyed.Once phage enters the lytic phase, sentinels immediately express Clustered Regularly Interspaced Short Palindromic Repeats (CRISPRs) [210-215] sequences specific to incoming phage DNA and *Shigella* specific bacteriocin on a high copy number plasmid. Engineered CRISPRs have already been shown to confer phage resistance [210, 213, 214]. CRISPRs are small repeated sequences separated by short spacer sequences that match bacteriophage and specify the targets of interference, a mechanism similar but not homologous to RNAi in eukarayotes **(Figure 45 (b)).** The repeat-spacer array is transcribed into a long RNA, and the repeats assume a secondary structure. Cas (CRISPR-associated) proteins naturally present in sentinel/killer cells will recognize the sequence or structure of the repeats and process the RNA to produce small RNAs (sRNAs), each of which contains a spacer and two half repeats. The sRNAs, complexed with additional Cas proteins, base pair with phage nucleic acids, leading to their degradation.

CRISPR can be engineered to target the most important genes of the phage, lytic gene lys, Shiga toxin gene Stx, replication and proliferation genes o and p. Having P_L on a high copy number plasmid further helps titrate away N and prevents expression of phage genes before CRISPR. Besides destroying phage and reducing its spread it is imperative to kill the pathogen safely. Conventional anti-microbial therapies are counterproductive since killing the bacteria may accelerate toxin release [216]. Hence it is necessary that the bacteria be killed without lysis in order to prevent toxin release and septic shock from the LPS outer membrane. This issue can be addressed by coupling secretion of engineered *Shigella* specific colicin (Colicin U [99, 217]) with CRISPR expression. Colicins are bacteriocins produced by certain bacterial strains of the family Enterobacteriae, and their toxic effects are limited to sensitive strains within the species of the producer strain. Group A, to which Colicin U belongs, has modular three-domain architecture. Their production is strictly regulated and coordinated with production of an Immunity Protein, which provides immunity to the producing cell, by binding and neutralizing colcin Killing Domain. Once these colcins are released into the extracellular space the Receptor Domain of the

bacteriocin binds a specific receptor on the outer memebrane of the target cell. Then the Translocase Domain forms a complex with the tol receptors on the surface of the cell and facilitates release of the Immunity Protein bound to the Killing/Nuclease Domain. The Killing Domain then enters the target cell and degrades the DNA/RNA without disrupting the outer membrane and hence this *Shigella* antimicrobial approach reduces the possibility of septic shock. Similar to CoPy, Receptor and Translocase Domain of colicin U can be fused to the nuclease and immunity domain of colicin E3 produced by *E. coli*. This will allow the new hybrid colicin, CoShi, to recognize and specifically kill *Shigella* strains while leaving the producing strain unharmed.

Response sensitivity of the sentinels can be characterized by growing them in filter sterilized supernatant of the pathogen (> 10^2 per ml for clinical relevance) and quantifying their response (with a response goal of 100 nM AI-3) by measuring fluorescence using flow cytometry. Immunofluorescent staining and epi-fluorescent microscopy can be used to assay sequestering of Stx by the sentinels [203, 204] and expression of YaeT on the surface of sentinels. CFU counting and efficiency of plaquing [206]can measure phage immunity and sensitivity. Western Blots and Bradford Assay can quantify the amount of killer protein secreted. Specific activity of the secreted protein can be determined by characterizing the amount of purified protein required to kill a specific number of pathogen. Fine-tuning analogous to that described in chapter 02 may be required to optimize the sentinel response to pathogens.

This system architecture is highly modular and every single module is responsible for addressing a different aspect of the pathogen. Hence the system is still useful even before all modules are made functional and fully optimized. Once individual parts are validated, the sentinels can be co-cultured with pathogen, as was done in chapter 02, to determine the ratio needed to inhibit the growth of *Shigella in vitro* with Vero/Caco-2 cell lines. Eventually microfluidic GI tract models can be used to accurately predict spatiotemporal parameters, which will then help us plan *in vivo* Human Intestinal Xenograft Infection [218] models to test the efficacy of the system.

b) *Vibrio cholerae* Sense and Destroy

Several enteric pathogens inhabit the lower gastrointestinal tract and cause-localized disease following their acquisition through the faecal–oral route [219]. *V. cholerae*, a motile gram-negative human pathogen, results in a wide spectrum of diseases with various severities, including a fatality rate of approximately 50% if untreated [219]. In my thesis I proposed a modified 'Sense

and Destroy' system against *V. cholerae*. The pathogen uses two QS pathways, one broad and the other species specific. Many pathogens, including *V. cholerae*, produce and respond to a set of interconverting molecules, together called AI-2 that are derived from the shared precursor 4,5-dihydroxy-2, 3-pentanedione (DPD) that is synthesized by the LuxS enzyme. CAI-1, (S)-3-hydroxytridecan-4-one is the major species-specific quorum-sensing signal in *V. cholerae* [45, 220].

Detection of the *V. cholerae* autoinducers occurs through membrane-bound histidine kinases that act as cognate receptors for the two autoinducers, as shown in the **Figure 46**. AI-2 is detected by the periplasmic protein LuxP in complex with LuxQ, while CAI-1 is detected by CqsS. LuxQ and CqsS are bi-functional two-component enzymes that possess both kinase and phosphatase activities. At low cell density (LCD), these two proteins are devoid of their respective ligands and act as kinases, resulting in phosphorylation of histidine residues by ATP. The phosphate group is next transferred to the conserved aspartate residue located in the receiver domain of each receptor. Phosphate from both the receptors is subsequently transduced to a single phosphotransfer protein, LuxU, which transfers the phosphate to a response regulator called LuxO [221]. LuxO belongs to the NtrC family of response regulators and requires phosphorylation to act as a transcriptional activator. Phosphorylated LuxO (LuxO-P) activates transcription of genes encoding four small regulatory RNAs (sRNAs) called *Qrr1–4* **(Figure 47 (a)).**

The main target of the *Qrr* sRNAs is mRNA encoding a master transcriptional regulator HapR. At LCD, the *Qrr* sRNAs are transcribed, and with the assistance of the RNA chaperone Hfq, these sRNAs destabilize the HapR mRNA transcript and prevent its translation. When autoinducer concentration is above the threshold level required for detection due to high cell density (HCD), autoinducers bind the cognate receptors and switches them from acting as kinases to phosphatases. Phosphate flow in the signal transduction pathway is reversed, resulting in dephosphorylation and inactivation of LuxO. Therefore, at HCD, *qrr1–4s* are not transcribed, HapR mRNA is stabilized, and HapR protein is produced.

At high cell density, quorum sensing represses both the expression of virulence factors and the formation of biofilms. These events allow *V. cholerae* to leave the host, re-enter the environment in large numbers and initiates a new cycle of infection. Ultrasensitive sentinels need to be engineered that will detect *V. cholerae* species specific CAI-1 by expressing codon optimized CqsS, LuxU and LuxO.

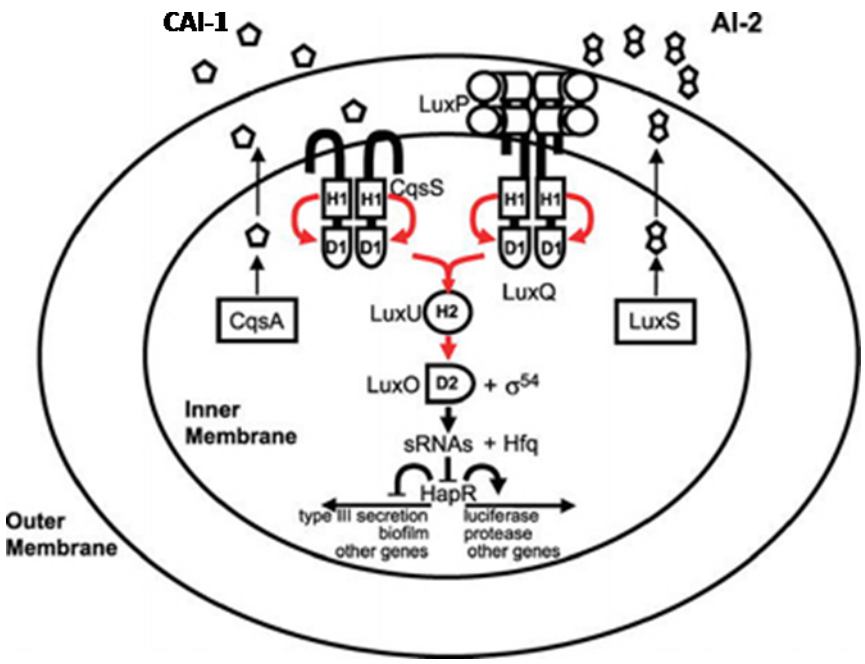

Figure 46: The *V. cholerae* quorum-sensing circuit.
This figure is adapted from [222] for illustrative purpose.

(a) (b)

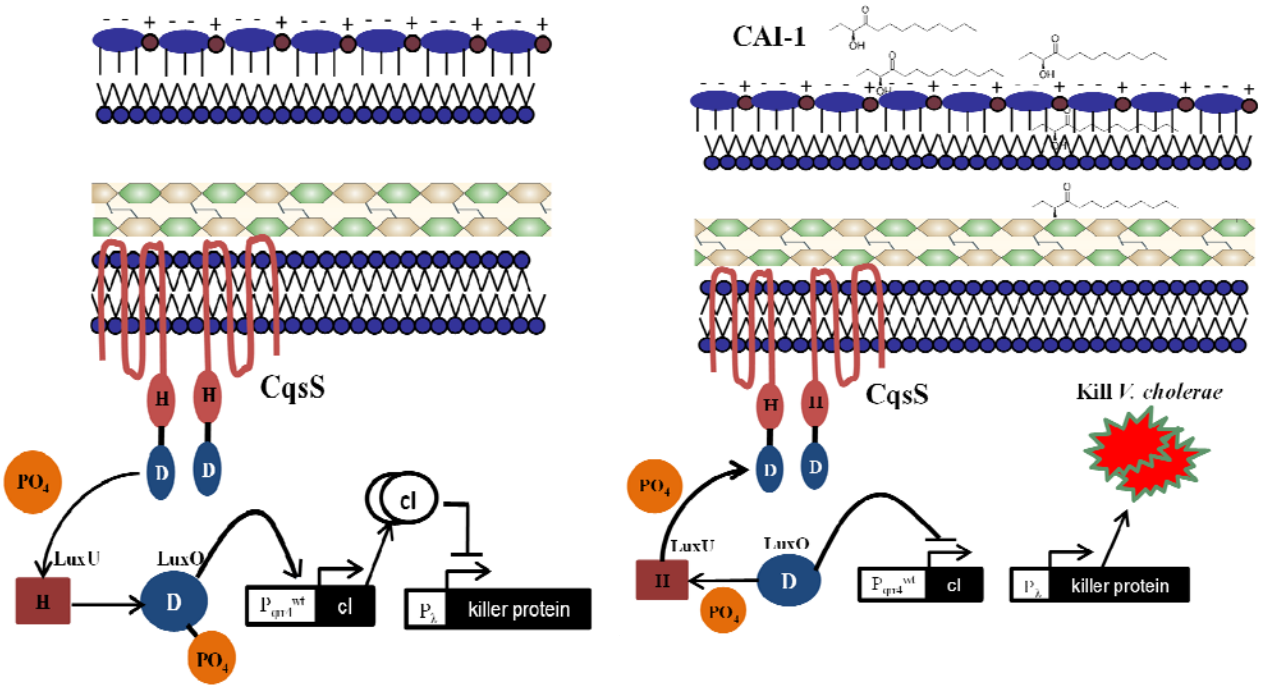

Figure 47: *Vibrio cholerae* 'Sense and Destroy' system.
(a)Sentinel activity when *V. cholerae* pathogen is at low cell density. (b) Expression and secretion of killer protein from the sentinels at high pathogen cell density.

As explained in chapter 02 earlier experience in building a signal amplifier will be useful in this scenario. **Figure 47 (b)** shows proposed *V. cholerae* sense and destroy circuit. In the absence of CAI-1, indicating low pathogen density, LuxO will be phosphorylated and promotes expression of a destabilized lambda repressor (cI-lva) [223] under P_{qrr4wt}. cI-LVA represses lambda promoter which regulates transcription of killer protein. As shown in **Figure 47 (a & b)** when pathogen density increases, the concentration of CAI-1 in the medium rises, causing it to bind CqsS and trigger the phosphatase which in turn deactivates LuxO and prevents the transcription of cI-lva. cI-LVA degrades quickly, allowing killer protein expression and secretion. This construct functions as a signal amplifier that detects even minute concentrations of CAI-1 in the medium when the pathogen is still in the early stages of infection. Function of signal amplifier is explained more in chapter 02.

Similar secretion mechanism as was demonstrated earlier in chapter 02 could be used to engineer secretion of a bacteriocin specific to *V. cholerae.* Five potential bacteriocins, all synthesized in a gram-positive soil bacterium *Bacillus thuringiensis*, are Morricin 269, Kurstacin 287, Kenyacin 404, Entomocin 420, Tolworthcin 524 [224]. These peptides are reported to selectively kill *V. cholerae* and are not effective against other gram-negative bacteria, including *E. coli, S, typhi, S. flexneri, S. sonnei* and *P.aeruginosa*. These bacteriocins are thermostable, resistant to α-amylase, RNAase and lysozyme, and show considerable activity at both low and high pH, which is characteristic of the stomach and gut environments [225]. They have a molecular mass between 10-25 kDa and no cystein residues. In my previous efforts proteins up to 90 kDa were secreted successfully, which likely indicates that FlgM can work as good secretion tag.

Again the sensitivity of the sentinels can be tested by growing them in filter sterilized supernatant of the pathogen and quantifying their response by measuring fluorescence using flow cytometer. Western Blots and Bradford Assay can quantify the amount of killer protein secreted. Specific activity of the secreted protein can be determined by characterizing the amount of purified protein required to kill a specific number of pathogen. Fine-tuning analogous to that described in chapter 02 may be required to optimize sentinel response to pathogens. Once the individual parts are tested, sentinels can be co-cultured with pathogen to determine a ratio needed to inhibit the growth of *V. cholerae.*

CHAPTER 6 -APPENDIX

I. Materials and Methods

a) Protein secretion, purification and concentration measurement

1L of *E. coli* (DH5 alpha-pro) cells containing His-FlgM-CoPY were grown to an optical density of 0.05 and their expression was induced by exogenous $3OC_{12}HSL$ (Cayman chemical Item Number 10007895). Induced culture was incubated at 37C at 280rpm for 4 hours. Subsequently the cells were pelleted by centrifugation of the culture at 6000rpm for 20 minutes. Supernatant was collected and filter sterilized by a 0.22micrometer NALGENE 500 ml, low protein binding, filter. This supernatant containing secreted His-FlgM-CoPy was concentrated by ultrafiltration using a 10-kDa molecular mass cut-off membrane in an AMICON stirred cell concentrator (Millipore, Billerica, MA, product number 8400) until the volume was decreased to approx 70 mL. The retained medium was further concentration using the smaller centricon plus-70 (Millipore) centrifuge filteration devices with Ultracel PL-10 regenrated cellulose 10,000 MWCO. (Catalog number UFC701008). Final volume of this retentate was 350 ul. This retentate was Histag purified under native conditions using Ni-NTA (Ni^{2+}-nitrilotriacetate) Superflow (Qiagen) column,washed with 50 mM sodium phosphate buffer, 300 mM NaCl and 10 mM imidazole (pH 7.4) and eluted with 50 mM NaPO4, 300 mM NaCl and 500 mM imidazole (pH 7.4). Purification using Co^{+2} ions from Clontech gave the same results. Its concentration was determined via UV spectroscopy using ThermoScientific, NanoDrop 2000c and the extinction coefficient (ε=0.781) as calculated by the ProtPram tool on the ExPASy toolserver [226].

b) Cell density and fluorescence measurements

Optical density (600 nm) readings were measured in a Tecan Safire² plate reader (Tecan-US, Durham, NC) at regular periods over the course of the experiment. Total volume of culture and purified CoPy or His-FlgM-CoPy in a well of a 96-clear-bottom microtiter plate (Falcon, Oxnard, CA) was 200 ul. To prevent evaporation of the culture for long experiments each well was covered with 40 ul of mineral oil (ACROS Organics, USA) and incubated at 37°C at 280 rpm. Green fluorescence was measured using a Becton-Dickinson FACSCAN flow cytometer with a 488-nm argon excitation laser and a 515-545 excitation filter as described in [54].

c) Strains and growth conditions

E. coli K-12 MG1655 (F- lambda- *ilvG- rfb*-50 *rph*-1) was obtained from the *E. coli* Genetic Stock Center at Yale University. *Escherichia coli* Nissle 1917 was a gift of Prof. Florian Gunzer from Technical University of Dresden, Germany. Wild type *Pseudomonas Aeruginosa* (PAO1) and a constitutively green strain of PAO1, *PAO-Tdk-gfp*, was a gift of Prof. Barbara H. Iglewski from University of Rochester Medical Center. *PAO-TdK-gfp* is resistant to 100 ug/mL ampicillin (Sigma, St. Louis, MO). *E. coli* DH5*a* (F- _80dlacZ_M15 _(lacZYA-argF)U169 recA1 endA1 hsdR17(rk - , mk+) phoA supE44 thi-1 gyrA96 relA1 E-) was used for plasmid building and propagation. LB broth (Difco, Detroit, MI) with the appropriate antibiotic(s) was used as a growth medium in all experiments. For direct detection experiments, 25 ug/mL Cholramphenicol (Shelton Scientific, Shelton, CT) and 100 ug/mL ampicillin (Sigma, St. Louis, MO) were used. Wild type PAO1 is naturally resistant to 25 ug/ml of Chloramphenicol. The AHLs butanoylhomoserine lactone (C4HSL), 3-oxohexanoyl-homoserine lactone (3OC6HSL) and 3-oxo-dodecanoyl-homoserine lactone (3OC12HSL) are from CAYMAN chemicals. For all growth experiments, cultures were incubated at 37°C in a shaker at 280 rpm.

HEK 293FT (Invitrogen) human embryonic kidney fibroblasts (stably expressing the SV40 large T antigen) were used for transfection experiments. To activate rtTA dependent Tet-ON promoter, Doxycycline (Clontech) was used at the indicated concentrations. All the cells were grown at 37°C and 5% CO2 in a sterile tissue culture incubator. Cell culture media for culturing 293FT/NIH3T3 cells is composed of 87.9% DMEM (Hyclone), 10% Tet-approved Fetal Bovine Serum (Clontech), 1% Penicillin-Streptomycin (Hyclone), 1% Non-Essential-Amino-Acids (Hyclone), 0.1% Fungin (Invivogen) filtered through a 0.45 micron filter (Nalgene).

d) Electrocompetent Cells

EcN and MG1655 cells were grown in S.O.B (Difco, Detroit, MI) to an O.D. of 0.55 at room temperature. They were spun down by centrifugation at 4000rpm for 20 minutes, re-suspended and washed with ice cold 10% glycerol. This procedure was repeated 4 times and the final suspension volume was 40X from the starting volume. 100 ul aliquots were quickly frozen in liquid nitrogen and stored at -80 C.

e) Microscopic Cell Imaging

For the images shown in **Figure 26**, 10 ul highly diluted droplets of cells (PAO1-red, *E. coli*, MG1655) were pipetted on an agar plug. The agar plugs were then inverted on a sterile WillCo glass-bottom dish with the cells touching the glass bottom. The plate was then incubated at 37° C, and images were taken from below every 60 min by using a Zeiss (Thornwood, NY) Axiovert 200M microscope equipped with an AxioCam MR CCD camera. Images were captured with a X40 brightfield objective. Once the cells started growing 1 uM concentration of CoPy was pippetd on the agar plug and images were taken after every 60 minutes. For the **Figure 26** the experimental setup is described in chapter two. The images were taken with 10X objective and a GFP filter with 470/40 excitation and 525/50 emission.

f) Western Blot

Anti-FlgM antibody [128] was kindly provided by Prof. Kelly Hughes from the University of Utah. Rabbit polyclonal antibody was raised against a maltose binding protein (MBP)-CpxR hybrid [227] was used at a 1: 30,000 dilution and revealed with horseradish-peroxidase conjugated goat anti-rabbit IgG. I used the following western blotting protocol:

- Obtain Gel in packet (4–20% Mini-PROTEAN® TGX™ precast polyacrylamide gels from BIO-RAD) and load it into the holder device (Mini-PROTEAN® Tetra System from BIO-RAD) with the lanes facing toward the center. Fill the gel device with running buffer.
- Load sample (several dilutions in loading buffer if desired) and ladder (pre-stained broad range protein ladder from cell signaling #7720). Fill any empty wells with loading buffer to prevent coffee cup effect.
- Run gel for 60 min at 120V or until blue line reaches bottom of gel.
- While gel is running soak the membrane (PDVF) in 100% methanol (>30min) and the two extra thick blotting paper pads in the transfer buffer (with methanol) for ~20 min. This is required because membrane needs to be activated. It is not needed for Nitrocellulose membrane.
- After running the gel remove it from the casket and soak it in the transfer buffer for 5 min to equilibrate otherwise the gel will shrivel. At this point if only Commassie Blot is needed then the gel can be directly transferred to the Commassie staining solution for 2 minutes and then to the de-staining solution until the gel is completely de-stained.
- Then transfer from gel to the Trans-Blot® SD Semi-Dry Transfer Cell from BIO-RAD. Make

the gel and membrane sandwich according to the semi-dry transfer instructions.

- Run the machine at ~10V for 60min (appropriate time may need several iterations)
- Make Blocking solution in TBST (TBS+0.05% tween-20) according to GE Healthcare Amersham ECL advance western blotting detection kit.
- Incubate the membrane in the blocking buffer for 15 min.
- Make up antibody solutions (according to antibody specifications) in blocking buffer.
- Incubate the membrane in the primary antibody solution for 1hr at room temperature.
- Wash the membrane 3X 5 min with TBST.
- Incubate the membrane in the secondary antibody solution for 1hr at room temperature.
- Wash the membrane 3X 5 min with TBST.
- Use GE Healthcare Amersham ECL advance western blotting detection kit for developing the membrane and BIO-RAD imager (Molecular Imager® Gel Doc™ XR+ System with Image Lab™ Software from BIO-RAD, Hercules, CA, USA) for taking gel picture.
- **NOTE:** antibody solutions can be saved for later use with .02% sodium azide

1X Tris-HEPES-SDS Running Buffer consists of:

100 mM Tris

100 mM HEPES

3 mM SDS

Coomasie Staining Solution (1 liter):

500 ml Methanol

400 ml Ultrapure water

100 ml Glacial Acetic Acid

2.5 g Coomassie Brilliant Blue R-250

Coomasie Destaining Solution (1 liter):

785 ml ultrapure water

165 ml Ethanol

50 ml Glacial Acetic Acid

g) Immunofluorescence staining protocol

Materials Needed:

- Cells grown on glass slips (see poly-D-Lysine protocol for preparing cells grown on glass cover slips)
- 1x TBS
- 1x PBS
- Paraformaldehyde Containing fixation buffer
- Tweezers
- Parafilm
- 1x PBS with .1% triton X-100 (permeabilization solution)
- 1x PBS with 1% BSA (blocking solutions).
- Two primary antibodies were used. First one is E7 against beta-tubulin mouse anti-mouse and the second one is 6X His-Tag goat anti-rabbit IgG from Rockland. Two secondary antibodies used were Alexa Fluor 488, goat anti-mouse IgG 2mg/ml and Alexa Fluor 610 R-phycoerythrin goat anti-rabbit respectively. Both are from Invitrogen.
- Mounting medium (mowiol)
- Glass slides for mounting

  Protocol :
- Remove cells culture media from the wells and very carefully wash them with 500ul 1x PBS (the PBS should contain Ca^{+2} and Mg^{+2}). Remove PBS and add 500ul Fixation Buffer. (or just remove as much media as possible and then add fixation buffer)
- Wash 3x 5min in 200 ul TBS (to neutralize the remaining fixation buffer)
- Incubate cells in 100 ul of PBS with 0.1% Triton X-100 for 10min
- Wash 3x 5min in 200 ul PBS
- Incubate Cells in 200 ul of PBS with 1% BSA for 15 min
- Incubate cells in 25 ul of Primary antibody solution for 1 hour. Cover the glass slides so that the samples don't dry out.
- Wash 3x 5min in 200 ul PBS
- Incubate cells in 25 ul of secondary antibody solution (1:200 to 1:2000) for 1 hour. Cover the glass slides so that the samples don't dry out. Keep it out of light.
- Wash 3x 5min in 200 ul PBS

- Mount these glass slips on a glass slide with a dab of the mowiol and let them dry in the dark for about 30 min
- Seal borders with clear nail polish. Observe them under microscope.

h) Poly-D-Lysine Protocol

- Poly-D-Lysine is used in a concentration of ~50 ug/ml
- Then apply to the glass slides and let sit for 1hour.
- Wash once with DI sterile Water
- Apply cells
- **NOTE**: Poly-D-Lysine should not be kept in polypropylene tubes. Polystyrene or PET are better.

i) Fast-Forward transfection of mammalian cells with DNA in 24 well plate using Attractene (Qiazen)

- Dilute 0.4 µg DNA dissolved in TE buffer, pH 7–8 (minimum DNA concentration: 0.1 µg/µl) with medium without serum, proteins, or antibiotics, to a total volume of 60 µl. For example, if the DNA concentration is 1 µg/µl, dilute 0.4 µl DNA in 59.6 µl medium.
- Add 1.5 µl Attractene Transfection Reagent. Mix by pipetting up and down or vortexing. Centrifuge for a few seconds to remove any liquid from the top of the tube if necessary.
- Incubate the samples for 10–15 min at room temperature (15–25ºC) to allow transfection complex formation. Transfection complex formation takes a minimum of 10–15 min. The transfection complexes will remain stable during the time it takes to prepare the cells for transfection. However, the incubation time should not be extended for longer than is necessary for cell preparation.
- Harvest the cells by trypsinization and suspend in culture medium containing serum and antibiotics. The cells should be healthy and in logarithmic growth phase. It is important that serum and antibiotics are present in the culture medium at this point because transfections are performed without changing the medium. The cultivation of cells over this time without serum would deprive the cells of essential growth factors. This does not apply to cells that are routinely cultivated without serum.
- Count the cells in the harvested cell suspension and adjust the cell density to 0.4–1.6 x 10^5 cells in 500 µl (depending on the cell line). The optimal cell density should be determined

for each cell line. For example, cell density should be adjusted to 0.8–3.2 x 10^5 cells per ml for a final cell density at transfection of 0.4–1.6 x 10^5 cells in 500 µl. As plating and transfection of cells are carried out on the same day, higher cell densities are required than would be necessary if the cells had a longer incubation time prior to transfection. As a guideline, the required cell number is usually 2–3 folds higher than that used for the Traditional Protocol (where cells are plated on the day before transfection).

- Add 500 µl of the cell suspension to a well of a 24-well plate. Next, add the transfection complexes to the well. Mix by pipetting up and down twice.
- Incubate the cells with the transfection complexes under their normal growth conditions (typically 37°C and 5% CO_2).
- In most cases, removal of transfection complexes is not necessary. However, if cytotoxicity is observed, remove the complexes after 6–18 hours and add fresh culture medium.
- Assay the cells for expression of the transfected gene after an appropriate incubation time. The length of the incubation time depends on the assay and the transfected gene.
- For stable transfections, passage the cells into the appropriate selection medium 24–48 h after transfection. Maintain the cells in selective culture medium until colonies appear.

j) Modified Modular Cloning(mod-MoClo) Strategy

Previous efforts in synthetic biology largely focused on the creation of genetic devices and small modules that are constructed from these devices [228-242]. But to truly program cells, significant advances in strategies to assemble devices and modules into large scale systems are needed. Recent progress in the field has seen organisms with entire genomes synthesized [243-245]. Recently Ernest Weber et al [246] published a modular cloning strategy using standard type IIs enzymes which allows rapid high throughput assembly of several multi-gene constructs. I developed a similar but slightly modified strategy for constructing bacterial plasmids.

MoClo strategy [246] involves assembling one promoter, one 5' untranslated region (UTR), one signal peptide, one coding sequence of a gene and a terminator from sets of pre-made standardized modules into one transcriptional unit (TU). This standardization works if the gene circuit is destined for eukaryotic systems but bacterial operons can be bi-cistronic which means one transcriptional unit can have a promoter, 5' UTR, signal peptide, gene, another RBS (different or similar from the one in 5'UTR), another gene and a terminator. In order to have that flexibility the original MoClo strategy was modified to construct bi-cistronic system in bacteria. This was

achieved by slightly modifying the flanking barcodes of different parts such that a bi-cistronic system can be constructed with the use of another type IIs enzyme, AarI, besides the regular enzymes. **Figure 48 (a)** shows the flanking bar codes for any part and the corresponding level zero destination vectors. According to the bar codes given in , the modified MoClo protocol is divided into three parts.

- If the transcriptional unit is (promoter_RBS_non-secreted gene_terminator) then the protocol is similar to running 4 part MoClo with pLo-P, pLo-U, pLo-SC, pLo-T as level zero vectors.
- If the transcriptional unit is (promoter_RBS_secretion-signal_secreted gene_terminator) then the protocol is similar to running 5 part MoClo with pLo-P, pLo-U, pLo-S, pLo-C, pLo-T as level zero vectors.
- If the transcriptional unit is (promoter_RBS1_non-secreted gene 1_RBS2_non-secreted gene 2_terminator) then the modified protocol is as follows
    i) First digest 40fmoles of gene1 and RBS2 with AarI at 37C for 3 hours and completely deactivate AarI by incubating the mixture for 20 minutes at 65C.
    ii) Add 40fmoles of gene2 and pLo-SC to above mixture with 10units of BpiI and 10units of T4 DNA ligase (using high concentration ligase, 20 U/ml) in Promega ligation buffer in a final reaction volume of 20 ul. The mix was incubated in a thermocycler with the following parameters: incubation for 2 minutes at 37C, 5 minutes at 16C, both steps repeated 45 times, followed by incubation for 5 minutes at 50uC and 10 minutes at 80C. The reaction mix was then added to 100 ul chemically competent DH10b cells, incubated for 30 min on ice and transformed by heat shock. 800 ul of liquid LB was then added to the transformation, and the cells were let to recover 60 min at 37C. Different aliquots of the transformation were plated on LB plates containing the appropriate antibiotic. The resulting plasmid will be pLo-gene1_RBS2_gene2 which then can be used to run a 4 part MoClo with pLo-promoter, pLo-RBS1 and pLo-Terminator.

Using the protocol and flanking bar codes discussed above a library of parts was constructed that is given in **Figure 48 (b)**. This library was then used to construct five level one transcriptional units given in **Figure 48 (c).** In future a level two vector can be constructed from these five transcriptional units.

(a)

1. ATAGAGgaagacttGGAG-**Promoters**-TACTttgtcttcCTCTAT----pLo-P
2. ATAGAGgaagacttTACTaacacctgcctagCTCG-**RBS**-ggagggAATGttgtcttcCTCTAT—pLo-U
3. ATAGAGgaagacttAATG-**Gene**- cacctgcctagCTCGGCTTttgtcttcCTCTAT—pLo-SC
   a) ATAGAGgaagacttAATG—**N terminal Secretion Signal**-gg-AGGTttgtcttcCTCTAT--pLo-S
   b) ATAGAGgaagacttAGGT-**Secreted Gene**- cacctgcctagCTCGGCTTttgtcttcCTCTAT--pLo-C
4. ATAGAGgaagacttGCTT-**Terminator**-CGCTttgtcttcCTCTAT—pLo-T

(b)

1) **Promoters**
   a) pConsensus
   b) pLAC-LacO
   c) pLAS
   d) pLacIq
   e) pLuxPr(luxICDABEG+cIORI)
2) **Secretion Signal**
   a) HisTag-FlgM
3) **RBS**
   a) RBSII
   b) RBSH
4) **Genes**
   a) DsRed
   b) ECFP
   c) EYFP
   d) cI
   e) LacI
   f) LasR
   g) Imm
   h) Tsi2
   i) LasR-RBSII-DsRed
   j) Imm-RBSII-Tsi2
   k) ECFP-RBSII-LacI
5) **Secreted Genes**
   a) CelY
6) **Terminators**
   a) Boot
   b) Double Terminator
   c) Terminator t
   d) Terminator 0

(c)

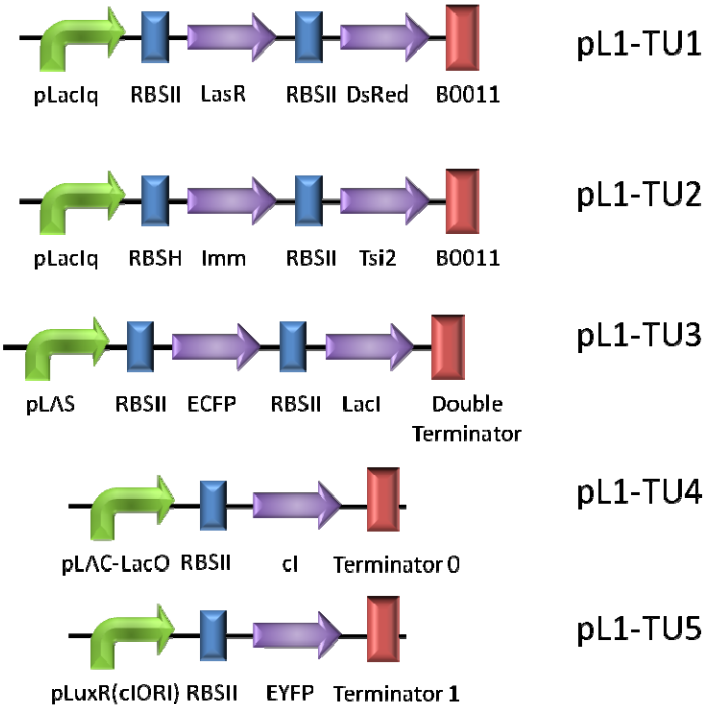

Figure 48 : Modified MoClo cloning strategy

(a) Flanking barcodes for different components and their different destination vectors. Enzyme (BpiI and AarI) cut sites are in black color, resulting overhangs after digestion from enzymes are in magenta color, filler sequences are in light gray and junk sequences which allow enzymes to sit and digest are in blue color. (b) All level zero vectors with promoters in pLo-P, RBS in pLo-U, Secretion signal in pLo-S, genes in pLo-SC, secreted genes in pLo-C and terminators in pLo-T. (c) Parts constructed in (b) were used to construct five transcriptional units which if combined for level two will result in bacterial adaptive response circuit with different fluorescent markers instead of toxins.

k) Supporting Figures

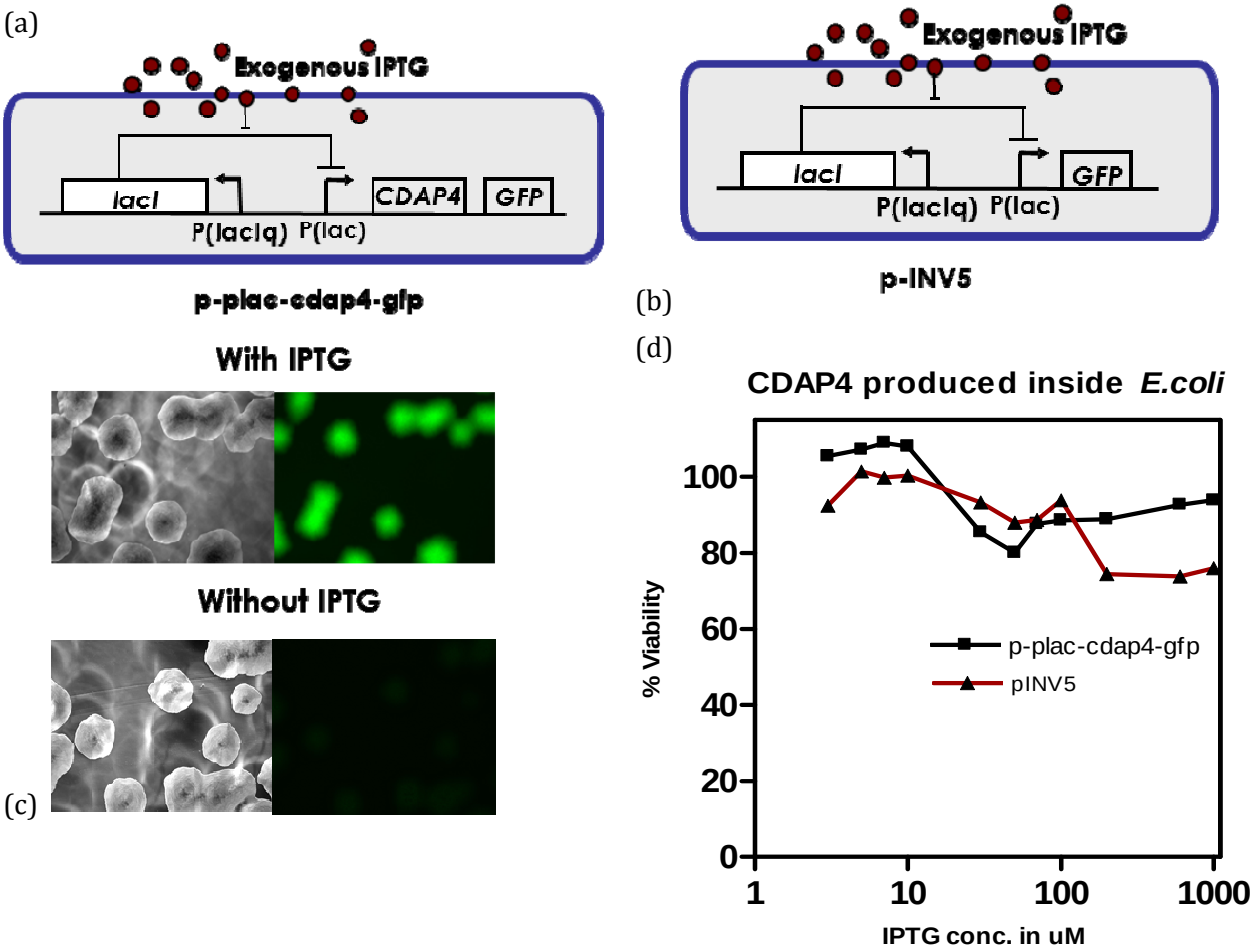

Figure 49: Expression of CDAP4 using IPTG induction.
(a) CDAP4 and GFP are cloned under IPTG inducible promoter. (b) Only GFP under IPTG control (c) Cells containing CDAP4 and GFP with and without IPTG. It shows that colonies expressing CDAP4 and GFP look healthy. The images were taken using 2.5X objective of a Zeiss Microscope. (d) cell viability when cells are expressing CDAP4. P-plac-cdap4-gfp is the plasmid shown in (a) while pINV5 is the plasmid shown in (b).

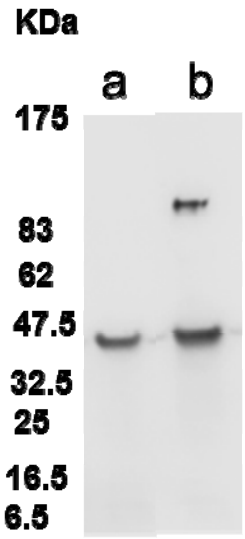

Figure 50: Western Blot of *E. coli* cells expressing FlgM-CoPy with and without FliCDST operon deletion in the chromosome.
Lane (a) is the supernatant collected from E. coli cells with FliCDST deletion. This deletion was achieved in the MAZE [247]strain EcNRZ[recA-, mutS-] using one step inactivation method described in Datsenko, KA, Wanner, BL [248]. Lane (b) is the supernatant from MG1655.

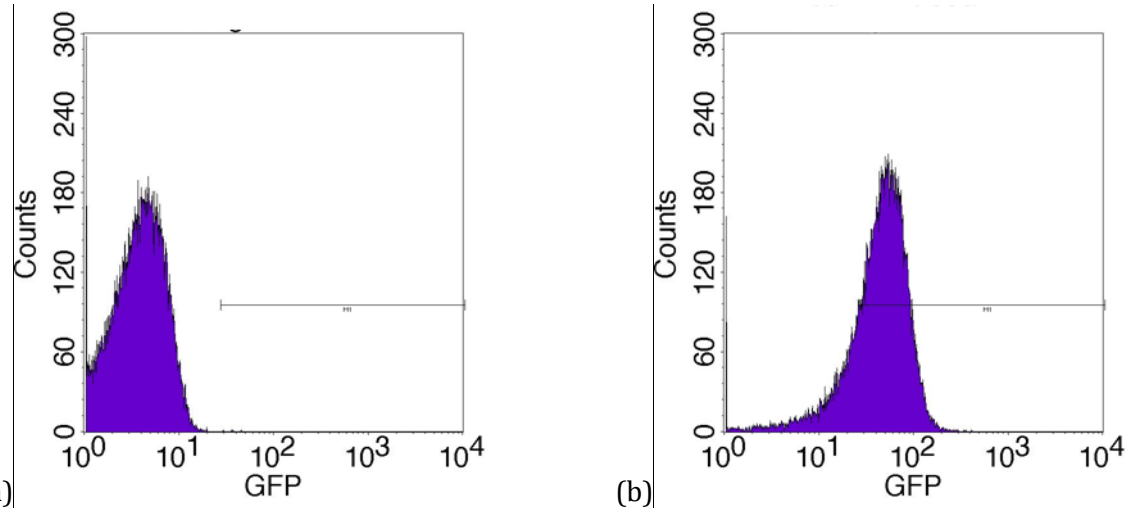

Figure 51: Histogram of the sentinels expressing FlgM-CoPy and GFP.
(a) uninduced sentinels (b) Fully induced sentinels with 10uM 3OC12HSL. This shows that the expression profile with or without induction is unimodal.

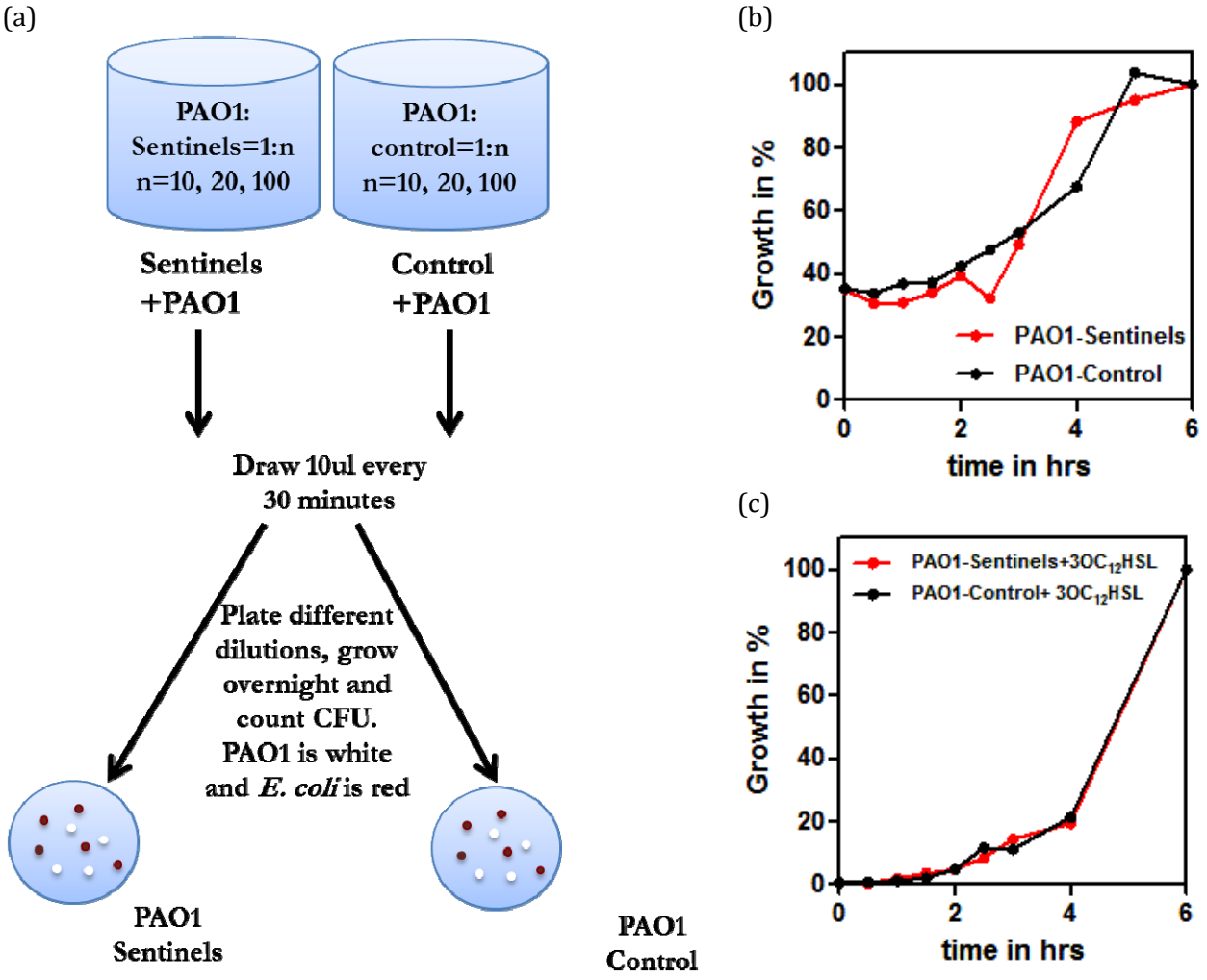

Figure 52 : Co-culture of PAO1 with the sentinels and control cells
(a) Experimental setup to co-culture PAO1 and *E. coli* in the liquid medium in different ratios starting from 1:10, 20 and 100. Starting culture was 4 ml and culture was drawn every 30 minutes for 6 hours. Various dilutions were plated on MaConkey agar and colonies were counted the next day. On this agar PAO1 forms white colonies and E. coli forms red colonies. (b) This figure shows that for 1:10 starting ratio the growth of PAO1 is same with or without the sentinels. (c) This figure shows that for 1:10 starting ratio the growth of PAO1 is same with or without the sentinels even when the cells are maximally induced with 10uM 3OC12HSL.

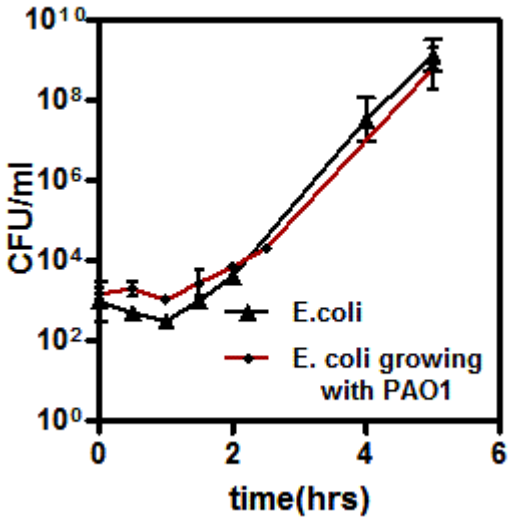

Figure 53: Growth of *E. coli* growing with and without PAO1.

l) List of Plasmids.

The following table provides an overview of the plasmids constructed for the various systems described in this thesis. All the plasmids for bacterial 'Sense and Destroy' system described in this study were constructed using basic molecular biology cloning techniques. The plasmid pLas-His-FlgM-CoPy-mRFP encodes *His-FlgM-CoPy* under control of the *P. aeruginosa* p(las) promoter, as well as constitutive LasR and mRFP production from a weakly constitutive *p(lacIq)* promoter. CoPy is a chimeric bacteriocin with receptor and translocase domain from pyocin S3 and nuclease and immunity domain from colicin E3. It was constructed as described in [109] and cloned under p(las) promoter. FlgM was pcr'd from E. coli MG1655 genome and PCR SOE'd to CoPy with FlgM being fused in frame to the N terminus of CoPy. LasR and pyocin S3 was pcr'd from PAO1 genome. All the plasmids for mammalian 'Sense and Destroy' system were constructed using Gateway and Gibson cloning methods from Invitrogen. pENTR are all entry vectors obtained after basic BP reaction. All pZDonor's are vector obtained after LR reaction.

Mammalian Sense and Destroy plasmids		
Entry Vectors		
Plasmid Name	**Antibiotic Resistance**	**Origin of Replication**
pENTR_L4_UbC_R1	Kanamycin	pUC origin
pENTR_L4_TRE-tight_R1	Kanamycin	pUC origin
pENTR-L1-TetR-mirff4-L2	Kanamycin	pUC origin
pENTR_L1_LacI-FF5-miRFF4_L2	Kanamycin	pUC origin
pENTR_L4_minCMVLoxO7_R1	Kanamycin	pUC origin
pENTR_L1_EBFP-4Xff4_L2	Kanamycin	pUC origin
pENTR_L1_EBFP-4xff5_L2	Kanamycin	pUC origin
pENTR_L1_EBFP2-AscI-SpeI_L2	Kanamycin	pUC origin
pENTR_L1_EBFP2_L2	Kanamycin	pUC origin
pENTR_L1_Ig-CDAP4_L2	Kanamycin	pUC origin
pENTR_L1_NOS2-HisTag_L2	Kanamycin	pUC origin
pENTR-L1-TetR-mirff4-L2	Kanamycin	pUC origin
pENTR_L1_LacI-FF5-miRFF4_L2	Kanamycin	pUC origin
pENTR_L1_TetR-mirFF5_L2	Kanamycin	pUC origin
pENTR_L1_Ig-CDAP4_L2 PCR Product	Kanamycin	pUC origin
pENTR_L1_SecTATk-VP16Gal4-His_L2	Kanamycin	pUC origin
pENTR_L1_SS-CDAP4_L2	Kanamycin	pUC origin
pENTR_L4_TRE-LacO1Oid-81.5_R1	Kanamycin	pUC origin
pENTR_L4_PacI-EcoRI_R1_ND	Kanamycin	pUC origin

pENTR_L4_CAGop_R1_ND	Kanamycin	pUC origin
pENTR_L1_mKate_L2	Kanamycin	pUC origin
pENTR_L1_LacI_L2	Kanamycin	pUC origin
pENTR_L1_LacI-FF5-miRFF4_L2	Kanamycin	pUC origin
pENTR_L1_EYFP-FF6x4-L2	Kanamycin	pUC origin
pENTR_L1_EYFP-FF4x4-L2	Kanamycin	pUC origin
pENTR_L1_EBFP2_L2	Kanamycin	pUC origin
pENTR_L1_AmCyan-mirFF4-L2	Kanamycin	pUC origin
pENTR-L4_Hef1a-tetO2-R1	Kanamycin	pUC origin
pENTR_L1_LacI-4Xff4-miRFF6_L2	Kanamycin	pUC origin
pENTR_L4_pLas-4-lasbox_R1_SG	Kanamycin	pUC origin
pENTR_L4_pLas-6-lasbox_R1_SG	Kanamycin	pUC origin
pENTR_L4_pLas-7-lasbox_R1_SG	Kanamycin	pUC origin
pENTR_L4_pLas-LacOid_R1_SG	Kanamycin	pUC origin
pENTR_L4_pLux-LacOid_R1_SG	Kanamycin	pUC origin
pENTR_L1_mCoPy_L2	Kanamycin	pUC origin
pENTR_L4_pLas-7-lasbox_R1	Kanamycin	pUC origin
pENTR_L1_p65H4LuxRFmNLS_L2	Kanamycin	pUC origin
LR Vectors		
pZDonor 1-GTW-2r-minCMVLoxO7-Ig-CDAP4	Ampicillin	pBR322
pZDonor 1-GTW-2r-minCMVLoxO7-mKate	Ampicillin	pBR322
pZDonor 1-GTW-2r-pLas-4-lasbox-mKate	Ampicillin	pBR322
pZDonor 1-GTW-2r-pLas-6-lasbox-mKate	Ampicillin	pBR322
pZDonor 1-GTW-2r-pLas-7-lasbox-Ig-CDAP4	Ampicillin	pBR322
pZDonor 1-GTW-2r-pLas-7-lasbox-mKate	Ampicillin	pBR322
pZDonor 1-GTW-2-UbC-RheoAct-2A-Rec-FF3	Ampicillin	pBR322
pZDonor 2-GTW-3r-Hef1a-tetO2-LacI-4Xff4-miRFF6	Ampicillin	pBR322
pZDonor 2-GTW-3-5xUAS-TetR-mirff4	Ampicillin	pBR322
pZDonor 3-GTW-4r-Hef1a-LacO1Oid-EYFP-FF6x4	Ampicillin	pBR322
pZDonor 3-GTW-4r-pLas-LacOid-EYFP-FF6x4	Ampicillin	pBR322
pZDonor 3-GTW-4r-pLux-LacOid-EYFP-FF6x4	Ampicillin	pBR322
pZDonor 3-GTW-4-Hef1a-tetO2-EYFP-FF4x4	Ampicillin	pBR322
pZDonor 4-GTW-5-minCMVLoxO7-TetR-mirff4	Ampicillin	pBR322
pZDonor 4-GTW-5-pLas-4-lasbox-TetR-mirff4	Ampicillin	pBR322
pZDonor 4-GTW-5-pLas-6-lasbox-TetR-mirff4	Ampicillin	pBR322
pZDonor 4-GTW-5-pLas-7-lasbox-TetR-mirff4	Ampicillin	pBR322
pZDonor 4-GTW-5-Rheo-5xUAS-AmCyan	Ampicillin	pBR322
pZDonor 5-GTW-6-Hef1a-tetO2-AmCyan-mirFF4	Ampicillin	pBR322

pZDonor 6-GTW-7-UbC-p65H4LuxRFmNLS	Ampicillin	pBR322
pZDonor 1-GTW-2r-minCMVLoxO7-SS-CDAP4	Ampicillin	pBR322
pZDonor 1-GTW-2r-pLas-7-lasbox-SS-CDAP4	Ampicillin	pBR322
pZDonor 2-GTW-3r-5xUAS_Rheo-TetR-mirFF5	Ampicillin	pBR322
pZDonor 2-GTW-3r-Hefıa-tetO2-EBFP-4xff5	Ampicillin	pBR322
pZDonor 3-GTW-4r-Hefıa-tetO2-mKate-FF5-FF4	Ampicillin	pBR322
pZDonor 3-GTW-4r-pLux-LacOid-NOS2-HisTag	Ampicillin	pBR322
pZDonor 4-GTW-5-minCMVLoxO7-LacI-FF5-miRFF4	Ampicillin	pBR322
pZDonor 4-GTW-5-minCMVLoxO7-TetR-mirFF5	Ampicillin	pBR322
pZDonor 4-GTW-5-pLas-7-lasbox-LacI-FF5-miRFF4	Ampicillin	pBR322
pZDonor 4-GTW-5-pLas-7-lasbox-TetR-mirFF5	Ampicillin	pBR322
pZDonor 6-GTW-7-UbC-p65H4LasRmNLS	Ampicillin	pBR322
pZDonor 1-GTW-2r-pLas-7-lasbox-mCoPy	Ampicillin	pBR322

Bacterial 'Sense and Destroy' plasmids		
Plasmid Name	**Antibiotic Resistance**	**Origin of replication**
pXL-101-contains CDAP4	Kanamycin	p15A
p-tetO-CoPy-Lys	Chloramphenicol	ColE1
pSDE-COL401	Kanamycin	p15A
p-SDECOL4012	Chloramphenicol	ColE1
p-SDECOL-4013	Chloramphenicol	ColE1
p-SDECOL-4014	Chloramphenicol	ColE1
p-plas-His-FlgM-CoPy	Chloramphenicol	ColE1
p-plas-FlgM	Chloramphenicol	ColE1
p-plas-CoPy-Lys	Chloramphenicol	ColE1
p-plas-CoPy	Chloramphenicol	ColE1

p-plac-cdap4-histag-gfp	Kanamycin	p15A
p-plac-cdap4-gfp-INV5	Kanamycin	p15A
p-FlgM-CoPy	Chloramphenicol	ColE1
p-FlgM	Chloramphenicol	ColE1
CRISPR into pProTET	Chloramphenicol	ColE1
pLas-His-FlgM-CoPy-mRFP	Ampicillin	ColE1
pLas-His-FlgM-CoPy-GFP-mcherry	Chloramphenicol	ColE1
pLas-His-CoPy-HlyA-RFP-Imm	Ampicillin	ColE1
pLas-His-CoPy-HlyA-RFP	Ampicillin	ColE1
p-teto-CoPy-Linker-FlgM	Chloramphenicol	ColE1
p-pconst-FlgM-CoPy	Chloramphenicol	ColE1
pET-24a(+) HisCoPy	Kanamycin	ColE1
pET-24a(+) HisCoPyHlyA	Kanamycin	ColE1
pET-24a(+) HisFlgMCoPy	Kanamycin	ColE1

II. MATLAB code

I did MATLAB simulations in order to understand the effect of various parameters on the adaptive response of mammalian 'Sense and Destroy' system described in chapter 04. In , and I've listed all the reactions and initial values of the parameters used in the model. The 'f' in parameter stands for forward reaction, and the 'r' stands for reverse.

	Type	Name	Expression
1	reaction	r1	AHL + pLux1 <-> [AHL-pLux1], k1f*AHL*pLux1 - k1r*[AHL-pLux1]
2	reaction	r2	[AHL-pLux1] -> [AHL-pLux1] + m_TetR + m_red, k2*[AHL-pLux1]
3	reaction	r3	TetR -> null, d3*TetR
4	reaction	r4	red -> null, d2*red
5	reaction	r5	TetR + Dox <-> [TetR-Dox], k4f*TetR*Dox - k4r*[TetR-Dox]
6	reaction	r6	TetR + tetO <-> [TetR-tetO], k5f*TetR*tetO - k5r*[TetR-tetO]
7	reaction	r7	tetO -> tetO + m_LacI, k6*tetO
8	reaction	r8	LacI -> null, d6*LacI
9	reaction	r9	LacI + IPTG <-> [LacI-IPTG], k7f*LacI*IPTG - k7r*[LacI-IPTG]
10	reaction	r10	LacI + LacO <-> [LacI-LacO], k8f*LacI*LacO - k8r*[LacI-LacO]
11	reaction	r11	[TetR-Dox] -> Dox, d4*[TetR-Dox]
12	reaction	r12	[TetR-tetO] -> tetO, d5*[TetR-tetO]
13	reaction	r13	[LacI-IPTG] -> IPTG, d7*[LacI-IPTG]
14	reaction	r14	[LacI-LacO] -> LacO, d8*[LacI-LacO]
15	reaction	r15	LacO + AHL <-> [LacO-AHL], k9f*LacO*AHL - k9r*[LacO-AHL]
16	reaction	r16	[LacO-AHL] + LacI <-> [LacI-LacO-AHL], k11f*[LacO-AHL]*LacI - k11r*[LacI-LacO-AHL]
17	reaction	r17	[LacI-LacO] + AHL <-> [LacI-LacO-AHL], k10f*[LacI-LacO]*AHL - k10r*[LacI-LacO-AHL]
18	reaction	r18	[LacI-LacO-AHL] -> [LacO-AHL], d10*[LacI-LacO-AHL]
19	reaction	r19	[LacO-AHL] -> [LacO-AHL] + m_green, k12*[LacO-AHL]
20	reaction	r20	green -> null, d12*green
21	reaction	r25	m_TetR -> m_TetR + TetR, k_tran*m_TetR
22	reaction	r26	m_red -> m_red + red, k_tran*m_red
23	reaction	r27	m_LacI -> m_LacI + LacI, k_tran*m_LacI
24	reaction	r28	m_green -> m_green + green, k_tran*m_green
25	event		time >= 50000, {AHL = AHL_high}

Figure 54: Various reactions used for modeling Adaptive response of Mammalian 'Sense and Destroy'.

	Ron Circuit	Cell	1.0	liter
	Cell	AHL	0.0	molarity
	Cell	pLux1	4.49E-7	molarity
	Cell	red	0.0	molarity
	Cell	Dox	0.0	molarity
	Cell	tetO	4.49E-7	molarity
	Cell	LacI	0.0	molarity
	Cell	IPTG	0.0	molarity
	Cell	LacI-IPTG	0.0	molarity
	Cell	LacO	4.49E-7	molarity
	Cell	LacI-LacO	0.0	molarity
	Cell	AHL-pLux1	0.0	molarity
	Cell	LacO-AHL	0.0	molarity
	Cell	LacI-LacO-AHL	0.0	molarity
	Cell	green	0.0	molarity
	Cell	m_red	0.0	molarity
	Cell	m_LacI	0.0	molarity
	Cell	m_green	0.0	molarity
	Cell	m_TetR	0.0	molarity
	Cell	TetR	0.0	molarity
	Cell	TetR-Dox	0.0	molarity
	Cell	TetR-tetO	0.0	molarity

Figure 55 : Initial concentrations (Molar) of various species used inside the cell model

Ron Circuit	AHL_high	3.0E-5	molarity
Ron Circuit	k_tran	0.02	1/second
Ron Circuit	d_rna	0.0020	1/second
AHL + pLux1 <-> [AHL-pLux1]	k1f	1.0E7	1/(molarity*second)
AHL + pLux1 <-> [AHL-pLux1]	k1r	0.01	1/second
[AHL-pLux1] -> [AHL-pLux1] + m_TetR + m_red	k2	0.1	1/second
TetR -> null	d3	2.0E-4	1/second
red -> null	d2	2.0E-4	1/second
TetR + Dox <-> [TetR-Dox]	k4f	1.0E7	1/(molarity*second)
TetR + Dox <-> [TetR-Dox]	k4r	0.01	1/second
TetR + tetO <-> [TetR-tetO]	k5f	1.0E7	1/(molarity*second)
TetR + tetO <-> [TetR-tetO]	k5r	0.01	1/second
tetO -> tetO + m_LacI	k6	1.0E-4	1/second
LacI -> null	d6	2.0E-4	1/second
LacI + IPTG <-> [LacI-IPTG]	k7f	1.0E7	1/(molarity*second)
LacI + IPTG <-> [LacI-IPTG]	k7r	0.01	1/second
LacI + LacO <-> [LacI-LacO]	k8f	1.0E7	1/(molarity*second)
LacI + LacO <-> [LacI-LacO]	k8r	0.01	1/second
[TetR-Dox] -> Dox	d4	2.0E-4	1/second
[TetR-tetO] -> tetO	d5	2.0E-4	1/second
[LacI-IPTG] -> IPTG	d7	2.0E-4	1/second
[LacI-LacO] -> LacO	d8	2.0E-4	1/second
LacO + AHL <-> [LacO-AHL]	k9f	1000000.0	1/(molarity*second)
LacO + AHL <-> [LacO-AHL]	k9r	0.01	1/second
[LacO-AHL] + LacI <-> [LacI-LacO-AHL]	k11f	1000000.0	1/(molarity*second)
[LacO-AHL] + LacI <-> [LacI-LacO-AHL]	k11r	0.01	1/second
[LacI-LacO] + AHL <-> [LacI-LacO-AHL]	k10f	1000000.0	1/(molarity*second)
[LacI-LacO] + AHL <-> [LacI-LacO-AHL]	k10r	0.01	1/second
[LacI-LacO-AHL] -> [LacO-AHL]	d10	2.0E-4	1/second
[LacO-AHL] -> [LacO-AHL] + m_green	k12	0.1	1/second
green -> null	d12	2.0E-4	1/second

Figure 56: Initial values of different parameters in the model

CHAPTER 7 - REFERENCES

1. Andrianantoandro, E., et al., *Synthetic biology: new engineering rules for an emerging discipline.* Mol Syst Biol, 2006. **2**: p. 2006 0028.
2. Purnick, P.E. and R. Weiss, *The second wave of synthetic biology: from modules to systems.* Nat Rev Mol Cell Biol, 2009. **10**(6): p. 410-22.
3. Auslander, S., M. Wieland, and M. Fussenegger, *Smart medication through combination of synthetic biology and cell microencapsulation.* Metab Eng, 2011.
4. Khalil, A.S. and J.J. Collins, *Synthetic biology: applications come of age.* Nat Rev Genet, 2010. **11**(5): p. 367-79.
5. Ruder, W.C., T. Lu, and J.J. Collins, *Synthetic biology moving into the clinic.* Science, 2011. **333**(6047): p. 1248-52.
6. Weber, W. and M. Fussenegger, *Emerging biomedical applications of synthetic biology.* Nat Rev Genet, 2012. **13**(1): p. 21-35.
7. Xie, Z., et al., *Multi-input RNAi-based logic circuit for identification of specific cancer cells.* Science, 2011. **333**(6047): p. 1307-11.
8. Subramanian, S., *Synthetic gene networks for differentiation of mouse embryonic stem cells*, 2008, Princeton University. p. xii, 154 leaves.
9. Morens, D.M., G.K. Folkers, and A.S. Fauci, *The challenge of emerging and re-emerging infectious diseases.* Nature, 2004. **430**(6996): p. 242-9.
10. Donadio, S., et al., *Antibiotic discovery in the twenty-first century: current trends and future perspectives.* J Antibiot (Tokyo), 2010. **63**(8): p. 423-30.
11. Kohanski, M.A., D.J. Dwyer, and J.J. Collins, *How antibiotics kill bacteria: from targets to networks.* Nat Rev Microbiol, 2010. **8**(6): p. 423-35.
12. Li, J.Z., et al., *Efficacy of short-course antibiotic regimens for community-acquired pneumonia: a meta-analysis.* Am J Med, 2007. **120**(9): p. 783-90.
13. Kohanski, M.A., M.A. DePristo, and J.J. Collins, *Sublethal antibiotic treatment leads to multidrug resistance via radical-induced mutagenesis.* Mol Cell, 2010. **37**(3): p. 311-20.
14. Na, X. and C. Kelly, *Probiotics in clostridium difficile Infection.* J Clin Gastroenterol, 2011. **45 Suppl**: p. S154-8.
15. Gough, E., H. Shaikh, and A.R. Manges, *Systematic review of intestinal microbiota transplantation (fecal bacteriotherapy) for recurrent Clostridium difficile infection.* Clin Infect Dis, 2011. **53**(10): p. 994-1002.
16. Echols, R.M., *Understanding the regulatory hurdles for antibacterial drug development in the post-Ketek world.* Ann N Y Acad Sci, 2011. **1241**(1): p. 153-61.
17. Gonzalez-Nicolini, V. and M. Fussenegger, *In vitro assays for anticancer drug discovery--a novel approach based on engineered mammalian cell lines.* Anticancer Drugs, 2005. **16**(3): p. 223-8.
18. Weber, W., et al., *A novel vector platform for vitamin H-inducible transgene expression in mammalian cells.* J Biotechnol, 2007. **131**(2): p. 150-8.
19. Weber, W. and M. Fussenegger, *The impact of synthetic biology on drug discovery.* Drug Discov Today, 2009. **14**(19-20): p. 956-63.
20. Weber, W., et al., *A synthetic mammalian gene circuit reveals antituberculosis compounds.* Proc Natl Acad Sci U S A, 2008. **105**(29): p. 9994-8.
21. Davies, J., *Darwin and microbiomes.* EMBO Rep, 2009. **10**(8): p. 805.
22. Rahme, L.G., et al., *Use of model plant hosts to identify Pseudomonas aeruginosa virulence factors.* Proc Natl Acad Sci U S A, 1997. **94**(24): p. 13245-50.

23. Favero, M.S., et al., *Pseudomonas aeruginosa: growth in distilled water from hospitals.* Science, 1971. **173**(3999): p. 836-8.
24. Stover, C.K., et al., *Complete genome sequence of Pseudomonas aeruginosa PAO1, an opportunistic pathogen.* Nature, 2000. **406**(6799): p. 959-64.
25. Atkinson, S. and P. Williams, *Quorum sensing and social networking in the microbial world.* J R Soc Interface, 2009. **6**(40): p. 959-78.
26. De Kievit, T.R., et al., *Quorum-sensing genes in Pseudomonas aeruginosa biofilms: their role and expression patterns.* Appl Environ Microbiol, 2001. **67**(4): p. 1865-73.
27. Jayaraman, A. and T.K. Wood, *Bacterial quorum sensing: signals, circuits, and implications for biofilms and disease.* Annu Rev Biomed Eng, 2008. **10**: p. 145-67.
28. Smith, R., *P. aeruginosa quorum-sensing systems and virulence.* Curr Opin Microbiol, 2003. **6**(1): p. 56-60.
29. Waters, C.M. and B.L. Bassler, *Quorum sensing: cell-to-cell communication in bacteria.* Annu Rev Cell Dev Biol, 2005. **21**: p. 319-46.
30. Whiteley, M., K.M. Lee, and E.P. Greenberg, *Identification of genes controlled by quorum sensing in Pseudomonas aeruginosa.* Proc Natl Acad Sci U S A, 1999. **96**(24): p. 13904-9.
31. Van Delden, C. and B.H. Iglewski, *Cell-to-cell signaling and Pseudomonas aeruginosa infections.* Emerg Infect Dis, 1998. **4**(4): p. 551-60.
32. Finch, R.G., *Antibiotic resistance: a view from the prescriber.* Nat Rev Microbiol, 2004. **2**(12): p. 989-94.
33. Hancock, R.E. and D.P. Speert, *Antibiotic resistance in Pseudomonas aeruginosa: mechanisms and impact on treatment.* Drug Resist Updat, 2000. **3**(4): p. 247-255.
34. Tenover, F.C., *Mechanisms of antimicrobial resistance in bacteria.* Am J Med, 2006. **119**(6 Suppl 1): p. S3-10; discussion S62-70.
35. van Hoek, A.H., et al., *Acquired antibiotic resistance genes: an overview.* Front Microbiol, 2011. **2**: p. 203.
36. McManus, M.C., *Mechanisms of bacterial resistance to antimicrobial agents.* Am J Health Syst Pharm, 1997. **54**(12): p. 1420-33; quiz 1444-6.
37. Stratton, C.W., *Mechanisms of bacterial resistance to antimicrobial agents.* J Med Liban, 2000. **48**(4): p. 186-98.
38. Rossolini, G.M. and E. Mantengoli, *Treatment and control of severe infections caused by multiresistant Pseudomonas aeruginosa.* Clin Microbiol Infect, 2005. **11 Suppl 4**: p. 17-32.
39. Mah, T.F., et al., *A genetic basis for Pseudomonas aeruginosa biofilm antibiotic resistance.* Nature, 2003. **426**(6964): p. 306-10.
40. Strateva, T. and D. Yordanov, *Pseudomonas aeruginosa - a phenomenon of bacterial resistance.* J Med Microbiol, 2009. **58**(Pt 9): p. 1133-48.
41. Bassler, B.L. and R. Losick, *Bacterially speaking.* Cell, 2006. **125**(2): p. 237-46.
42. Miller, M.B. and B.L. Bassler, *Quorum sensing in bacteria.* Annu Rev Microbiol, 2001. **55**: p. 165-99.
43. Henke, J.M. and B.L. Bassler, *Bacterial social engagements.* Trends Cell Biol, 2004. **14**(11): p. 648-56.
44. March, J.C. and W.E. Bentley, *Quorum sensing and bacterial cross-talk in biotechnology.* Curr Opin Biotechnol, 2004. **15**(5): p. 495-502.
45. Ng, W.L. and B.L. Bassler, *Bacterial quorum-sensing network architectures.* Annu Rev Genet, 2009. **43**: p. 197-222.

46. Rinaudo, K., et al., *A universal RNAi-based logic evaluator that operates in mammalian cells.* Nat Biotechnol, 2007. **25**(7): p. 795-801.
47. Arai, R., et al., *Design of the linkers which effectively separate domains of a bifunctional fusion protein.* Protein Eng, 2001. **14**(8): p. 529-32.
48. Coloma, M.J., et al., *Novel vectors for the expression of antibody molecules using variable regions generated by polymerase chain reaction.* J Immunol Methods, 1992. **152**(1): p. 89-104.
49. Greber, D. and M. Fussenegger, *Mammalian synthetic biology: engineering of sophisticated gene networks.* J Biotechnol, 2007. **130**(4): p. 329-45.
50. Cookson, N.A., L.S. Tsimring, and J. Hasty, *The pedestrian watchmaker: genetic clocks from engineered oscillators.* FEBS Lett, 2009. **583**(24): p. 3931-7.
51. Garcia-Ojalvo, J., M.B. Elowitz, and S.H. Strogatz, *Modeling a synthetic multicellular clock: repressilators coupled by quorum sensing.* Proc Natl Acad Sci U S A, 2004. **101**(30): p. 10955-60.
52. Mondragon-Palomino, O., et al., *Entrainment of a population of synthetic genetic oscillators.* Science, 2011. **333**(6047): p. 1315-9.
53. Stricker, J., et al., *A fast, robust and tunable synthetic gene oscillator.* Nature, 2008. **456**(7221): p. 516-9.
54. Gardner, T.S., C.R. Cantor, and J.J. Collins, *Construction of a genetic toggle switch in Escherichia coli.* Nature, 2000. **403**(6767): p. 339-42.
55. Lu, T.K., A.S. Khalil, and J.J. Collins, *Next-generation synthetic gene networks.* Nat Biotechnol, 2009. **27**(12): p. 1139-50.
56. Nandagopal, N. and M.B. Elowitz, *Synthetic biology: integrated gene circuits.* Science, 2011. **333**(6047): p. 1244-8.
57. Basu, S., et al., *Spatiotemporal control of gene expression with pulse-generating networks.* Proc Natl Acad Sci U S A, 2004. **101**(17): p. 6355-60.
58. Hooshangi, S., *Sensitivity and noise propagation in complex synthetic gene networks*, 2006, Princeton University. p. xiii, 90 leaves.
59. Hooshangi, S., S. Thiberge, and R. Weiss, *Ultrasensitivity and noise propagation in a synthetic transcriptional cascade.* Proc Natl Acad Sci U S A, 2005. **102**(10): p. 3581-6.
60. Karig, D. and R. Weiss, *Signal-amplifying genetic circuit enables in vivo observation of weak promoter activation in the Rhl quorum sensing system.* Biotechnol Bioeng, 2005. **89**(6): p. 709-18.
61. Basu, S., et al., *A synthetic multicellular system for programmed pattern formation.* Nature, 2005. **434**(7037): p. 1130-4.
62. Hasty, J., et al., *Noise-based switches and amplifiers for gene expression.* Proc Natl Acad Sci U S A, 2000. **97**(5): p. 2075-80.
63. Ptashne, M., *Principles of a switch.* Nat Chem Biol, 2011. **7**(8): p. 484-7.
64. Karig, D.K., *Engineering multi-signal synthetic biological systems*, 2007, Princeton University. p. xiii, 138 leaves.
65. Georgiou, G. and L. Segatori, *Preparative expression of secreted proteins in bacteria: status report and future prospects.* Curr Opin Biotechnol, 2005. **16**(5): p. 538-45.
66. Mergulhao, F.J., D.K. Summers, and G.A. Monteiro, *Recombinant protein secretion in Escherichia coli.* Biotechnol Adv, 2005. **23**(3): p. 177-202.
67. Saier, M.H., Jr., *Protein secretion and membrane insertion systems in gram-negative bacteria.* J Membr Biol, 2006. **214**(2): p. 75-90.
68. Sandkvist, M. and M. Bagdasarian, *Secretion of recombinant proteins by Gram-negative bacteria.* Curr Opin Biotechnol, 1996. **7**(5): p. 505-11.

69. Wickner, W. and R. Schekman, *Protein translocation across biological membranes.* Science, 2005. **310**(5753): p. 1452-6.
70. Sorensen, H.P. and K.K. Mortensen, *Advanced genetic strategies for recombinant protein expression in Escherichia coli.* J Biotechnol, 2005. **115**(2): p. 113-28.
71. Filloux, A., A. Hachani, and S. Bleves, *The bacterial type VI secretion machine: yet another player for protein transport across membranes.* Microbiology, 2008. **154**(Pt 6): p. 1570-83.
72. San Miguel, M., et al., *An Escherichia coli twin-arginine signal peptide switches between helical and unstructured conformations depending on the hydrophobicity of the environment.* European Journal of Biochemistry, 2003. **270**(16): p. 3345-3352.
73. Bernard, C.S., et al., *Nooks and crannies in type VI secretion regulation.* J Bacteriol, 2010. **192**(15): p. 3850-60.
74. Bingle, L.E., C.M. Bailey, and M.J. Pallen, *Type VI secretion: a beginner's guide.* Curr Opin Microbiol, 2008. **11**(1): p. 3-8.
75. Feltcher, M.E., J.T. Sullivan, and M. Braunstein, *Protein export systems of Mycobacterium tuberculosis: novel targets for drug development?* Future Microbiol, 2010. **5**(10): p. 1581-97.
76. Delepelaire, P., *Type I secretion in gram-negative bacteria.* Biochim Biophys Acta, 2004. **1694**(1-3): p. 149-61.
77. Desvaux, M., et al., *The general secretory pathway: a general misnomer?* Trends Microbiol, 2004. **12**(7): p. 306-9.
78. Michiels, T. and G.R. Cornelis, *Secretion of hybrid proteins by the Yersinia Yop export system.* J Bacteriol, 1991. **173**(5): p. 1677-85.
79. Anderson, D.M. and O. Schneewind, *A mRNA signal for the type III secretion of Yop proteins by Yersinia enterocolitica.* Science, 1997. **278**(5340): p. 1140-3.
80. Birtalan, S.C., R.M. Phillips, and P. Ghosh, *Three-dimensional secretion signals in chaperone-effector complexes of bacterial pathogens.* Mol Cell, 2002. **9**(5): p. 971-80.
81. Henderson, I.R., et al., *Type V protein secretion pathway: the autotransporter story.* Microbiol Mol Biol Rev, 2004. **68**(4): p. 692-744.
82. Zechner, E.L., S. Lang, and J.F. Schildbach, *Assembly and mechanisms of bacterial type IV secretion machines.* Philos Trans R Soc Lond B Biol Sci, 2012. **367**(1592): p. 1073-87.
83. Cascales, E., *The type VI secretion toolkit.* EMBO Rep, 2008. **9**(8): p. 735-41.
84. Hood, R.D., et al., *A type VI secretion system of Pseudomonas aeruginosa targets a toxin to bacteria.* Cell Host Microbe, 2010. **7**(1): p. 25-37.
85. Jani, A.J. and P.A. Cotter, *Type VI secretion: not just for pathogenesis anymore.* Cell Host Microbe, 2010. **8**(1): p. 2-6.
86. Basler, M., et al., *Type VI secretion requires a dynamic contractile phage tail-like structure.* Nature, 2012. **483**(7388): p. 182-6.
87. Mancias, J.D. and J. Goldberg, *Exiting the endoplasmic reticulum.* Traffic, 2005. **6**(4): p. 278-85.
88. Dupont, E., A. Prochiantz, and A. Joliot, *Identification of a signal peptide for unconventional secretion.* J Biol Chem, 2007. **282**(12): p. 8994-9000.
89. Schlatter, S., et al., *SAMY, a novel mammalian reporter gene derived from Bacillus stearothermophilus alpha-amylase.* Gene, 2002. **282**(1-2): p. 19-31.
90. Zhang, L., Q. Leng, and A.J. Mixson, *Alteration in the IL-2 signal peptide affects secretion of proteins in vitro and in vivo.* J Gene Med, 2005. **7**(3): p. 354-65.
91. Chun, C.K., et al., *Inactivation of a Pseudomonas aeruginosa quorum-sensing signal by human airway epithelia.* Proc Natl Acad Sci U S A, 2004. **101**(10): p. 3587-90.

92. Son, M.S., et al., *In vivo evidence of Pseudomonas aeruginosa nutrient acquisition and pathogenesis in the lungs of cystic fibrosis patients.* Infect Immun, 2007. **75**(11): p. 5313-24.
93. Charlton, T.S., et al., *A novel and sensitive method for the quantification of N-3-oxoacyl homoserine lactones using gas chromatography-mass spectrometry: application to a model bacterial biofilm.* Environ Microbiol, 2000. **2**(5): p. 530-41.
94. Smith, R.S., et al., *The Pseudomonas aeruginosa quorum-sensing molecule N-(3-oxododecanoyl)homoserine lactone contributes to virulence and induces inflammation in vivo.* J Bacteriol, 2002. **184**(4): p. 1132-9.
95. Cotter, P.D., C. Hill, and R.P. Ross, *Bacteriocins: developing innate immunity for food.* Nat Rev Microbiol, 2005. **3**(10): p. 777-88.
96. Field, D., et al., *The dawning of a 'Golden era' in lantibiotic bioengineering.* Mol Microbiol, 2010. **78**(5): p. 1077-87.
97. Parret, A.H. and R. De Mot, *Bacteria killing their own kind: novel bacteriocins of Pseudomonas and other gamma-proteobacteria.* Trends Microbiol, 2002. **10**(3): p. 107-12.
98. Piper, C., et al., *Discovery of medically significant lantibiotics.* Curr Drug Discov Technol, 2009. **6**(1): p. 1-18.
99. Cascales, E., et al., *Colicin biology.* Microbiol Mol Biol Rev, 2007. **71**(1): p. 158-229.
100. Mulec, J., et al., *A cka-gfp transcriptional fusion reveals that the colicin K activity gene is induced in only 3 percent of the population.* J Bacteriol, 2003. **185**(2): p. 654-9.
101. Goodwin, K., R.E. Levin, and R.G. Doggett, *Autosensitivity of Pseudomonas aeruginosa to its own pyocin.* Infect Immun, 1972. **6**(5): p. 889-92.
102. Michel-Briand, Y. and C. Baysse, *The pyocins of Pseudomonas aeruginosa.* Biochimie, 2002. **84**(5-6): p. 499-510.
103. Duport, C., C. Baysse, and Y. Michel-Briand, *Molecular characterization of pyocin S3, a novel S-type pyocin from Pseudomonas aeruginosa.* J Biol Chem, 1995. **270**(15): p. 8920-7.
104. Sano, Y. and M. Kageyama, *Purification and properties of an S-type pyocin, pyocin AP41.* J Bacteriol, 1981. **146**(2): p. 733-9.
105. Sano, Y., M. Kobayashi, and M. Kageyama, *Functional domains of S-type pyocins deduced from chimeric molecules.* J Bacteriol, 1993. **175**(19): p. 6179-85.
106. Sano, Y., et al., *Molecular structures and functions of pyocins S1 and S2 in Pseudomonas aeruginosa.* J Bacteriol, 1993. **175**(10): p. 2907-16.
107. Bonsor, D.A., N.A. Meenan, and C. Kleanthous, *Colicins exploit native disorder to gain cell entry: a hitchhiker's guide to translocation.* Biochem Soc Trans, 2008. **36**(Pt 6): p. 1409-13.
108. Soelaiman, S., et al., *Crystal structure of colicin E3: implications for cell entry and ribosome inactivation.* Mol Cell, 2001. **8**(5): p. 1053-62.
109. Kageyama, M., et al., *Construction and characterization of pyocin-colicin chimeric proteins.* J Bacteriol, 1996. **178**(1): p. 103-10.
110. Zwietering, M.H., et al., *Modeling of the bacterial growth curve.* Appl Environ Microbiol, 1990. **56**(6): p. 1875-81.
111. You, L., et al., *Programmed population control by cell-cell communication and regulated killing.* Nature, 2004. **428**(6985): p. 868-71.
112. Bernhardt, T.G., W.D. Roof, and R. Young, *Genetic evidence that the bacteriophage phi X174 lysis protein inhibits cell wall synthesis.* Proc Natl Acad Sci U S A, 2000. **97**(8): p. 4297-302.

113. Bernhardt, T.G., W.D. Roof, and R. Young, *The Escherichia coli FKBP-type PPIase SlyD is required for the stabilization of the E lysis protein of bacteriophage phi X174.* Mol Microbiol, 2002. **45**(1): p. 99-108.
114. Bernhardt, T.G., D.K. Struck, and R. Young, *The lysis protein E of phi X174 is a specific inhibitor of the MraY-catalyzed step in peptidoglycan synthesis.* J Biol Chem, 2001. **276**(9): p. 6093-7.
115. Haidinger, W., et al., *Escherichia coli ghost production by expression of lysis gene E and Staphylococcal nuclease.* Appl Environ Microbiol, 2003. **69**(10): p. 6106-13.
116. Witte, A. and W. Lubitz, *Biochemical characterization of phi X174-protein-E-mediated lysis of Escherichia coli.* Eur J Biochem, 1989. **180**(2): p. 393-8.
117. Choi, J.H. and S.Y. Lee, *Secretory and extracellular production of recombinant proteins using Escherichia coli.* Appl Microbiol Biotechnol, 2004. **64**(5): p. 625-35.
118. Gupta, P. and K.H. Lee, *Silent mutations result in HlyA hypersecretion by reducing intracellular HlyA protein aggregates.* Biotechnol Bioeng, 2008. **101**(5): p. 967-74.
119. Cornelis, G.R. and F. Van Gijsegem, *Assembly and function of type III secretory systems.* Annu Rev Microbiol, 2000. **54**: p. 735-74.
120. Macnab, R.M., *Type III flagellar protein export and flagellar assembly.* Biochim Biophys Acta, 2004. **1694**(1-3): p. 207-17.
121. Majander, K., et al., *Extracellular secretion of polypeptides using a modified Escherichia coli flagellar secretion apparatus.* Nat Biotechnol, 2005. **23**(4): p. 475-81.
122. Troisfontaines, P. and G.R. Cornelis, *Type III secretion: more systems than you think.* Physiology (Bethesda), 2005. **20**: p. 326-39.
123. Aldridge, P., et al., *Transcriptional and translational control of the Salmonella fliC gene.* J Bacteriol, 2006. **188**(12): p. 4487-96.
124. Chilcott, G.S. and K.T. Hughes, *Coupling of flagellar gene expression to flagellar assembly in Salmonella enterica serovar typhimurium and Escherichia coli.* Microbiol Mol Biol Rev, 2000. **64**(4): p. 694-708.
125. Karlinsey, J.E., et al., *Completion of the hook-basal body complex of the Salmonella typhimurium flagellum is coupled to FlgM secretion and fliC transcription.* Mol Microbiol, 2000. **37**(5): p. 1220-31.
126. Aldridge, P. and K.T. Hughes, *Regulation of flagellar assembly.* Curr Opin Microbiol, 2002. **5**(2): p. 160-5.
127. Chevance, F.F. and K.T. Hughes, *Coordinating assembly of a bacterial macromolecular machine.* Nat Rev Microbiol, 2008. **6**(6): p. 455-65.
128. Hughes, K.T., et al., *Sensing structural intermediates in bacterial flagellar assembly by export of a negative regulator.* Science, 1993. **262**(5137): p. 1277-80.
129. Lee, S.H. and J.E. Galan, *Salmonella type III secretion-associated chaperones confer secretion-pathway specificity.* Mol Microbiol, 2004. **51**(2): p. 483-95.
130. Thomas, N.A. and B. Brett Finlay, *Establishing order for type III secretion substrates – a hierarchical process.* Trends in Microbiology, 2003. **11**(8): p. 398-403.
131. Sorenson, M.K., S.S. Ray, and S.A. Darst, *Crystal structure of the flagellar sigma/anti-sigma complex sigma(28)/FlgM reveals an intact sigma factor in an inactive conformation.* Mol Cell, 2004. **14**(1): p. 127-38.
132. Aldridge, P.D., et al., *The flagellar-specific transcription factor, sigma28, is the Type III secretion chaperone for the flagellar-specific anti-sigma28 factor FlgM.* Genes Dev, 2006. **20**(16): p. 2315-26.
133. Rosu, V., et al., *Translation inhibition of the Salmonella fliC gene by the fliC 5′ untranslated region, fliC coding sequences, and FlgM.* J Bacteriol, 2006. **188**(12): p. 4497-507.

134. Josenhans, C., et al., *Functional characterization of the antagonistic flagellar late regulators FliA and FlgM of Helicobacter pylori and their effects on the H. pylori transcriptome.* Mol Microbiol, 2002. **43**(2): p. 307-22.
135. Chadsey, M.S. and K.T. Hughes, *A multipartite interaction between Salmonella transcription factor sigma28 and its anti-sigma factor FlgM: implications for sigma28 holoenzyme destabilization through stepwise binding.* J Mol Biol, 2001. **306**(5): p. 915-29.
136. Chilcott, G.S. and K.T. Hughes, *The type III secretion determinants of the flagellar anti-transcription factor, FlgM, extend from the amino-terminus into the anti-sigma28 domain.* Mol Microbiol, 1998. **30**(5): p. 1029-40.
137. Chadsey, M.S., J.E. Karlinsey, and K.T. Hughes, *The flagellar anti-sigma factor FlgM actively dissociates Salmonella typhimurium sigma28 RNA polymerase holoenzyme.* Genes Dev, 1998. **12**(19): p. 3123-36.
138. Daughdrill, G.W., et al., *The C-terminal half of the anti-sigma factor, FlgM, becomes structured when bound to its target, sigma 28.* Nat Struct Biol, 1997. **4**(4): p. 285-91.
139. Gillen, K.L. and K.T. Hughes, *Transcription from two promoters and autoregulation contribute to the control of expression of the Salmonella typhimurium flagellar regulatory gene flgM.* J Bacteriol, 1993. **175**(21): p. 7006-15.
140. Gillen, K.L. and K.T. Hughes, *Molecular characterization of flgM, a gene encoding a negative regulator of flagellin synthesis in Salmonella typhimurium.* J Bacteriol, 1991. **173**(20): p. 6453-9.
141. Schultz, M., *Clinical use of E. coli Nissle 1917 in inflammatory bowel disease.* Inflamm Bowel Dis, 2008. **14**(7): p. 1012-8.
142. Vasile, N., R. Ghindea, and T. Vassu, *Probiotics--an alternative treatment for various diseases.* Roum Arch Microbiol Immunol, 2011. **70**(2): p. 54-9.
143. Sun, J., et al., *Genomic peculiarity of coding sequences and metabolic potential of probiotic Escherichia coli strain Nissle 1917 inferred from raw genome data.* J Biotechnol, 2005. **117**(2): p. 147-61.
144. Rao, S., et al., *Toward a live microbial microbicide for HIV: commensal bacteria secreting an HIV fusion inhibitor peptide.* Proc Natl Acad Sci U S A, 2005. **102**(34): p. 11993-8.
145. Collins, C.H., F.H. Arnold, and J.R. Leadbetter, *Directed evolution of Vibrio fischeri LuxR for increased sensitivity to a broad spectrum of acyl-homoserine lactones.* Mol Microbiol, 2005. **55**(3): p. 712-23.
146. Saeidi, N., et al., *Engineering microbes to sense and eradicate Pseudomonas aeruginosa, a human pathogen.* Mol Syst Biol, 2011. **7**: p. 521.
147. Filloux, A., *Secretion signal and protein targeting in bacteria: a biological puzzle.* J Bacteriol, 2010. **192**(15): p. 3847-9.
148. Bendtsen, J.D., et al., *Non-classical protein secretion in bacteria.* BMC Microbiol, 2005. **5**: p. 58.
149. Koster, M., W. Bitter, and J. Tommassen, *Protein secretion mechanisms in Gram-negative bacteria.* Int J Med Microbiol, 2000. **290**(4-5): p. 325-31.
150. Abajy, M.Y., et al., *A type IV-secretion-like system is required for conjugative DNA transport of broad-host-range plasmid pIP501 in gram-positive bacteria.* J Bacteriol, 2007. **189**(6): p. 2487-96.
151. Fernandez-Gonzalez, E., et al., *Transfer of R388 derivatives by a pathogenesis-associated type IV secretion system into both bacteria and human cells.* J Bacteriol, 2011. **193**(22): p. 6257-65.

152. Saini, S., et al., *Continuous control of flagellar gene expression by the sigma28-FlgM regulatory circuit in Salmonella enterica.* Mol Microbiol, 2011. **79**(1): p. 264-78.
153. Chevance, F.F., et al., *A little gene with big effects: a serT mutant is defective in flgM gene translation.* J Bacteriol, 2006. **188**(1): p. 297-304.
154. Daughdrill, G.W., L.J. Hanely, and F.W. Dahlquist, *The C-terminal half of the anti-sigma factor FlgM contains a dynamic equilibrium solution structure favoring helical conformations.* Biochemistry, 1998. **37**(4): p. 1076-82.
155. Frisk, A., et al., *Identification and functional characterization of flgM, a gene encoding the anti-sigma 28 factor in Pseudomonas aeruginosa.* J Bacteriol, 2002. **184**(6): p. 1514-21.
156. Schmitt, C.K., S.C. Darnell, and A.D. O'Brien, *The attenuated phenotype of a Salmonella typhimurium flgM mutant is related to expression of FliC flagellin.* J Bacteriol, 1996. **178**(10): p. 2911-5.
157. Schmitt, C.K., et al., *Mutation of flgM attenuates virulence of Salmonella typhimurium, and mutation of fliA represses the attenuated phenotype.* J Bacteriol, 1994. **176**(2): p. 368-77.
158. Yokoseki, T., T. Iino, and K. Kutsukake, *Negative regulation by fliD, fliS, and fliT of the export of the flagellum-specific anti-sigma factor, FlgM, in Salmonella typhimurium.* J Bacteriol, 1996. **178**(3): p. 899-901.
159. Rauhut, R. and G. Klug, *mRNA degradation in bacteria.* FEMS Microbiol Rev, 1999. **23**(3): p. 353-70.
160. Regnier, P. and C.M. Arraiano, *Degradation of mRNA in bacteria: emergence of ubiquitous features.* Bioessays, 2000. **22**(3): p. 235-44.
161. Lopez, P.J., et al., *The C-terminal half of RNase E, which organizes the Escherichia coli degradosome, participates in mRNA degradation but not rRNA processing in vivo.* Mol Microbiol, 1999. **33**(1): p. 188-99.
162. Zalucki, Y.M., I.R. Beacham, and M.P. Jennings, *Coupling between codon usage, translation and protein export in Escherichia coli.* Biotechnol J, 2011. **6**(6): p. 660-7.
163. Dieci, G., et al., *tRNA-assisted overproduction of eukaryotic ribosomal proteins.* Protein Expr Purif, 2000. **18**(3): p. 346-54.
164. Hoffmann, F., J. Weber, and U. Rinas, *Metabolic adaptation of Escherichia coli during temperature-induced recombinant protein production: 1. Readjustment of metabolic enzyme synthesis.* Biotechnol Bioeng, 2002. **80**(3): p. 313-9.
165. Chang, D.E., D.J. Smalley, and T. Conway, *Gene expression profiling of Escherichia coli growth transitions: an expanded stringent response model.* Mol Microbiol, 2002. **45**(2): p. 289-306.
166. Dong, H., L. Nilsson, and C.G. Kurland, *Gratuitous overexpression of genes in Escherichia coli leads to growth inhibition and ribosome destruction.* J Bacteriol, 1995. **177**(6): p. 1497-504.
167. Jonasson, P., et al., *Genetic design for facilitated production and recovery of recombinant proteins in Escherichia coli.* Biotechnol Appl Biochem, 2002. **35**(Pt 2): p. 91-105.
168. Miroux, B. and J.E. Walker, *Over-production of proteins in Escherichia coli: mutant hosts that allow synthesis of some membrane proteins and globular proteins at high levels.* J Mol Biol, 1996. **260**(3): p. 289-98.
169. Lee, P.S. and K.H. Lee, *Engineering HlyA hypersecretion in Escherichia coli based on proteomic and microarray analyses.* Biotechnol Bioeng, 2005. **89**(2): p. 195-205.

170. Kim, J., M. Hegde, and A. Jayaraman, *Co-culture of epithelial cells and bacteria for investigating host-pathogen interactions.* Lab Chip, 2010. **10**(1): p. 43-50.
171. Nahum, J.R., B.N. Harding, and B. Kerr, *Evolution of restraint in a structured rock-paper-scissors community.* Proc Natl Acad Sci U S A, 2011. **108 Suppl 2**: p. 10831-8.
172. Haase, J., M. Kalkum, and E. Lanka, *TrbK, a small cytoplasmic membrane lipoprotein, functions in entry exclusion of the IncP alpha plasmid RP4.* J Bacteriol, 1996. **178**(23): p. 6720-9.
173. Thomas, C.M. and K.M. Nielsen, *Mechanisms of, and barriers to, horizontal gene transfer between bacteria.* Nat Rev Microbiol, 2005. **3**(9): p. 711-21.
174. Wilkins, B.M., et al., *Distribution of restriction enzyme recognition sequences on broad host range plasmid RP4: molecular and evolutionary implications.* J Mol Biol, 1996. **258**(3): p. 447-56.
175. Frost, L.S., K. Ippen-Ihler, and R.A. Skurray, *Analysis of the sequence and gene products of the transfer region of the F sex factor.* Microbiol Rev, 1994. **58**(2): p. 162-210.
176. Hochhut, B., et al., *Formation of chromosomal tandem arrays of the SXT element and R391, two conjugative chromosomally integrating elements that share an attachment site.* J Bacteriol, 2001. **183**(4): p. 1124-32.
177. Purdy, D., et al., *Conjugative transfer of clostridial shuttle vectors from Escherichia coli to Clostridium difficile through circumvention of the restriction barrier.* Mol Microbiol, 2002. **46**(2): p. 439-52.
178. Favre-Bonte, S., T. Kohler, and C. Van Delden, *Biofilm formation by Pseudomonas aeruginosa: role of the C4-HSL cell-to-cell signal and inhibition by azithromycin.* J Antimicrob Chemother, 2003. **52**(4): p. 598-604.
179. Smiley, A.K., et al., *Expression of human beta defensin 4 in genetically modified keratinocytes enhances antimicrobial activity.* J Burn Care Res, 2007. **28**(1): p. 127-32.
180. Supp, D.M., *Gene therapy to fight infection in skin transplants.* Pharmacogenomics, 2007. **8**(5): p. 483-6.
181. Gravante, G., et al., *A randomized trial comparing ReCell system of epidermal cells delivery versus classic skin grafts for the treatment of deep partial thickness burns.* Burns, 2007. **33**(8): p. 966-72.
182. Aubel, D. and M. Fussenegger, *Mammalian synthetic biology--from tools to therapies.* Bioessays, 2010. **32**(4): p. 332-45.
183. Weber, W. and M. Fussenegger, *Engineering of synthetic mammalian gene networks.* Chem Biol, 2009. **16**(3): p. 287-97.
184. Weber, W. and M. Fussenegger, *Synthetic gene networks in mammalian cells.* Curr Opin Biotechnol, 2010. **21**(5): p. 690-6.
185. Wieland, M., D. Auslander, and M. Fussenegger, *Engineering of ribozyme-based riboswitches for mammalian cells.* Methods, 2012.
186. Draganov, D.I., et al., *Human paraoxonases (PON1, PON2, and PON3) are lactonases with overlapping and distinct substrate specificities.* J Lipid Res, 2005. **46**(6): p. 1239-47.
187. Ng, C.J., et al., *Paraoxonase-2 is a ubiquitously expressed protein with antioxidant properties and is capable of preventing cell-mediated oxidative modification of low density lipoprotein.* J Biol Chem, 2001. **276**(48): p. 44444-9.
188. Yang, F., et al., *Quorum quenching enzyme activity is widely conserved in the sera of mammalian species.* FEBS Lett, 2005. **579**(17): p. 3713-7.
189. Andersen, D.C. and L. Krummen, *Recombinant protein expression for therapeutic applications.* Curr Opin Biotechnol, 2002. **13**(2): p. 117-23.

190. Barnes, L.M. and A.J. Dickson, *Mammalian cell factories for efficient and stable protein expression.* Curr Opin Biotechnol, 2006. **17**(4): p. 381-6.
191. Pechere, J.C., et al., *Non-compliance with antibiotic therapy for acute community infections: a global survey.* Int J Antimicrob Agents, 2007. **29**(3): p. 245-53.
192. Thomas, J.K., et al., *Pharmacodynamic evaluation of factors associated with the development of bacterial resistance in acutely ill patients during therapy.* Antimicrob Agents Chemother, 1998. **42**(3): p. 521-7.
193. Rosenfeld, N. and U. Alon, *Response delays and the structure of transcription networks.* J Mol Biol, 2003. **329**(4): p. 645-54.
194. Weber, W., et al., *A synthetic time-delay circuit in mammalian cells and mice.* Proc Natl Acad Sci U S A, 2007. **104**(8): p. 2643-8.
195. Martinez-Becerra, F., et al., *Analysis of the antimicrobial activities of a chemokine-derived peptide (CDAP-4) on Pseudomonas aeruginosa.* Biochem Biophys Res Commun, 2007. **355**(2): p. 352-8.
196. Gossling, J. and J.M. Slack, *Predominant gram-positive bacteria in human feces: numbers, variety, and persistence.* Infect Immun, 1974. **9**(4): p. 719-29.
197. van de Verg, L.L., et al., *Antibody and cytokine responses in a mouse pulmonary model of Shigella flexneri serotype 2a infection.* Infect Immun, 1995. **63**(5): p. 1947-54.
198. Clarke, M.B., et al., *The QseC sensor kinase: a bacterial adrenergic receptor.* Proc Natl Acad Sci U S A, 2006. **103**(27): p. 10420-5.
199. Hughes, D.T. and V. Sperandio, *Inter-kingdom signalling: communication between bacteria and their hosts.* Nat Rev Microbiol, 2008. **6**(2): p. 111-20.
200. Moreira, C.G., D. Weinshenker, and V. Sperandio, *QseC mediates Salmonella enterica serovar typhimurium virulence in vitro and in vivo.* Infect Immun, 2010. **78**(3): p. 914-26.
201. Rasko, D.A., et al., *Targeting QseC signaling and virulence for antibiotic development.* Science, 2008. **321**(5892): p. 1078-80.
202. Vendeville, A., et al., *Making 'sense' of metabolism: autoinducer-2, LuxS and pathogenic bacteria.* Nat Rev Microbiol, 2005. **3**(5): p. 383-96.
203. Paton, A.W., R. Morona, and J.C. Paton, *A new biological agent for treatment of Shiga toxigenic Escherichia coli infections and dysentery in humans.* Nat Med, 2000. **6**(3): p. 265-70.
204. Paton, A.W., R. Morona, and J.C. Paton, *Designer probiotics for prevention of enteric infections.* Nat Rev Microbiol, 2006. **4**(3): p. 193-200.
205. Schmidt, H., *Shiga-toxin-converting bacteriophages.* Res Microbiol, 2001. **152**(8): p. 687-95.
206. Smith, D.L., et al., *Short-tailed stx phages exploit the conserved YaeT protein to disseminate Shiga toxin genes among enterobacteria.* J Bacteriol, 2007. **189**(20): p. 7223-33.
207. James, C.E., et al., *Lytic and lysogenic infection of diverse Escherichia coli and Shigella strains with a verocytotoxigenic bacteriophage.* Appl Environ Microbiol, 2001. **67**(9): p. 4335-7.
208. Wagner, P.L., et al., *Role for a phage promoter in Shiga toxin 2 expression from a pathogenic Escherichia coli strain.* J Bacteriol, 2001. **183**(6): p. 2081-5.
209. Wagner, P.L. and M.K. Waldor, *Bacteriophage control of bacterial virulence.* Infect Immun, 2002. **70**(8): p. 3985-93.
210. Marraffini, L.A. and E.J. Sontheimer, *CRISPR interference: RNA-directed adaptive immunity in bacteria and archaea.* Nat Rev Genet, 2010. **11**(3): p. 181-90.

211. Sorek, R., V. Kunin, and P. Hugenholtz, *CRISPR--a widespread system that provides acquired resistance against phages in bacteria and archaea.* Nat Rev Microbiol, 2008. **6**(3): p. 181-6.
212. Barrangou, R., et al., *CRISPR provides acquired resistance against viruses in prokaryotes.* Science, 2007. **315**(5819): p. 1709-12.
213. Labrie, S.J., J.E. Samson, and S. Moineau, *Bacteriophage resistance mechanisms.* Nat Rev Microbiol, 2010. **8**(5): p. 317-27.
214. Marraffini, L.A. and E.J. Sontheimer, *Self versus non-self discrimination during CRISPR RNA-directed immunity.* Nature, 2010. **463**(7280): p. 568-71.
215. Pul, U., et al., *Identification and characterization of E. coli CRISPR-cas promoters and their silencing by H-NS.* Mol Microbiol, 2010. **75**(6): p. 1495-512.
216. Johannes, L. and W. Romer, *Shiga toxins--from cell biology to biomedical applications.* Nat Rev Microbiol, 2010. **8**(2): p. 105-16.
217. Smajs, D., H. Pilsl, and V. Braun, *Colicin U, a novel colicin produced by Shigella boydii.* J Bacteriol, 1997. **179**(15): p. 4919-28.
218. Huh, D., et al., *Acoustically detectable cellular-level lung injury induced by fluid mechanical stresses in microfluidic airway systems.* Proc Natl Acad Sci U S A, 2007. **104**(48): p. 18886-91.
219. Nelson, E.J., et al., *Cholera transmission: the host, pathogen and bacteriophage dynamic.* Nat Rev Microbiol, 2009. **7**(10): p. 693-702.
220. Higgins, D.A., et al., *The major Vibrio cholerae autoinducer and its role in virulence factor production.* Nature, 2007. **450**(7171): p. 883-6.
221. Freeman, J.A. and B.L. Bassler, *A genetic analysis of the function of LuxO, a two-component response regulator involved in quorum sensing in Vibrio harveyi.* Mol Microbiol, 1999. **31**(2): p. 665-77.
222. Wingreen, N.S. and S.A. Levin, *Cooperation among microorganisms.* PLoS Biol, 2006. **4**(9): p. e299.
223. Svenningsen, S.L., C.M. Waters, and B.L. Bassler, *A negative feedback loop involving small RNAs accelerates Vibrio cholerae's transition out of quorum-sensing mode.* Genes Dev, 2008. **22**(2): p. 226-38.
224. Barboza-Corona, J.E., et al., *Bacteriocin-like inhibitor substances produced by Mexican strains of Bacillus thuringiensis.* Arch Microbiol, 2007. **187**(2): p. 117-26.
225. Duquesne, S., et al., *Microcins, gene-encoded antibacterial peptides from enterobacteria.* Nat Prod Rep, 2007. **24**(4): p. 708-34.
226. Gasteiger, E., et al., *ExPASy: The proteomics server for in-depth protein knowledge and analysis.* Nucleic Acids Res, 2003. **31**(13): p. 3784-8.
227. Raivio, T.L. and T.J. Silhavy, *Transduction of envelope stress in Escherichia coli by the Cpx two-component system.* J Bacteriol, 1997. **179**(24): p. 7724-33.
228. Lynch, S.A. and R.T. Gill, *Synthetic biology: New strategies for directing design.* Metab Eng, 2011.
229. Muller, K.M. and K.M. Arndt, *Standardization in synthetic biology.* Methods Mol Biol, 2012. **813**: p. 23-43.
230. Boyle, P.M. and P.A. Silver, *Parts plus pipes: Synthetic biology approaches to metabolic engineering.* Metab Eng, 2011.
231. Wang, B., et al., *Engineering modular and orthogonal genetic logic gates for robust digital-like synthetic biology.* Nat Commun, 2011. **2**: p. 508.
232. Sarrion-Perdigones, A., et al., *GoldenBraid: an iterative cloning system for standardized assembly of reusable genetic modules.* PLoS One, 2011. **6**(7): p. e21622.

233. Leguia, M., et al., *Automated assembly of standard biological parts.* Methods Enzymol, 2011. **498**: p. 363-97.
234. Tsvetanova, B., et al., *Genetic assembly tools for synthetic biology.* Methods Enzymol, 2011. **498**: p. 327-48.
235. Shetty, R., et al., *Assembly of BioBrick standard biological parts using three antibiotic assembly.* Methods Enzymol, 2011. **498**: p. 311-26.
236. Xia, B., et al., *Developer's and user's guide to Clotho v2.0 A software platform for the creation of synthetic biological systems.* Methods Enzymol, 2011. **498**: p. 97-135.
237. Galdzicki, M., et al., *Standard biological parts knowledgebase.* PLoS One, 2011. **6**(2): p. e17005.
238. Huang, H.H., et al., *Design and characterization of molecular tools for a Synthetic Biology approach towards developing cyanobacterial biotechnology.* Nucleic Acids Res, 2010. **38**(8): p. 2577-93.
239. Cooling, M.T., et al., *Standard virtual biological parts: a repository of modular modeling components for synthetic biology.* Bioinformatics, 2010. **26**(7): p. 925-31.
240. Lucks, J.B., et al., *Toward scalable parts families for predictable design of biological circuits.* Curr Opin Microbiol, 2008. **11**(6): p. 567-73.
241. Shetty, R.P., D. Endy, and T.F. Knight, Jr., *Engineering BioBrick vectors from BioBrick parts.* J Biol Eng, 2008. **2**: p. 5.
242. Murphy, K.F., G. Balazsi, and J.J. Collins, *Combinatorial promoter design for engineering noisy gene expression.* Proc Natl Acad Sci U S A, 2007. **104**(31): p. 12726-31.
243. Benders, G.A., et al., *Cloning whole bacterial genomes in yeast.* Nucleic Acids Res, 2010. **38**(8): p. 2558-69.
244. Gibson, D.G., et al., *Creation of a bacterial cell controlled by a chemically synthesized genome.* Science, 2010. **329**(5987): p. 52-6.
245. Noskov, V.N., et al., *Isolation of circular yeast artificial chromosomes for synthetic biology and functional genomics studies.* Nat Protoc, 2011. **6**(1): p. 89-96.
246. Weber, E., et al., *A modular cloning system for standardized assembly of multigene constructs.* PLoS One, 2011. **6**(2): p. e16765.
247. Wang, H.H., et al., *Programming cells by multiplex genome engineering and accelerated evolution.* Nature, 2009. **460**(7257): p. 894-8.
248. Datsenko, K.A. and B.L. Wanner, *One-step inactivation of chromosomal genes in Escherichia coli K-12 using PCR products.* Proc Natl Acad Sci U S A, 2000. **97**(12): p. 6640-5.